

**MODELING OF A HIGH FREQUENCY FIELD
EFFECT TRANSISTOR ON INDIUM GALLIUM
NITRIDE:
THE METAL OXIDE SEMICONDUCTOR CAPACITOR
1-CHANNEL MODEL**

By

Tarik Menkad

A thesis presented to

Lakehead University

in fulfillment of

the thesis requirement for the degree of Masters of Science in Electrical
Engineering

Thunder Bay ON, Canada

April 1st,2012

Abstract

Quantum devices are an important class of modern heterostructure devices in which quantum effects are exploited directly. A Gallium Nitride high frequency field effect transistor (FET), the subject of this work, exploits a newly found exciton source in Indium Gallium Nitride $\text{In}_x\text{Ga}_{1-x}\text{N}$. These quasi-particles are used as a quantum electron source for the FET channel, made of Intrinsic Gallium Nitride (GaN). The present work addresses the natural need for providing this high frequency transistor with a device model. Following the same steps as those used in classical Metal-Oxide-Semiconductor Field Effect Transistor (MOSFET) modeling, a model for the metal oxide heterojunction capacitor; core of this high frequency field effect transistor, is first developed.

The first challenge is to define the free charge carrier concentration distribution, the electric field and the potential drop at any point inside the intrinsic Gallium Nitride layer. This layer plays the role of the channel of a proposed MOSFET device on Indium gallium Nitride.

A new analytical model for a two terminal Metal-Oxide-Gallium Nitride/Indium Gallium Nitride heterojunction structure (MOS capacitor) is presented. This model characterizes the space charge layer created by electron tunneling in the structure's channel which is made of intrinsic Gallium Nitride. A one dimensional (1-D) analysis is adopted, and a set of hypotheses is stated to frame the present work. In this analysis two Gallium Nitride channel models are suggested. The need for such models is demonstrated by the quasi-static analysis of the 2-terminal MOS capacitor. The comparison of these two models is performed through the concordance of the results with the exciton theory in Wurtzite Indium Gallium Nitride ($\text{In}_x\text{Ga}_{1-x}\text{N}$).

Acknowledgements

I would like to thank my supervisors; Professor Dimiter Alexandrov and Professor Kenneth Scott Alexander Butcher for their support and encouragement during this research work. In many stages of this research, I benefited from their advices, particularly so when exploring new ideas. Theirs positive outlook and confidence in my research inspired me.

I would like also to thank Dr. Christoffersen for his trust and help during tough moments.

Finally, I would like to thank all Faculty of Engineering and Graduate Studies members.

Table of contents

Abstract	ii
Acknowledgements	iii
List of figures	viii
List of tables	xii
List of Symbols	xiii
List of Abbreviations	xiv
Chapter 1: Introduction.....	1
1.1 Background	1
1.2 Motivation	2
1.3 Objectives	3
1.2 Organization of the manuscript.....	3
1.5 Conclusion.....	3
Chapter 2 : The High Frequency Field Effect Transistor on $\text{In}_x\text{Ga}_{1-x}\text{N}$	4
2.1 Introduction	4
2.2 Structure	4
2.3 Functioning.....	5
2.4 Conclusion.....	7
Chapter 3 : The ideal MOS capacitor on $\text{In}_{0.5}\text{Ga}_{0.5}\text{N}$	8
3.1 Introduction	8
3.2 Nomenclature	8
3.3 The ideal MOS Capacitor on $\text{In}_{0.5}\text{Ga}_{0.5}\text{N}$	9

3.4	Analysis of the ideal MOS capacitor on $\text{In}_{0.5}\text{Ga}_{0.5}\text{N}$	10
3.5	Conclusion.....	14
Chapter 4 : Channel model 1		15
4.1	Introduction	15
4.2	Exposition of the problem	15
4.3	Mathematical formulation	17
4.4	Domain of validity	23
4.5	Simulation results and discussion	26
4.6	Conclusion.....	48
Chapter 5 : Channel model 2		49
5.1	Introduction	49
5.2	Mathematical formulation	50
5.3	Simulation results and Discussion	56
5.4	Conclusion.....	95
Chapter 6 : Comparison.....		96
6.1	Introduction	96
6.2	Comparison	96
6.3	Set of equations.....	97
6.4	Conclusion.....	98
Chapter 7 : Conclusion.....		99
7.1	Conclusion.....	99
7.2	Future work	99
REFERENCES		101
Appendix A.....		103
A.1	Introduction	103

A.2	Proof.....	103
A.3	Conclusion.....	105
Appendix B.....		106
B.1	Introduction	106
B.2	Proof.....	106
B.3	Computation of the solution	109
B.4	Conclusion.....	110
Appendix C.....		111
C.1	Introduction	111
C.2	Proof.....	111
C.3	Computation of the solution	115
C.4	Conclusion.....	115

List of figures

Figure 2-1 : Cross-section of the High Frequency transistor on $\text{In}_x\text{Ga}_{1-x}\text{N}$	5
Figure 2-2: Creation and drift of mobile charge carriers in the HF FET on $\text{In}_x\text{Ga}_{1-x}\text{N}$	6
Figure 3-1: Structure of the 2-terminal MOS capacitor on $\text{In}_{0.5}\text{Ga}_{0.5}\text{N}$	9
Figure 3-2: A cross-sectional schematics of MOS heterojunction capacitor, with the corresponding referenced potential drops across the regions of interest.	11
Figure 4-1: Channel model 1 block diagram	15
Figure 4-2: Charge distribution through a hypothetical i-GaN rectangular cuboid	16
Figure 4-3: One (1-D) dimension illustration of the charge distribution through an i-GaN hypothetical rectangular cuboid	18
Figure 4-4: Solution algorithm of the proposed channel model.....	22
Figure 4-5: Domain of validity of the proposed channel model for any i-GaN layer thickness value in the range 20nm-160nm.....	24
Figure 4-6: Free electron concentration, electric field, and potential drop for $(n_{\text{ch ave}}, th_{\text{GaN}})=(10^{-9}\text{cm}^{-3}, 50\text{nm})$	28
Figure 4-7: Free electron concentration, electric field, and potential drop for $(n_{\text{ch ave}}, th_{\text{GaN}})=(10^{-8}\text{cm}^{-3}, 50\text{nm})$	28
Figure 4-8: Free electron concentration, electric field, and potential drop for $(n_{\text{ch ave}}, th_{\text{GaN}})=(10^{-7}\text{cm}^{-3}, 50\text{nm})$	29
Figure 4-9: Free electron concentration, electric field, and potential drop for $(n_{\text{ch ave}}, th_{\text{GaN}})=(10^{-6}\text{cm}^{-3}, 50\text{nm})$	29
Figure 4-10: Free electron concentration, electric field, and potential drop for $(n_{\text{ch ave}}, th_{\text{GaN}})=(10^{-5}\text{cm}^{-3}, 50\text{nm})$	30
Figure 4-11: Free electron concentration, electric field, and potential drop for $(n_{\text{ch ave}}, th_{\text{GaN}})=(10^{-4}\text{cm}^{-3}, 50\text{nm})$	30
Figure 4-12: Free electron concentration, electric field, and potential drop for $(n_{\text{ch ave}}, th_{\text{GaN}})=(10^{-3}\text{cm}^{-3}, 50\text{nm})$	31
Figure 4-13: Free electron concentration, electric field, and potential drop for $(n_{\text{ch ave}}, th_{\text{GaN}})=(10^{-2}\text{cm}^{-3}, 50\text{nm})$	31
Figure 4-14: Free electron concentration, electric field, and potential drop for $(n_{\text{ch ave}}, th_{\text{GaN}})=(10^{-1}\text{cm}^{-3}, 50\text{nm})$	32
Figure 4-15: Free electron concentration, electric field, and potential drop for $(n_{\text{ch ave}}, th_{\text{GaN}})=(10^0\text{cm}^{-3}, 50\text{nm})$	32

Figure 4-16: Free electron concentration, electric field, and potential drop for ($n_{ch\ ave}, th_{GaN}$)= $(10^{+1}cm^{-3}, 50nm)$	33
Figure 4-17: Free electron concentration, electric field, and potential drop for ($n_{ch\ ave}, th_{GaN}$)= $(10^{+2}cm^{-3}, 50nm)$	33
Figure 4-18: Free electron concentration, electric field, and potential drop for ($n_{ch\ ave}, th_{GaN}$)= $(10^{+3}cm^{-3}, 50nm)$	34
Figure 4-19: Free electron concentration, electric field, and potential drop for ($n_{ch\ ave}, th_{GaN}$)= $(10^{+4}cm^{-3}, 50nm)$	34
Figure 4-20: Free electron concentration, electric field, and potential drop for ($n_{ch\ ave}, th_{GaN}$)= $(10^{+5}cm^{-3}, 50nm)$	35
Figure 4-21: Free electron concentration, electric field, and potential drop for ($n_{ch\ ave}, th_{GaN}$)= $(10^{+6}cm^{-3}, 50nm)$	35
Figure 4-22: Free electron concentration, electric field, and potential drop for ($n_{ch\ ave}, th_{GaN}$)= $(10^{+7}cm^{-3}, 50nm)$	36
Figure 4-23: Free electron concentration, electric field, and potential drop for ($n_{ch\ ave}, th_{GaN}$)= $(10^{+8}cm^{-3}, 50nm)$	36
Figure 4-24: Free electron concentration, electric field, and potential drop for ($n_{ch\ ave}, th_{GaN}$)= $(10^{+9}cm^{-3}, 50nm)$	37
Figure 4-25: Free electron concentration, electric field, and potential drop for ($n_{ch\ ave}, th_{GaN}$)= $(10^{+10}cm^{-3}, 50nm)$	37
Figure 4-26: Free electron concentration, electric field, and potential drop for ($n_{ch\ ave}, th_{GaN}$)= $(10^{+11}cm^{-3}, 50nm)$	38
Figure 4-27: Free electron concentration, electric field, and potential drop for ($n_{ch\ ave}, th_{GaN}$)= $(10^{+12}cm^{-3}, 50nm)$	38
Figure 4-28: Free electron concentration, electric field, and potential drop for ($n_{ch\ ave}, th_{GaN}$)= $(10^{+13}cm^{-3}, 50nm)$	39
Figure 4-29: Free electron concentration, electric field, and potential drop for ($n_{ch\ ave}, th_{GaN}$)= $(10^{+14}cm^{-3}, 50nm)$	39
Figure 4-30: Free electron concentration, electric field, and potential drop for ($n_{ch\ ave}, th_{GaN}$)= $(10^{+15}cm^{-3}, 50nm)$	40
Figure 4-31: Free electrons concentration, electric field, and potential drop for ($n_{ch\ ave}, th_{GaN}$)= $(10^{+16}cm^{-3}, 50nm)$	40
Figure 4-32: Free electron concentration, electric field, and potential drop for ($n_{ch\ ave}, th_{GaN}$)= $(10^{+17}cm^{-3}, 50nm)$	41

Figure 4-33: Free electron concentration, electric field, and potential drop for $(n_{ch\ ave}, th_{GaN})=(10^{+18}cm^{-3}, 50nm)$	41
Figure 4-34: Free electron concentration for $(n_{ch\ ave}, th_{GaN})=(10^{+11\12\13\14\15\16\17\18}cm^{-3}, 50nm)$	42
Figure 4-35: Electric field for $(n_{ch\ ave}, th_{GaN})=(10^{+11\12\13\14\15\16\17\18}cm^{-3}, 50nm)$	42
Figure 4-36: Potential drop for $(n_{ch\ ave}, th_{GaN})=(10^{+11\12\13\14\15\16\17\18}cm^{-3}, 50nm)$	43
Figure 4-37: Free electron concentration for $(n_{ch\ ave}, th_{GaN})=(10^{+16}cm^{-3}, 25-50-75-100-125nm)$	43
Figure 4-38: Electric field for $(n_{ch\ ave}, th_{GaN})=(10^{+16}cm^{-3}, 25-50-75-100-125nm)$	44
Figure 4-39: Potential drop for $(n_{ch\ ave}, th_{GaN})=(10^{+16}cm^{-3}, 25-50-75-100-125nm)$	44
Figure 4-40: Electric field deviation from its initial value for $(n_{ch\ ave}, th_{GaN})=(10^{-9}\ to\ 10^{+18}cm^{-3}, 50nm)$	45
Figure 5-1: Block diagram of i-GaN channel model 2	50
Figure 5-2: A cross-sectional schematics of the intrinsic GaN layer, with the corresponding referenced potential drop, and electric field.....	50
Figure 5-3: Solution flowchart for intrinsic GaN channel model 2.....	55
Figure 5-4: (n_{ch}, F, v) for input $(n_{ch\ ave}, th_{GaN})=(10^{+17}cm^{-3}, 10^{-2}\10^{-1}V/cm, 50nm)$	60
Figure 5-5: (n_{ch}, F, v) for input $(n_{ch\ ave}, th_{GaN})=(10^{+16}cm^{-3}, 10^{-2}\10^{-1}V/cm, 50nm)$	60
Figure 5-6: (n_{ch}, F, v) for input $(n_{ch\ ave}, th_{GaN})=(10^{+15}cm^{-3}, 10^{-2}\10^{-1}V/cm, 50nm)$	61
Figure 5-7: (n_{ch}, F, v) for input $(n_{ch\ ave}, th_{GaN})=(10^{+14}cm^{-3}, 10^{-2}\10^{-1}V/cm, 50nm)$	61
Figure 5-8: (n_{ch}, F, v) for input $(n_{ch\ ave}, th_{GaN})=(10^{+13}cm^{-3}, 10^{-2}\10^{-1}V/cm, 50nm)$	62
Figure 5-9: (n_{ch}, F, v) for input $(n_{ch\ ave}, th_{GaN})=(10^{+12}cm^{-3}, 10^{-2}\10^{-1}V/cm, 50nm)$	62
Figure 5-10: (n_{ch}, F, v) for input $(n_{ch\ ave}, th_{GaN})=(10^{+11}cm^{-3}, 10^{-2}\10^{-1}V/cm, 50nm)$	63
Figure 5-11: (n_{ch}, F, v) for input $(n_{ch\ ave}, th_{GaN})=(10^{+10}cm^{-3}, 10^{-2}\10^{-1}V/cm, 50nm)$	63
Figure 5-12: (n_{ch}, F, v) for input $(n_{ch\ ave}, th_{GaN})=(10^{+9}cm^{-3}, 10^{-2}\10^{-1}V/cm, 50nm)$	64
Figure 5-13: (n_{ch}, F, v) for input $(n_{ch\ ave}, th_{GaN})=(10^{+8}cm^{-3}, 10^{-2}\10^{-1}V/cm, 50nm)$	64
Figure 5-14: (n_{ch}, F, v) for input $(n_{ch\ ave}, th_{GaN})=(10^{+7}cm^{-3}, 10^{-2}\10^{-1}V/cm, 50nm)$	65
Figure 5-15: (n_{ch}, F, v) for input $(n_{ch\ ave}, th_{GaN})=(10^{+6}cm^{-3}, 10^{-3}\10^{-2}V/cm, 50nm)$	65
Figure 5-16: (n_{ch}, F, v) for input $(n_{ch\ ave}, th_{GaN})=(10^{+5}cm^{-3}, 10^{-3}\10^{-2}V/cm, 50nm)$	66
Figure 5-17: (n_{ch}, F, v) for input $(n_{ch\ ave}, th_{GaN})=(10^{+4}cm^{-3}, 10^{-4}\10^{-3}V/cm, 50nm)$	66
Figure 5-18: (n_{ch}, F, v) for input $(n_{ch\ ave}, th_{GaN})=(10^{+3}cm^{-3}, 10^{-4}\10^{-3}V/cm, 50nm)$	67
Figure 5-19: (n_{ch}, F, v) for input $(n_{ch\ ave}, th_{GaN})=(10^{+2}cm^{-3}, 10^{-5}\10^{-4}V/cm, 50nm)$	67
Figure 5-20: (n_{ch}, F, v) for input $(n_{ch\ ave}, th_{GaN})=(10^{+1}cm^{-3}, 10^{-5}\10^{-4}V/cm, 50nm)$	68
Figure 5-21: (n_{ch}, F, v) for input $(n_{ch\ ave}, th_{GaN})=(1cm^{-3}, 10^{-6}\10^{-5}V/cm, 50nm)$	68
Figure 5-22: (n_{ch}, F, v) for input $(n_{ch\ ave}, th_{GaN})=(10^{-1}cm^{-3}, 10^{-6}\10^{-5}V/cm, 50nm)$	69
Figure 5-23: (n_{ch}, F, v) for input $(n_{ch\ ave}, th_{GaN})=(10^{-2}cm^{-3}, 10^{-7}\10^{-6}V/cm, 50nm)$	69
Figure 5-24: (n_{ch}, F, v) for input $(n_{ch\ ave}, th_{GaN})=(10^{-3}cm^{-3}, 10^{-7}\10^{-6}V/cm, 50nm)$	70

Figure 5-25: (n_{ch}, F, v) for input $(n_{ch\ ave}, th_{GaN})=(10^{-4}cm^{-3}, 10^{-8}\backslash 10^{-7}V/cm, 50nm)$	70
Figure 5-26: (n_{ch}, F, v) for input $(n_{ch\ ave}, th_{GaN})=(10^{-5}cm^{-3}, 10^{-8}\backslash 10^{-7}V/cm, 50nm)$	71
Figure 5-27: (n_{ch}, F, v) for input $(n_{ch\ ave}, th_{GaN})=(10^{-6}cm^{-3}, 10^{-9}\backslash 10^{-8}V/cm, 50nm)$	71
Figure 5-28: (n_{ch}, F, v) for input $(n_{ch\ ave}, th_{GaN})=(10^{-7}cm^{-3}, 10^{-9}\backslash 10^{-8}V/cm, 50nm)$	72
Figure 5-29: (n_{ch}, F, v) for input $(n_{ch\ ave}, th_{GaN})=(10^{-8}cm^{-3}, 10^{-10}\backslash 10^{-9}V/cm, 50nm)$	72
Figure 5-30: (n_{ch}, F, v) for input $(n_{ch\ ave}, th_{GaN})=(10^{-9}cm^{-3}, 10^{-10}\backslash 10^{-9}V/cm, 50nm)$	73
Figure 5-31: (n_{ch}, F, v) for input $(n_{ch\ ave}, th_{GaN})=(10^{+18}cm^{-3}, 5*10^{+3}\backslash 10^{+4}V/cm, 50nm)$	78
Figure 5-32: (n_{ch}, F, v) for input $(n_{ch\ ave}, th_{GaN})=(10^{+18}cm^{-3}, 5*10^{+4}\backslash 10^{+5}V/cm, 50nm)$	78
Figure 5-33: (n_{ch}, F, v) for input $(n_{ch\ ave}, th_{GaN})=(10^{+17}cm^{-3}, 5*10^{+4}\backslash 10^{+5}V/cm, 50nm)$	79
Figure 5-34: (n_{ch}, F, v) for input $(n_{ch\ ave}, th_{GaN})=(10^{+16}cm^{-3}, 5*10^{+4}\backslash 10^{+5}V/cm, 50nm)$	79
Figure 5-35: (n_{ch}, F, v) for input $(n_{ch\ ave}, th_{GaN})=(10^{+15}cm^{-3}, 5*10^{+4}\backslash 10^{+5}V/cm, 50nm)$	80
Figure 5-36: (n_{ch}, F, v) for input $(n_{ch\ ave}, th_{GaN})=(10^{+14}cm^{-3}, 5*10^{+4}\backslash 10^{+5}V/cm, 50nm)$	80
Figure 5-37: (n_{ch}, F, v) for input $(n_{ch\ ave}, th_{GaN})=(10^{+13}cm^{-3}, 5*10^{+4}\backslash 10^{+5}V/cm, 50nm)$	81
Figure 5-38: (n_{ch}, F, v) for input $(n_{ch\ ave}, th_{GaN})=(10^{+12}cm^{-3}, 5*10^{+4}\backslash 10^{+5}V/cm, 50nm)$	81
Figure 5-39: (n_{ch}, F, v) for input $(n_{ch\ ave}, th_{GaN})=(10^{+11}cm^{-3}, 5*10^{+4}\backslash 10^{+5}V/cm, 50nm)$	82
Figure 5-40: (n_{ch}, F, v) for input $(n_{ch\ ave}, th_{GaN})=(10^{+10}cm^{-3}, 5*10^{+4}\backslash 10^{+5}V/cm, 50nm)$	82
Figure 5-41: (n_{ch}, F, v) for input $(n_{ch\ ave}, th_{GaN})=(10^{+9}cm^{-3}, 5*10^{+4}\backslash 10^{+5}V/cm, 50nm)$	83
Figure 5-42: (n_{ch}, F, v) for input $(n_{ch\ ave}, th_{GaN})=(10^{+8}cm^{-3}, 5*10^{+4}\backslash 10^{+5}V/cm, 50nm)$	83
Figure 5-43: (n_{ch}, F, v) for input $(n_{ch\ ave}, th_{GaN})=(10^{+7}cm^{-3}, 5*10^{+4}\backslash 10^{+5}V/cm, 50nm)$	84
Figure 5-44: (n_{ch}, F, v) for input $(n_{ch\ ave}, th_{GaN})=(10^{+6}cm^{-3}, 5*10^{+3}\backslash 5*10^{+4}V/cm, 50nm)$	84
Figure 5-45: (n_{ch}, F, v) for input $(n_{ch\ ave}, th_{GaN})=(10^{+5}cm^{-3}, 5*10^{+3}\backslash 10^{+4}V/cm, 50nm)$	85
Figure 5-46: (n_{ch}, F, v) for input $(n_{ch\ ave}, th_{GaN})=(10^{+4}cm^{-3}, 5*10^{+3}\backslash 10^{+4}V/cm, 50nm)$	85
Figure 5-47: (n_{ch}, F, v) for input $(n_{ch\ ave}, th_{GaN})=(10^{+3}cm^{-3}, 5*10^{+3}\backslash 10^{+4}V/cm, 50nm)$	86
Figure 5-48: (n_{ch}, F, v) for input $(n_{ch\ ave}, th_{GaN})=(10^{+2}cm^{-3}, 5*10^{+3}\backslash 10^{+4}V/cm, 50nm)$	86
Figure 5-49: (n_{ch}, F, v) for input $(n_{ch\ ave}, th_{GaN})=(10^{+1}cm^{-3}, 5*10^{+3}\backslash 10^{+4}V/cm, 50nm)$	87
Figure 5-50: (n_{ch}, F, v) for input $(n_{ch\ ave}, th_{GaN})=(100cm^{-3}, 5*10^{+2}\backslash 5*10^{+3}V/cm, 50nm)$	87
Figure 5-51: (n_{ch}, F, v) for input $(n_{ch\ ave}, th_{GaN})=(10^{+14}\backslash 15\backslash 16\backslash 17\ cm^{-3}, 5*10^{+2}V/cm, 50nm)$	88
Figure 5-52 (a) Free electron concentration, (b) Electric field, and (c) Potential drop are plotted as functions of the normalized abscissa for inputs $(n_{ch\ ave}, F_0, th_{GaN})=(10^{+14}\backslash 15\backslash 16\ cm^{-3}, 5*10^{+4}\backslash 10^{+5}V/cm, 50nm)$	89
Figure 5-53: (a) Free electron concentration, (b) Electric field, and (c) Potential drop are plotted as functions of the normalized abscissa for inputs $(n_{ch\ ave}, F_0, th_{GaN})=(10^{+16}cm^{-3}, 10^{+4}V/cm, 50\backslash 75\backslash 100\backslash 125nm)$	91

List of tables

Table 4-1: Maximum values of average concentrations for GaN layer thicknesses in the range 20nm-160nm.....	25
Table 4-2: Initial and final values of free electron concentration, electric field and potential drop for ($n_{ch\ ave}=10^{-9}$ to 10^{+17} cm ⁻³ , $th_{GaN}=50$ nm)	46
Table 5-1: Initial and final values for the free electron concentration, and the electric field, and the voltage drop across GaN layer of 50nm thickness (weak initial field).....	74
Table 5-2: Initial and final values for the free electron concentration and the electric field, and the voltage drop across GaN layer of 50nm thickness	92

List of Symbols

Symbol	Meaning
Q'_G, Q'_{GaN}	Charge per unit area on the gate and in GaN layer
$Q'_{p-In_{0.5}Ga_{0.5}N}$	Charge per unit area in the Space Charge Region (SCR) located in p-type $In_{0.5}Ga_{0.5}N$ side of i-GaN/p- $In_{0.5}Ga_{0.5}N$ heterojunction
α_p	Coefficient that depends on the lifetime of injected electrons in p- $In_{0.5}Ga_{0.5}N$
n_0''	Concentration of electrons occupying the state Γ_{cl}^1 in non equilibrium
α_{e-ex}	Creation efficiency of excitons current
v_{Gg}	DC sweep gate voltage
α_{n-p}	Efficiency of the electron injection through the p-n homojunction
F	Electric field
F_0	Electric field in GaN layer at the i-GaN/p- $In_{0.5}Ga_{0.5}N$ heterojunction.
Q	Elementary charge
n_{ch}	Free electrons concentration present in intrinsic Gallium Nitride layer
V_{Gg}	Front gate to back substrate voltage
C'_{Gg}	Gate capacitance per unit area
th_{ox}, th_{GaN}	Oxide and GaN layers thicknesses
$E_n(0)$	Position of the hydrogen like electron energy level E_n for $F = 0$
ξ	Potential barrier width for level E_n
φ_1, φ_2	Potential drops across $In_{0.5}Ga_{0.5}N$ pn junction and across the SCR in p-type $In_{0.5}Ga_{0.5}N$ side of the i-GaN/p- $In_{0.5}Ga_{0.5}N$ heterojunction
φ_3, φ_4	Potential drop across i-GaN, oxide layers
v	Potential drop
$\epsilon_{In_{0.5}Ga_{0.5}N}, \epsilon_0$	Relative permittivity of $In_{0.5}Ga_{0.5}N$, and permittivity of vacuum
$\epsilon_{ox}, \epsilon_{GaN}$	Relative permittivity of oxide and GaN
$\epsilon_{ox}, \epsilon_{GaN}$	Relative permittivity of oxide and GaN
u_T	Thermal voltage

List of Abbreviations

Abbreviation	Meaning
HF	High Frequency
FET	Field Effect Transistor
MOS	Metal Oxide Semiconductor
SCR	Space Charge Region
HBT	Hetero-junction Bipolar Transistor
DHBT	Double-Heterojunction bipolar Transistor
HEMT	High Electron Mobility Transistor
HFET	Hetero-structure Field Effect Transistor
MBE	Molecular beam Epitaxy
MOCVD	Metalorganic Chemical Vapour Deposition
MODFET	Modulation-Doped Field-Effect Transistor
SDHT	Selectively Doped Heterojunction Transistor
TEGFET	Two-dimensional Electron Gas Field Effect Transistor

Chapter 1 : Introduction

1.1 Background

The Metal-Oxide-Semiconductor Field Effect Transistor (MOSFET) is the most important device in the design of high-density integrated circuits such as microprocessors and memories. It is also important for power applications. The principle of the surface field effect transistor was first proposed in the early 1930's by Lilienfeld [1-3] and Heil [4]. Shockley and Pearson [5] studied this effect in the late 1940's. The first device –quality Si-SiO₂ (Silicon-Silicon Dioxide) was produced by Ligenza and Spitzer using thermal oxidation [6]. The basic MOSFET structure, which uses the Si-SiO₂ system, was proposed by Khahng and Atalla [7] in 1960. The device characteristics were initially studied by Ihantola and Moll [8], Sah [9], and Hofstein and Heiman [10]. The technology, application, and device physics have been reviewed by many books [11-15].

For the classical MOSFET conduction occurs when there is a charge inversion in its channel. The application of a positive (negative) and sufficient gate voltage on a n (p) MOSFET creates an accumulation Space Charge Region (SCR) at the surface of the p (n) semiconductor underneath the interface oxide/semiconductor. This accumulation region is of opposite type compared to that of the bulk semiconductor. The creation of an inversion region is accompanied with the existence of a depletion SCR. Under a transverse electric field free charge carriers (electrons for n-MOSFET and holes for p-MOSFET) move in a doped semiconductor and are subject to ionic and phonon scattering.

In the Modulation Doped Field Effect Transistor (MODFET), known also as the High Electron Mobility Transistor (HEMT), and for the Two-dimensional Electron-Gas Field Effect Transistor (TEGFET), and Selectively Doped Heterojunction Transistor (SDHT), the wide-energy-gap material of the heterostructure is doped and carriers diffuse to the undoped narrow-bandgap layer at which heterointerface the channel is formed. As a result, channel carriers in the undoped heterointerface are spatially separated from the doped region and have high mobilities because there is no impurity scattering. Carrier transport parallel to the layers of a superlattice was first considered by Esaki and Tsu in 1969 [16]. The development of Molecular Beam Epitaxy (MBE) and Metalorganic Chemical Vapour

Deposition (MOCVD) technologies in the 1970's made heterostructures, quantum wells and superlattices practical and more accessible. The enhanced mobility in the AlGaAs/GaAs modulation doped superlattice was first demonstrated by Dingle et al in 1978 [17]. Stormer et al subsequently obtained a similar effect using a single AlGaAs/GaAs heterojunction in 1979 [18]. This effect was applied to the field effect transistor by Mimura et al in 1980 [19-20] and later by Delagebeaudeuf et al in the same year [21]. For an in-depth treatment of the MODFET, readers are referred to Refs [22-25]. The main difference between the classic MOSFET and the MODFET aside from their structure resides in the fact that charge carriers move in a doped semiconductor for the MOSFET and in an intrinsic semiconductor for the MODFET offering a higher mobility and resulting in a faster device more suitable for high frequency applications.

The present work deals with a novel device, the High Frequency Field Effect Transistor on Indium Gallium Nitride [26]. Unlike the MODFET, the free charges carriers result from quantum tunnelling through the heterojunction instead of resulting from diffusion, as is the case for MODFET. However, in both devices, charge carriers move in an intrinsic semiconductor layer and observe reduced scattering.

1.2 Motivation

It is the trend in the silicon and compound microelectronics industries to continuously develop semiconductor circuits which are faster, smaller, and consume less power for a similar level of integration. This trend is fueled by the rapid growth of digital wireless communication and high frequency analog circuits. Both silicon and compound state-of-the-art integrated circuits rely on high-speed submicron devices. New hetero-structure devices are continuously being developed, such as the Heterojunction Bipolar Transistor (HBT), the Double-Heterojunction Bipolar Transistor (DHBT), the High-Electron-Mobility Transistor (HEMT), and the Hetero-structure Field-Effect Transistor (HFET).

Quantum devices are an important class of these modern hetero-structure devices in which quantum effects are exploited. The high frequency field effect transistor, which is the subject of this work, exploits recently identified quasi-particles in Indium Gallium Nitride $\text{In}_x\text{Ga}_{1-x}\text{N}$, called excitons of the structure. These excitons of structure are used as a quantum electron source for the channel of the High Frequency Metal Oxide Semiconductor Field effect

Chapter 1. Introduction
Section 1.2 Motivation
Section 1.3 Objectives
Section 1.4 Organization of the manuscript
Section 1.5 Conclusion

Transistor (HF MOSFET) made of Intrinsic Gallium Nitride GaN [26]. The present work aims to provide a stepping stone towards this novel structure by establishing a device model.

1.3 Objectives

Following the same steps as those used in classical MOSFET theory, a model for the metal oxide heterojunction capacitor - the core of this HF MOSFET- is first developed. To achieve this, the intrinsic Gallium Nitride channel was first modeled, and then used in the analysis of the 2-terminal MOS heterojunction capacitor on Indium gallium nitride.

The present work introduces this quasi-static analysis of the 2-terminal device and demonstrates the need to model its intrinsic GaN channel. Two channel models are presented, compared, and one of them is incorporated in the quasi static analysis of the 2-terminal MOS capacitor on Indium Gallium Nitride.

1.4 Organization of the manuscript

Chapter 2 contains a brief explanation of the structure and the functioning of the HF MOSFET on Indium Gallium Nitride. An ideal model of this transistor's core, the MOS capacitor is presented in chapter 3. Chapters 4 and 5 propose two models for the channel; model 1 and model 2 respectively. A comparison of these two channel models is performed in chapter 6. Chapter 7 wraps up this work. Three appendices A, B, and C are added at the end of this manuscript, they contain mathematical proofs that are essential to the analysis. References used to perform this present work are listed at the end of the manuscript.

1.5 Conclusion

The motivation of this work is not only about introducing a new analytical model for the practical situation where free charge carriers of electron origin are injected into a thin intrinsic semiconductor (Gallium Nitride), but is also about demonstrating the need for having such a model. The reader will realize that this model is a standalone entity, thus it can be introduced separately from the device analysis.

The channel model is presented as a part of the 2-terminal device analysis to show its necessity for the analysis of the MOS capacitor.

Chapter 2:

The High Frequency Field Effect Transistor on $\text{In}_x\text{Ga}_{1-x}\text{N}$ [26]

2.1 Introduction

The current chapter presents a brief qualitative description of the HF MOSFET on $\text{In}_x\text{Ga}_{1-x}\text{N}$ [26]. First, the different layers and regions forming this device are listed, their roles are stated. Second, a concise explanation of the functioning of this device is presented.

2.2 Structure

The HF MOSFET on $\text{In}_x\text{Ga}_{1-x}\text{N}$ has a multi-layer structure (see figure 2-1). The oxide layer is deposited on an intrinsic GaN region called the channel, on both sides of this channel there is a local heavily n-type doped GaN region called the drain or the source. These appellations are interchangeable depending on the applied external bias, making the high frequency transistor on $\text{In}_x\text{Ga}_{1-x}\text{N}$, like the classic MOSFET, a symmetric device. Underneath the GaN layer there is a p-type $\text{In}_x\text{Ga}_{1-x}\text{N}$ layer, forming together with the intrinsic GaN layer at their common frontier a semiconductor heterojunction. The p-type $\text{In}_x\text{Ga}_{1-x}\text{N}$ is implemented as a local diffusion area in a common layer of $\text{In}_x\text{Ga}_{1-x}\text{N}$. The non doped parts of $\text{In}_x\text{Ga}_{1-x}\text{N}$ are between the grounded n-type $\text{In}_x\text{Ga}_{1-x}\text{N}$ and the two n^+ -type GaN islands, their role is to prevent charge transmission between the n-type $\text{In}_x\text{Ga}_{1-x}\text{N}$ layer and the two n^+ -type GaN islands. Finally a thin film made of a metal or a highly degenerate semiconductor is deposited on both the oxide and the ground n-type $\text{In}_x\text{Ga}_{1-x}\text{N}$ layer to form the transistor gate and back substrate contacts respectively, in addition to the drain and source contacts. This makes the HF MOSFET on $\text{In}_x\text{Ga}_{1-x}\text{N}$ a 4-terminal device.

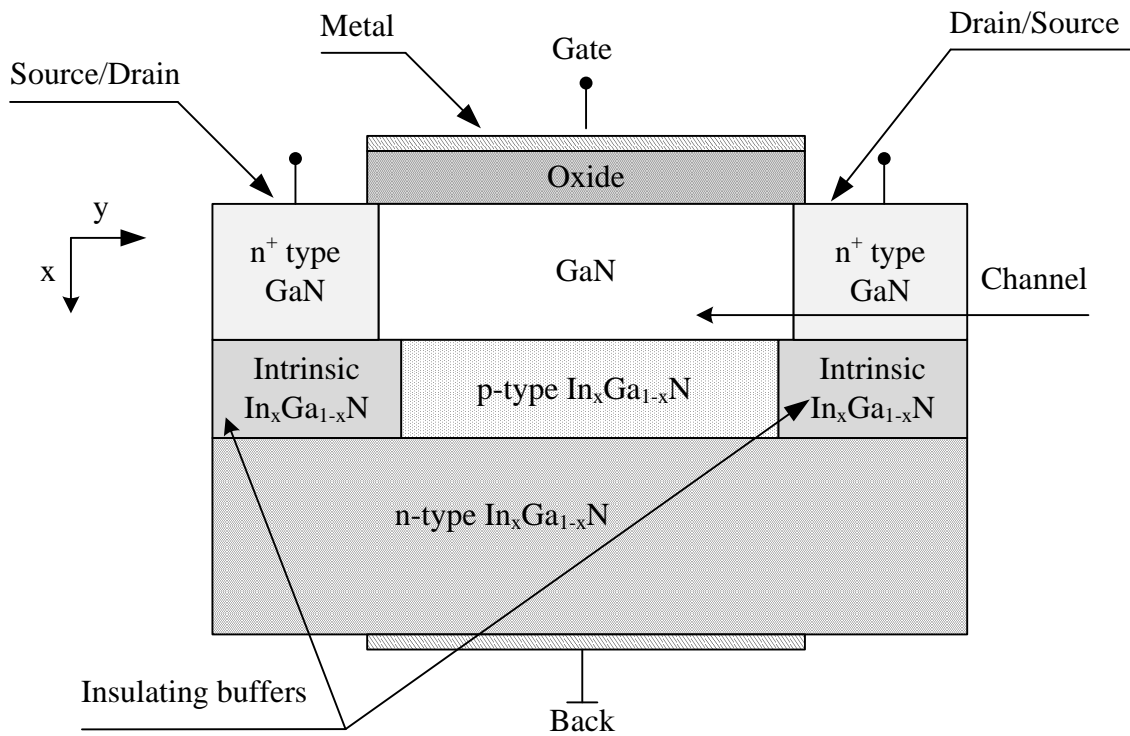


Figure 2-1 : Cross-section of the High Frequency transistor on $\text{In}_x\text{Ga}_{1-x}\text{N}$

2.3 Functioning

The HF MOSFET on $\text{In}_x\text{Ga}_{1-x}\text{N}$ uses excitons of the structure as a free electron source. The concentration of these free charge carriers in the channel made of intrinsic GaN material modulates the device's conductivity. Under the influence of an external electric field, the electrons move in an intrinsic semiconductor and experience reduced scattering (no impurity scattering). The high mobility in the channel allows low noise and high-speed performance. The application of a sufficiently high positive voltage on the gate with respect to the back (see Figure 2-2) forward biases the $\text{In}_x\text{Ga}_{1-x}\text{N}$ p-n homojunction. This positive applied potential drop allows electrons from the n-type $\text{In}_x\text{Ga}_{1-x}\text{N}$ region to move to the p-type side and form with holes quasi-particles called excitons with a zero net electric charge. The positive gate voltage must be high enough to produce a potential drop across the p-n $\text{In}_x\text{Ga}_{1-x}\text{N}$ homojunction that is bigger than an engineered threshold in order to generate excitons, see [26]. The production of these quasi-particles can be pictured as happening following the x-axis direction (see figure 2.2).

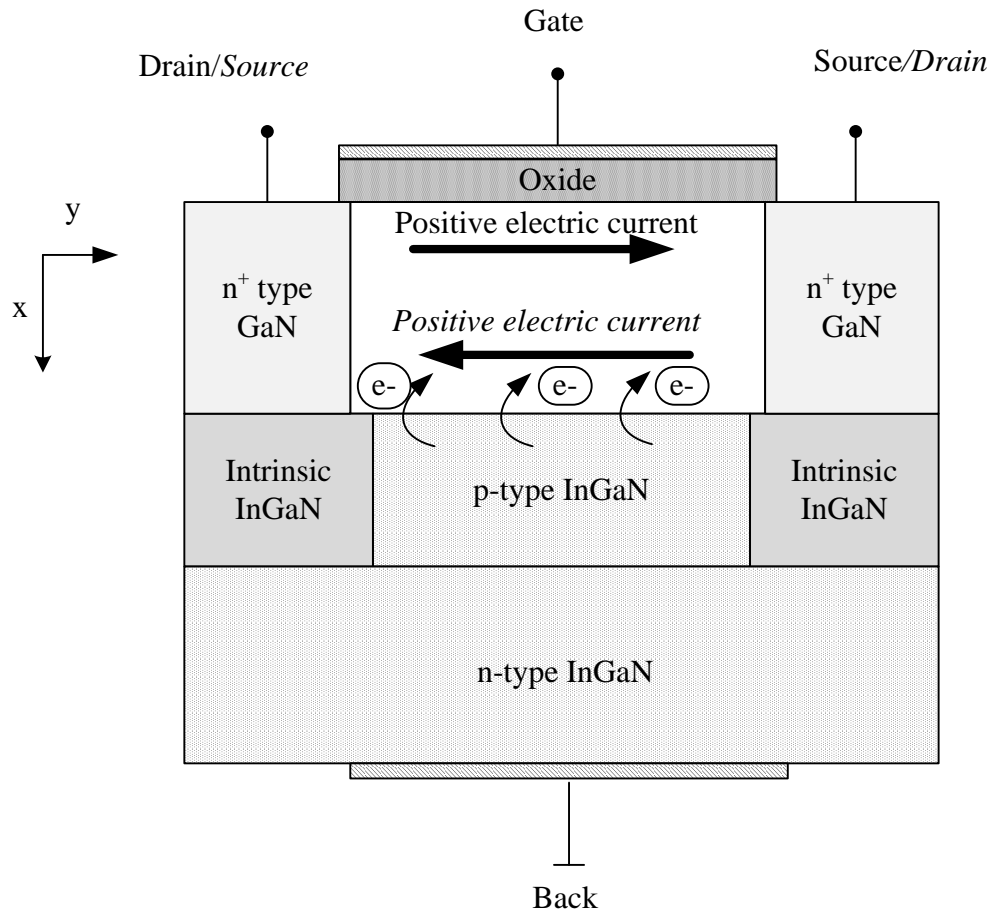


Figure 2-2: Creation and drift of mobile charge carriers in the HF FET on $In_xGa_{1-x}N$

The excitons present in the p-type $In_xGa_{1-x}N$ interacts with the i-GaN/p- $In_xGa_{1-x}N$ semiconductor heterojunction, this interaction leads to their destruction and to the tunneling of the corresponding electrons into the intrinsic GaN layer (channel). The concentration of excitons formed in p-type $In_xGa_{1-x}N$ at the p- $In_xGa_{1-x}N$ /i-GaN boundary is expressed in terms of the potential drop across the p-n $In_xGa_{1-x}N$ homojunction [26]. The transmission coefficient expresses the ratio of excitons that interact with the semiconductor heterojunction to the total amount of excitons present in the p- $In_{0.5}Ga_{0.5}N$ next to the heterojunction, this transmission coefficient is expressed in terms of the electric field applied to the GaN side of the p- $In_xGa_{1-x}N$ /i-GaN semiconductor heterojunction [26][27]. The application of a potential drop between the two n+-type GaN regions creates an electric field through the sandwiched i-GaN layer according to the y-axis direction; see Figure 2-2.

Free electrons present in the i-GaN layer (Channel) drift under the influence of this electric field producing an electric current.

2.4 Conclusion

Brief qualitative descriptions of the structure and of the functioning of this novel device were presented. A Complete description of this HF MOSFET on Indium Gallium Nitride is found in [26].

Chapter 3 : The ideal MOS capacitor on $In_{0.5}Ga_{0.5}N$ [28]

3.1 Introduction

A model for the real world device is presented. A set of hypotheses is stated. It defines the scope and sets the domain for the validity of this analysis. The quasi-static analysis performed on the ideal MOS capacitor demonstrates the need to investigate the charge distribution in its channel.

3.2 Nomenclature

V_{Gg}	Front gate to back substrate voltage
φ_1, φ_2	Potential drops across $In_{0.5}Ga_{0.5}N$ p-n junction and across the Space Charge Region (SCR) in p-type $In_{0.5}Ga_{0.5}N$ side of the i-GaN/p- $In_{0.5}Ga_{0.5}N$
φ_3, φ_4	Potential drop across i-GaN, oxide layers
th_{ox}, th_{GaN}	Oxide and GaN layers thicknesses
Q'_G, Q'_{GaN}	Charge per unit area on the gate and in the i-GaN layer
$Q'_{p-In_{0.5}Ga_{0.5}N}$	Charge per unit area in the SCR located in the p-type $In_{0.5}Ga_{0.5}N$ side of the i-GaN/p- $In_{0.5}Ga_{0.5}N$ heterojunction
n_{ch}	Free electrons concentration present in i-GaN layer
F_0	Electric field in i-GaN layer at the i-GaN/p- $In_{0.5}Ga_{0.5}N$ heterojunction.
P_{p0}, N_{p0}	Thermal equilibrium holes and electrons concentrations in p-type $In_{0.5}Ga_{0.5}N$
$\epsilon_{ox}, \epsilon_{GaN}$	Relative permittivities of oxide and GaN respectively
$\epsilon_{In_{0.5}Ga_{0.5}N}, \epsilon_0$	Relative permittivity of $In_{0.5}Ga_{0.5}N$, and permittivity of vacuum
u_T	Thermal voltage
q	Elementary charge

3.3 The ideal MOS Capacitor on $\text{In}_{0.5}\text{Ga}_{0.5}\text{N}$

The MOS structure (see figure 3-1), consisting of a metal-oxide-semiconductor sandwich, is the core of the HF MOSFET on $\text{In}_x\text{Ga}_{1-x}\text{N}$. It functions as a 2-terminal capacitor in which a metal contact is separated from the semiconductor by a thin insulator, which can be a thermally grown SiO_2 layer. The metal contact can be made of materials like aluminum or heavily doped polysilicon. A second metal layer along the back provides an electrical contact with the semiconductor material.

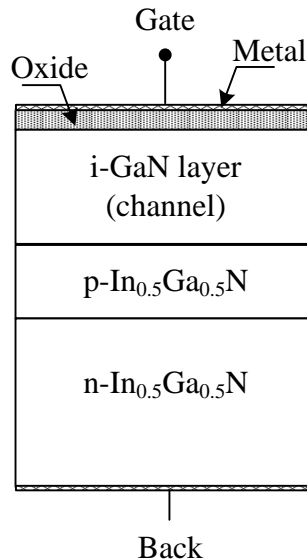


Figure 3-1: Structure of the 2-terminal MOS capacitor on $\text{In}_{0.5}\text{Ga}_{0.5}\text{N}$

The ideal MOS structure has the following properties:

- P1) The metal gate is equipotential.
- P2) The oxide is a perfect insulator with zero transport current. No trapped charges exist inside it or at its interfaces.
- P3) All doped semiconductors have a uniform profile.
- P4) All doped semiconductors are sufficiently thick, so that a field free (neutral) region exists in the bulk semiconductors.
- P5) The intrinsic GaN material is considered to be depleted of free charge carriers.

- P6) The semiconductor heterojunction is realized with a state-of-the art technique; polarization effects are negligible.
- P7) Both the oxide and the GaN material have the same work function.
- P8) The structure is one-dimensional; the electric field lines are perpendicular to the surfaces.
- P9) Metal/semiconductor interfaces are ohmic contacts, the potential contact is zero.

3.4 Analysis of the ideal MOS capacitor on In_{0.5}Ga_{0.5}N

The analysis of the ideal MOS capacitor on In_{0.5}Ga_{0.5}N is justified because all the idealized properties in section 3.3 are approached in a real device except properties P7) and P9). The inclusion of the potential contact and the work function difference in the model only requires a simple voltage shift of the capacitive characteristics. To define the scope and the domain for the validity of this quasi-static analysis, the following set of hypotheses is stated;

- H1) All semiconductors are considered to be non-degenerate, so that Boltzmann statistics can be used.
- H2) No temperature gradient is present. The device dimensions are small enough, that we assume that heat distributes evenly throughout the device.
- H3) Charge neutrality is assumed
- H4) The i-GaN/p-In_{0.5}Ga_{0.5}N semiconductor heterojunction is approximated by an abrupt junction.
- H5) The gate voltage varies slowly enough, so we can consider a zero-valued gate current.

Figure 3-2 illustrates a cross-section of the MOS structure including the referenced potential drops across regions of interest. The gate voltage breaks down to four potential drops φ_1 , φ_2 , φ_3 , and φ_4 .

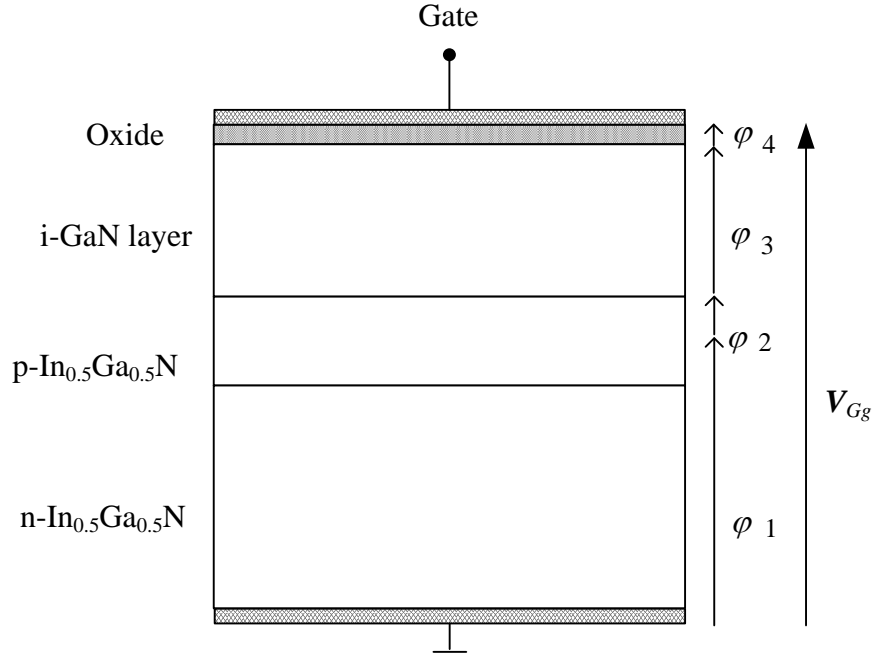


Figure 3-2: A cross-sectional schematic of the MOS heterojunction capacitor, with the corresponding referenced potential drops across the regions of interest.

A first set of relations, valid under any case of operation, is derived from global equilibrium and Gauss's Law:

$$V_{Gg} = \sum_{i=1}^4 \varphi_i \quad (3-1)$$

$$Q'_G + Q'_{p-In_{0.5}Ga_{0.5}N} + Q'_{GaN} = 0 \quad (3-2)$$

$$Q'_G = \frac{\epsilon_o \epsilon_{ox}}{th_{ox}} \varphi_4 \quad (3-3)$$

$$Q'_{p-In_{0.5}Ga_{0.5}N} = -\epsilon_o \epsilon_{GaN} F_0 \quad (3-4)$$

$$Q'_{GaN} = -q \overline{n_{ch}} th_{GaN} \quad (3-5)$$

Relations 3-2 to 3-5 are grouped in one relation.

$$\varepsilon_o \left(\varepsilon_{ox} \frac{\varphi_4}{th_{ox}} - \varepsilon_{GaN} F_0 \right) = q \overline{n_{ch}} th_{GaN} \quad (3-6)$$

To relate the electric field F_0 to potential drops, the (1-D) Poisson equation is solved for the SCR in p-type $In_{0.5}Ga_{0.5}N$ at the semiconductor heterojunction. The electric field F_0 is given as,

$$F_0 = sgn(V_{Gg}) \left(\frac{2qu_T \varepsilon_{InGaN}}{\varepsilon_o \varepsilon_{GaN}^2} \right)^{1/2} \left\{ P_{p_0} \left[\exp\left(-\frac{\varphi_2}{u_T}\right) + \frac{\varphi_2}{u_T} - 1 \right] + N_{p_0} \left[\exp\left(\frac{\varphi_2}{u_T}\right) - \frac{\varphi_2}{u_T} - 1 \right] \right\}^{1/2} \quad (3-7)$$

An expression for the free electron concentration average value was obtained in terms of the potential drop φ_1 across the $In_{0.5}Ga_{0.5}N$ p-n junction and the electric field F_0 in the i-GaN layer at the i-GaN/p- $In_{0.5}Ga_{0.5}N$ heterojunction [26]. A good approximation of this value is given by the expression 3-8

$$\overline{n_{ch}} = \beta \cdot \exp\left(\frac{\varphi_1}{u_T}\right) \cdot \exp\left\{-\frac{4\xi}{3\delta\hbar} \cdot \frac{1}{F_0} \left[\gamma^{3/2} - (\gamma - \delta F_0)^{3/2} \right]\right\} \quad (3-8),$$

where $\beta = \alpha_{n-p} \alpha_p \alpha_{e-ex} n_0'' \left[\sum_{i \in [1.5], i \neq 4} \exp\left(\frac{\Delta\Gamma_{cl}^i}{kT}\right) \right]$, $\gamma = 2m_{c\Gamma}^4 (\Gamma_{cl}^1(0) - E_n(0))$,

and $\delta = 2m_{c\Gamma}^4 q \varepsilon_{GaN} \xi$

Coefficient α_{n-p} represents the efficiency of the electron injection through the p-n homojunction ($0 < \alpha_{n-p} < 1$); α_p is a coefficient that depends on the lifetime of injected electrons in p-type $In_{0.5}Ga_{0.5}N$ ($0 < \alpha_p < 1$); α_{e-ex} is the creation efficiency for the excitonic current ($0 < \alpha_{e-ex} < 1$); n_0'' is the concentration of electrons occupying the state Γ_{cl}^1 in non equilibrium; $E_n(0)$ is the position of the hydrogen like electron energy level E_n for $F = 0$, and ξ is the potential barrier width for level E_n [26][27].

Two equations of four unknowns ($\varphi_1, \varphi_2, \varphi_3, \varphi_4$) are obtained; the first equation is given in 3-1, and the second equation is obtained by substituting the electric field F_0 and the average concentration $\overline{n_{ch}}$ by their expressions given in 3-7 and 3-8 respectively in 3-6.

A system of two equations for four unknowns ($\varphi_1, \varphi_2, \varphi_3, \varphi_4$) is not sufficient to solve for ($\varphi_1, \varphi_2, \varphi_3, \varphi_4$) given a value for the gate voltage V_{Gg} . The remaining two equations are obtained through modeling of the i-GaN layer.

In modeling the i-GaN channel, the charge distribution across the layer, the electric field through it and the potential drop at any point need to be determined. Although they are not final results, their determination imposes itself as an intermediate step in order to obtain the two additional equations in terms of the four potential drops ($\varphi_1, \varphi_2, \varphi_3, \varphi_4$). The average concentration value $\overline{n_{ch}}$ of free electrons that have tunneled into the i-GaN layer, the i-GaN layer thickness th_{GaN} , and the initial field value F_0 , are three natural candidates for a channel model input. Two approaches have been considered; the first one assumes that the initial field is inherent to the average concentration value, while the second one treats them as independent. The first model will have the average concentration $\overline{n_{ch}}$ and the GaN layer thickness th_{GaN} as inputs, while the second one will have one more input which is the initial field F_0 . Both models will generate the free electron concentration, the electric field, and the potential drop profiles (n_{ch}, F, v).

The determination of the charge density distribution, the electric field, and the potential drop across the channel are essential to relate the electric charge per unit area Q'_G present on the gate to the corresponding applied gate voltage V_{Gg} . Once a system of four equations in terms of the unknowns ($\varphi_1, \varphi_2, \varphi_3, \varphi_4$) is obtained, we can solve them for a given value of the applied gate voltage V_{Gg} . The gate capacitance C'_{Gg} per unit area will be given as follows;

$$C'_{Gg}(V_{Gg}) = \left. \frac{dQ'_G}{dv_{Gg}} \right|_{v_{Gg}=V_{Gg}} \quad (3-9)$$

Where v_{Gg} denotes the dc sweep gate voltage.

3.5 Conclusion

The concept of an ideal MOS capacitor structure on In_{0.5}Ga_{0.5}N is introduced and its use as a valid approximation of the real device is justified. The necessity of analyzing the charge distribution inside the i-GaN layer is demonstrated by performing a quasi-static analysis on the 2-terminal structure. Two Channel models were suggested, their inputs and outputs were determined. The quasi static analysis is not carried out. This will be done once a channel model is obtained and a complete system of four equations with respect to the potential drops ($\varphi_1, \varphi_2, \varphi_3, \varphi_4$) is found. Its resolution allows the computation of the quasi-static C-V curve of the ideal capacitor.

Chapter 4 : Channel model 1

4.1 Introduction

A first model for the channel made of intrinsic GaN is presented; it uses the average value of the free electron concentration present in the channel and its thickness as inputs. It gives the free electron concentration distribution, the potential drop, and the electric field at any point. Figure 4-1 represents a block diagram of this channel model.

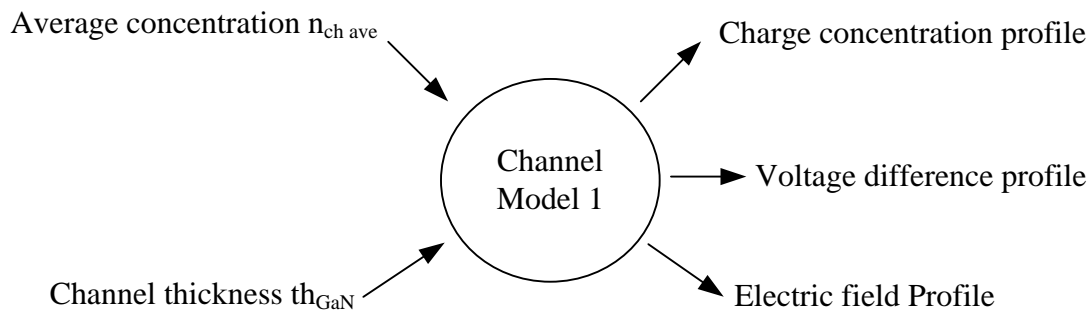


Figure 4-1: Channel model 1 block diagram

4.2 Exposition of the problem

It has been shown [29] that for any semiconductor material under the influence of an electric field, and with a zero net current (open circuit situation), it is possible to obtain a neutral region where both the voltage drop and the electric field are null. For this to happen, the semiconductor material must be thick enough. An estimation of this required thickness is deduced from the depth that an electric field can penetrate such a material. A common measure of this penetration is expressed in terms of The Debye length. Let us consider a hypothetical rectangular cuboid of i-GaN material, an electric field is applied on one side, it penetrates the semiconductor and dies out at a certain distance inside the layer. The neutral region begins at that location and extends all the way to the opposite side of the layer.

Figure 4-2 illustrates a rectangular cuboid made of intrinsic GaN material with a perpendicular electric field applied on one side, and also the existence of a quasi neutral region underneath (and including) the opposite side. If an electric charge is injected into this layer, it will distribute through it. The charge distribution will be constant in the neutral region and equal to the intrinsic free charge carriers concentration $n_{i,GaN}$. Outside the neutral (field free) region, the free electron concentration continuously increases to reach its maximum value at the surface on which the electric field is applied. This charge distribution occurs at steady state condition; when charge diffusion and drift currents cancel each other out, resulting in a zero value net current.

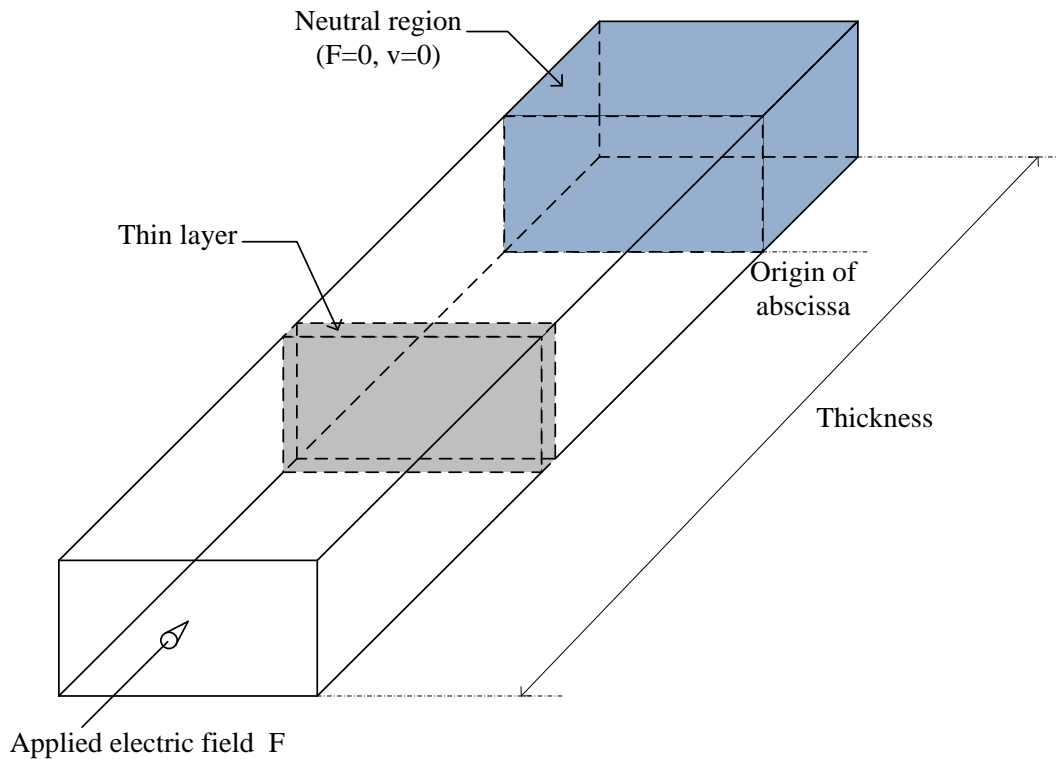


Figure 4-2: Charge distribution through a hypothetical i-GaN rectangular cuboid

For any value n of the free electron concentration, bigger than the intrinsic value, there exists a location, precisely a plane, where the free electron concentration gets this value n . The injected charge will determine the upper bound value that the free electron concentration will reach.

It will be proven shortly after that, for any value of the free electron concentration n , bigger than the intrinsic value, there is a thin region of known thickness where the average concentration, calculated over its thickness, gets the value n (see figure 4-2).

If the i-GaN channel is assimilated to this thin region, then the problem of finding the free electron concentration, the electric field, and the potential drop profiles at any point inside the channel is resolved by localizing this thin region in the i-GaN rectangular cuboid.

4.3 Mathematical formulation

Figure 4-3 illustrates a 1-D representation of the distribution of the injected charge in the i-GaN rectangular cuboid. Application of (1-D) Poisson equation to the i-GaN rectangular cuboid leads to the following initial conditions problem [30]

$$\begin{cases} \frac{d^2 v}{dx^2} = \frac{qn_{GaN}}{\epsilon_0 \epsilon_{GaN}} \\ \frac{dv}{dx}(0) = 0 \\ v(0) = 0 \end{cases} ,$$

where the free electron concentration n_{GaN} at any point x is related to the value of the potential drop $v(x)$ at that point by the relation

$$n(v) = n_{i,GaN} \exp\left(\frac{v}{u_T}\right)$$

$n_{i,GaN}$ is the intrinsic free carrier concentration of GaN, and u_T is the thermal voltage.

The solution for this initial condition problem is given as follows:

$$\begin{cases} v(x) = u_T \ln \left[\sec^2 \left(\frac{x}{L_D \sqrt{2}} \right) \right] \\ x \in \left[0, L_D \frac{\pi}{2} \sqrt{2} \right] \end{cases} ,$$

The Debye length for intrinsic GaN is denoted as L_D . It is expressed by the relation

$$L_D = \left(\frac{\epsilon_0 \epsilon_{GaN} u_T}{qn_{i,GaN}} \right)^{1/2}$$

$L_D \cong 2.46 * 10^7 \text{ cm}$ at room temperature

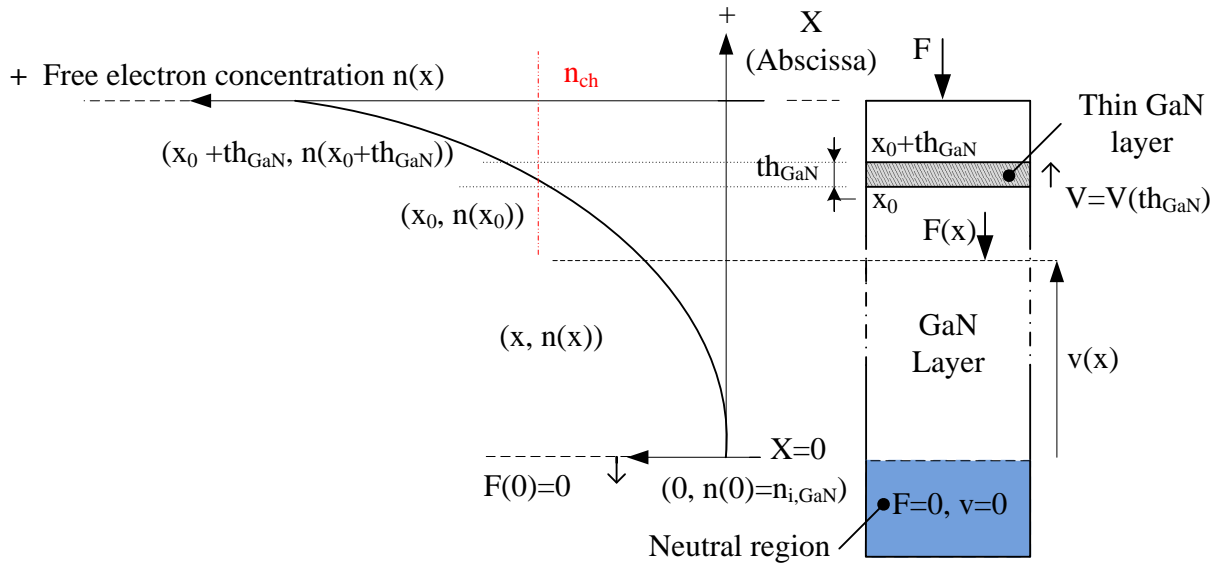


Figure 4-3: One (1-D) dimension illustration of the charge distribution through an i-GaN hypothetical rectangular cuboid

The free electron concentration $n(x)$ at a point x is

$$\begin{cases} n(x) = n_{i,GaN} \sec^2\left(\frac{x}{L_D\sqrt{2}}\right) \\ x \in \left[0, L_D \frac{\pi}{2}\sqrt{2}\right[\end{cases} \quad (4-1)$$

If we consider an infinite electric charge injected in a hypothetical i-GaN rectangular cuboid whose thickness can be made as close as needed to $(\frac{\pi}{2}\sqrt{2})L_D$, the free electron concentration $n(x)$ gets all values of the interval $[n_{i,GaN}, +\infty[$. In other words, for any given value n_{ch} of the concentration, there is a plane located at abscissa $x_0 \in \left[0, L_D \frac{\pi}{2}\sqrt{2}\right[$ where

$$n(x_0) = n_{ch}$$

This plane is unique because the free electron concentration n is expressed by a bijective function of the variable x (see equation 4-1). The intervals $\left[0, L_D \frac{\pi}{2}\sqrt{2}\right[$ and $[n_{i,GaN}, +\infty[$ are the domain of definition and the image set of the function n .

Let us consider the following bijective function N of variable x and parameter th_{GaN} defined as

$$\left\{ \begin{array}{l} N(x, th_{GaN}) = \frac{1}{th_{GaN}} \int_x^{x+th_{GaN}} n(w)dw \\ x \in \left[0, L_D \frac{\pi}{2} \sqrt{2} \right], th_{GaN} > 0, \text{ and } (x + th_{GaN}) \in \left[0, L_D \frac{\pi}{2} \sqrt{2} \right] \end{array} \right.$$

The value of N represents the free electron concentration average value calculated over a layer of thickness th_{GaN} . This thin layer is located at a point x inside the i-GaN rectangular cuboid. We can look at the i-GaN thin layer, of thickness th_{GaN} , that contains an electric charge of electron origin whose average concentration is equal to $\overline{n_{ch}}$, as a slice of thickness th_{GaN} taken from the i-GaN rectangular cuboid. Function N locates this slice. Calculating the integral in the expression of N results in to the following expression,

$$\left\{ \begin{array}{l} N(x, th_{GaN}) = \frac{n_{i,GaN} L_D \sqrt{2}}{th_{GaN}} \left[\tan \left(\frac{x + th_{GaN}}{L_D \sqrt{2}} \right) - \tan \left(\frac{x}{L_D \sqrt{2}} \right) \right] \\ x \in \left[0, L_D \frac{\pi}{2} \sqrt{2} \right], th_{GaN} > 0, \text{ and } (x + th_{GaN}) \in \left[0, L_D \frac{\pi}{2} \sqrt{2} \right] \end{array} \right.$$

For all values of $(\overline{n_{ch}}, th_{GaN})$ that satisfy the following condition;

$$\overline{n_{ch}} > \frac{n_{i,GaN} L_D \sqrt{2}}{th_{GaN}} \frac{2 \left(-1 + \sqrt{1 + \tan^2 \left(\frac{th_{GaN}}{L_D \sqrt{2}} \right)} \right)}{\tan \left(\frac{th_{GaN}}{L_D \sqrt{2}} \right)} \quad (4-2)$$

Equation $N(x_0, th_{GaN}) = \overline{n_{ch}}$ has a unique solution x_0 , it is given by the following expression

$$\left\{ \begin{array}{l} x_0 = L_D \sqrt{2} \cdot \arctan \left(-\frac{a}{2} + \frac{1}{2} \cotan \left(\frac{th_{GaN}}{L_D \sqrt{2}} \right) \cdot \Delta^{1/2} \right) \\ \text{where } a = \frac{\overline{n_{ch}} th_{GaN}}{n_{i,GaN} L_D \sqrt{2}}, \\ \text{and } \Delta = a^2 \tan^2 \left(\frac{th_{GaN}}{L_D \sqrt{2}} \right) + 4a \cdot \tan \left(\frac{th_{GaN}}{L_D \sqrt{2}} \right) - 4 \tan^2 \left(\frac{th_{GaN}}{L_D \sqrt{2}} \right) \end{array} \right.$$

In the case of an i-GaN thin layer, the condition given in equality 4-2 can be expressed as

$$\overline{n_{ch}} > n_{i,GaN}$$

Appendix A contains a demonstration of the condition 4-2

The initial value (and the lowest value) n_0 of free electron concentration on one side of our i-GaN thin layer is given as

$$n_0 = n(x_0) = n_{i,GaN} \left[\frac{a^2}{2} + \frac{1}{2} \left(1 - \frac{1}{2} \Delta^{1/2} \right) \cotan \left(\frac{th_{GaN}}{L_D \sqrt{2}} \right) \right] \quad (4-3)$$

The final value n_1 (and the highest value) of free electron concentration at the opposite side;

$n_1 = n(x_0 + th_{GaN})$, has the following expression,

$$n_1 = n_{i,GaN} \sec^2 \left\{ \arctan \left[-\frac{a}{2} + \frac{1}{2} \cotan \left(\frac{th_{GaN}}{L_D \sqrt{2}} \right) \Delta^{1/2} \right] + \frac{th_{GaN}}{L_D \sqrt{2}} \right\} \quad (4-4)$$

To see how the free electron concentration evolves across the layer thickness th_{GaN} , the normalized abscissa λ is used, it is defined as;

$$\left\{ \begin{array}{l} \lambda = \frac{x - x_0}{th_{GaN}} \\ \text{where } x \in [x_0, x_0 + th_{GaN}], \\ \text{so } \lambda \in [0, 1] \end{array} \right.$$

The free electron concentration n at any point $x \in [x_0, x_0 + th_{GaN}]$, which corresponds to a unique value of $\lambda = \frac{x - x_0}{th_{GaN}}$, is given by the following expression;

$$\left\{ \begin{array}{l} n(\lambda, \overline{n_{ch}}, th_{GaN}) = n_{i,GaN} \sec^2 \left\{ \arctan \left[-\frac{a}{2} + \frac{1}{2} \cotan \left(\frac{th_{GaN}}{L_D \sqrt{2}} \right) \Delta^{1/2} \right] + \lambda \frac{th_{GaN}}{L_D \sqrt{2}} \right\} \\ \text{where } \lambda \in [0, 1] \end{array} \right. \quad (4-5)$$

Notice that $n(0, \overline{n_{ch}}, th_{GaN}) = n_0$, and $n(1, \overline{n_{ch}}, th_{GaN}) = n_1$.

The voltage drop at any point λ is defined as;

$$\left\{ \begin{array}{l} v(\lambda, \overline{n_{ch}}, th_{GaN}) = v(x_0 + \lambda th_{GaN}) - v(x_0) \\ \text{where } \lambda \in [0, 1] \end{array} \right.$$

It is given by the following expression;

$$\left\{ v = u_T \ln \left\{ \frac{\sec^2 \left\{ \arctan \left[-\frac{a}{2} + \frac{1}{2} \cotan \left(\frac{th_{GaN}}{L_D \sqrt{2}} \right) \Delta^{1/2} \right] + \lambda \frac{th_{GaN}}{L_D \sqrt{2}} \right\}}{\frac{a^2}{2} + a \left(1 - \frac{1}{2} \Delta^{1/2} \right) \cotan \left(\frac{th_{GaN}}{L_D \sqrt{2}} \right)} \right\} \right. \quad (4-6)$$

where $\lambda \in [0,1]$

The voltage drop value across the thin i-GaN layer is obtained from equation 4-6 for $\lambda = 1$

$$V = u_T \ln \left\{ \frac{\sec^2 \left\{ \arctan \left[-\frac{a}{2} + \frac{1}{2} \cotan \left(\frac{th_{GaN}}{L_D \sqrt{2}} \right) \Delta^{1/2} \right] + \frac{th_{GaN}}{L_D \sqrt{2}} \right\}}{\frac{a^2}{2} + a \left(1 - \frac{1}{2} \Delta^{1/2} \right) \cotan \left(\frac{th_{GaN}}{L_D \sqrt{2}} \right)} \right\} \quad (4-7)$$

The electric field intensity F at any point λ is expressed as;

$$\left\{ F(\lambda, \overline{n_{ch}}, th_{GaN}) = \frac{1}{th_{GaN}} \frac{\partial v(\lambda, \overline{n_{ch}}, th_{GaN})}{\partial \lambda}, \right.$$

where $\lambda \in [0,1]$

and it is given by

$$\left\{ F(\lambda, \overline{n_{ch}}, th_{GaN}) = \frac{u_T \sqrt{2}}{L_D} \tan \left\{ \arctan \left[-\frac{a}{2} + \frac{1}{2} \cotan \left(\frac{th_{GaN}}{L_D \sqrt{2}} \right) \Delta^{1/2} \right] + \lambda \frac{th_{GaN}}{L_D \sqrt{2}} \right\} \right. \quad (4-8)$$

where $\lambda \in [0,1]$

Electric field initial and final values F_0 and F_1 respectively at both sides of the i-GaN layer are;

$$F_0 = F(0, \overline{n_{ch}}, th_{GaN}) = \frac{u_T \sqrt{2}}{L_D} \left[-\frac{a}{2} + \frac{1}{2} \cotan \left(\frac{th_{GaN}}{L_D \sqrt{2}} \right) \Delta^{1/2} \right] \quad (4-9)$$

$$F_1 = F(1, \overline{n_{ch}}, th_{GaN}) = \frac{u_T \sqrt{2}}{L_D} \tan \left\{ \arctan \left[-\frac{a}{2} + \frac{1}{2} \cotan \left(\frac{th_{GaN}}{L_D \sqrt{2}} \right) \Delta^{1/2} \right] + \frac{th_{GaN}}{L_D \sqrt{2}} \right\} \quad (4-10)$$

For any given values of the average concentration and the i-GaN layer thickness $(\overline{n_{ch}}, th_{GaN})$ that satisfy condition 4-2, the proposed channel model, for injected charges in an i-GaN thin layer, allows computation of the free electron concentration distribution (equation 4-5), the potential drop and (equation 4-6) and the electric field at any point λ (equation 4-8).

Initial and final values of the free electron concentration are given by equations 4-3 and 4-4 respectively. Those of the electric field are given by equations 4-9 and 4-10 respectively. Finally, the voltage drop across the i-GaN thin layer is given by Equation 4-7. Figure 4-4 represents the solution algorithm for the present i-GaN channel model.

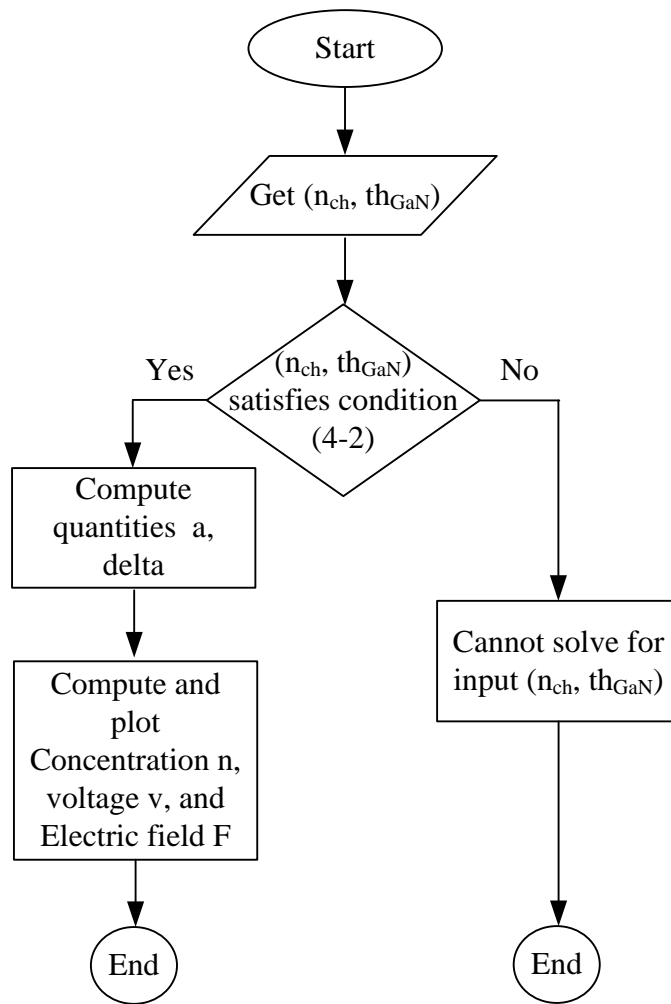


Figure 4-4: Solution algorithm of the proposed channel model

4.4 Domain of validity

The effective room temperature density of states for the conduction band in intrinsic GaN material has a value of $1.2 \cdot 10^{18} \text{ cm}^{-3}$ for the Zincblend crystal structure and $2.3 \cdot 10^{18} \text{ cm}^{-3}$ for the Wurtzite crystal structure [31][32]. These values set the upper bound limit of the free electron concentration as it is described using Boltzmann statistics. The present model is not valid for concentration values of the same order as that of the density of state for the conduction band where GaN becomes degenerate. Points $((\bar{n}_{ch})_{max}, th_{GaN})$ of the frontier of the domain of validity satisfy the following equation,

$$n(1, (\bar{n}_{ch})_{max}, th_{GaN}) = N_c ,$$

where N_c is the density of states for the conduction band in intrinsic GaN. These values can be determined by solving the previous equation. The maximum value of the average concentration of free electrons at which the model is still valid is given as,

$$(\bar{n}_{ch})_{max} = n_{i,GaN} \frac{L_D \sqrt{2}}{th_{GaN}} \frac{\tan\left(\frac{th_{GaN}}{L_D \sqrt{2}}\right) \left\{ 1 + \tan^2 \left[\arctan\left(\frac{N_c}{n_{i,GaN}} - 1\right)^{1/2} + \frac{th_{GaN}}{L_D \sqrt{2}} \right] \right\}}{1 + \tan\left(\frac{th_{GaN}}{L_D \sqrt{2}}\right) \tan \left[\arctan\left(\frac{N_c}{n_{i,GaN}} - 1\right)^{1/2} + \frac{th_{GaN}}{L_D \sqrt{2}} \right]}$$

$$(4-11)$$

For the case of a thin i-GaN layer, equation 4-11 can be simplified using the following approximations,

$$\left\{ \begin{array}{l} \tan\left(\frac{th_{GaN}}{L_D \sqrt{2}}\right) \sim \frac{th_{GaN}}{L_D \sqrt{2}} \\ \frac{N_c}{n_{i,GaN}} - 1 \sim \frac{N_c}{n_{i,GaN}} \\ \arctan\left(\frac{N_c}{n_{i,GaN}} - 1\right)^{1/2} + \frac{th_{GaN}}{L_D \sqrt{2}} \sim \arctan\left(\frac{N_c}{n_{i,GaN}} - 1\right)^{1/2} \end{array} \right.$$

Equation 4-11 can be put in a simpler form

$$(\overline{n_{ch}})_{max} = \frac{N_c}{1 + \left(\frac{th_{GaN}}{L_D\sqrt{2}}\right) \left(\frac{N_c}{n_{i,GaN}}\right)^{1/2}} \quad (4-12)$$

Expression 4-12 can be used to get a quick estimation of the value of $(\overline{n_{ch}})_{max}$. Figure 4-5 shows the domain of validity for the current model. Both values of the effective density of states are considered (both zincblend and wurtzite) for an i-GaN layer thickness range of [25nm, 125nm].

As the i-GaN layer thickness increases, the charge distribution gets steeper, in other words, the charge distribution span, above and below the average value, increases. For this reason, $(\overline{n_{ch}})_{ave}$ has to decrease to keep all values within the domain of validity. Figure 4-5 and table 4-1 confirm the effect of increasing the i-GaN layer thickness on the maximum average concentration value allowed to maintain the i-GaN material in a non degenerate state. For instance, for the case of 50nm thickness, the maximum average concentration allowed is $1.4886 \times 10^{17} \text{ cm}^{-3}$ for i-GaN Wurtzite crystal structure and $1.0498 \times 10^{17} \text{ cm}^{-3}$ for i-GaN Zinc Blend crystal structure.

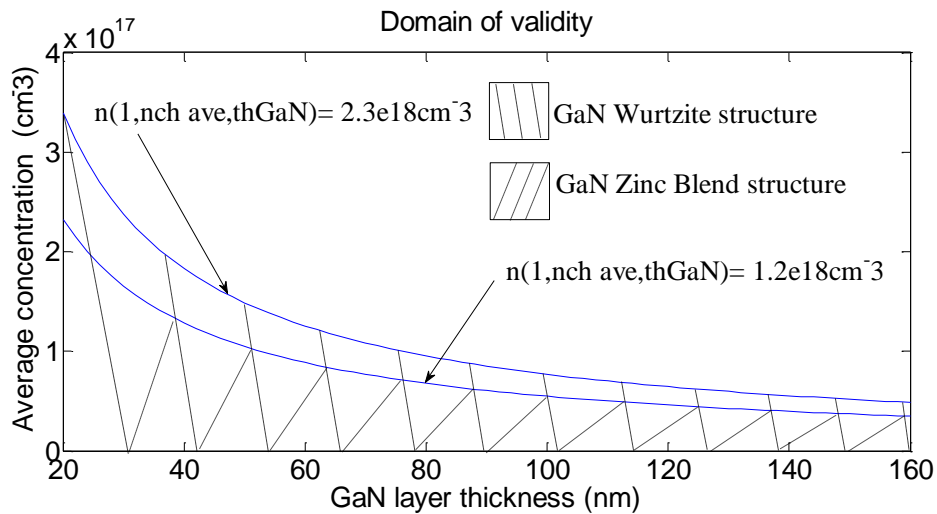


Figure 4-5: Domain of validity of the proposed channel model for any i-GaN layer thickness value in the range 20nm-160nm

Table 4-1: Maximum values of average concentrations for i-GaN layer thicknesses in the range 20nm-160nm

$th_{GaN}(nm)$	$(\overline{n_{ch}})_{max}$ (cm ⁻³) (GaN Wurtzite structure)	$(\overline{n_{ch}})_{max}$ (cm ⁻³) (GaN Zinc Blend crystal structure)
20	3.3957E+17	2.3235E+17
25	2.7982E+17	1.9327E+17
30	2.3795E+17	1.6544E+17
35	2.0698E+17	1.4462E+17
40	1.8314E+17	1.2845E+17
45	1.6423E+17	1.1554E+17
50	1.4886E+17	1.0498E+17
55	1.3612E+17	9.6193E+16
60	1.2538E+17	8.8762E+16
65	1.1622E+17	8.2397E+16
70	1.0830E+17	7.6884E+16
75	1.0140E+17	7.2062E+16
80	9.5321E+16	6.7810E+16
85	8.9931E+16	6.4031E+16
90	8.5117E+16	6.0651E+16
95	8.0793E+16	5.7610E+16
100	7.6887E+16	5.4860E+16
105	7.3341E+16	5.2360E+16
110	7.0107E+16	5.0078E+16
115	6.7147E+16	4.7987E+16
120	6.4427E+16	4.6063E+16

Table 4-1(cont'd): Maximum values of average concentrations for i-GaN layer thicknesses in the range 20nm-160nm

$th_{GaN}(nm)$	$(\overline{n_{ch}})_{max}$ (cm ⁻³) (GaN Wurtzite structure)	$(\overline{n_{ch}})_{max}$ (cm ⁻³) (GaN Zinc Blend crystal structure)
125	6.1918E+16	4.4288E+16
130	5.9598E+16	4.2644E+16
135	5.7445E+16	4.1118E+16
140	5.5442E+16	3.9698E+16
145	5.3574E+16	3.8372E+16
150	5.1828E+16	3.7132E+16
155	5.0192E+16	3.5970E+16
160	4.8657E+16	3.4878E+16

4.5 Simulation results and discussion

For a given i-GaN layer thickness, here it is considered that $th_{GaN} = 50nm$ as in [26]. Constants a and Δ can be computed if $\overline{n_{ch}}$ satisfies condition 4-2. Free charge concentration, electric field, and potential drop profiles can be defined. Figures 4-5 to 4-32 represent these three profiles for an average concentration $\overline{n_{ch}} = 10^{-9}$ to 10^{+18} cm⁻³ respectively, with an increment of one order each time. Although free electron concentration values smaller than unity have no physical meaning, they were considered in the simulation to illustrate the validity of the analysis performed. This free electron concentration values range represents all the states on which the i-GaN can be; from highly depleted (insulator) i-GaN material to heavily charged (conductor) i-GaN material. As the average concentration increases, the slice gets closer to the cuboid surface on which the electric field is applied. This fact justifies the increase in the electric field initial value. Figures 4-24 and 4-25 for example show this tendency.

Table 4-2 contains all values F_0 of the electric field. Gauss's law predicts an increase of the electric field final value F_1 as the average value of free electron concentration increases for a fixed i-GaN layer thickness. Final values F_1 in table 4-2 confirm this tendency. The effect of changing the average concentration while maintaining the same i-GaN layer thickness of 50nm is presented in figures 4-33, 4-34, and 4-35. Figure 4-33 shows that the distribution of electrons gets steeper as the average concentration increases. This can be explained as follow; as the average concentration increases, the thin i-GaN layer is identified to a thin slice of same thickness from the cuboid that gets closer to the surface on which the electric field is applied. This leads to an increase in two quantities; first the initial value of the electric field and second the difference between its final and initial values increases (the encapsulated charge is directly proportional to the difference between the electric field final and initial values), a higher electric field initial value pushes away more electrons from the corresponding i-GaN layer side, increasing the charge depletion on this side. On the other side, a stronger accumulation region is created.

To this point, the thickness has been kept constant. The effect of changing this quantity while keeping the average concentration constant is presented in figures 4-36, 4-37, and 4-38. Figure 4-36 shows the concentration distribution for the same average value of 10^{16}cm^{-3} and for different values of i-GaN layer thickness. For a constant value of the average concentration, as the thickness increases, the range of values taken by the concentration above and under the average value increases. This leads to a steeper distribution as shown in Figure 4-36. The potential drop across the thin i-GaN layer increases as it becomes thicker. Finally, the deviation of the electric field from its initial value is shown in Figure 4-39 for inputs $(\overline{n_{ch}}, th_{GaN}) = (10^{-9} \text{ to } 10^{+18} \text{cm}^{-3}, 50 \text{ nm})$, this gives a rough estimation about the range of the average concentration values on which the constant electric field approximation can be applied. For an i-GaN layer thickness of 50nm, the constant field approximation holds for $\overline{n_{ch}}$ values up to 10^{+12}cm^{-3} .

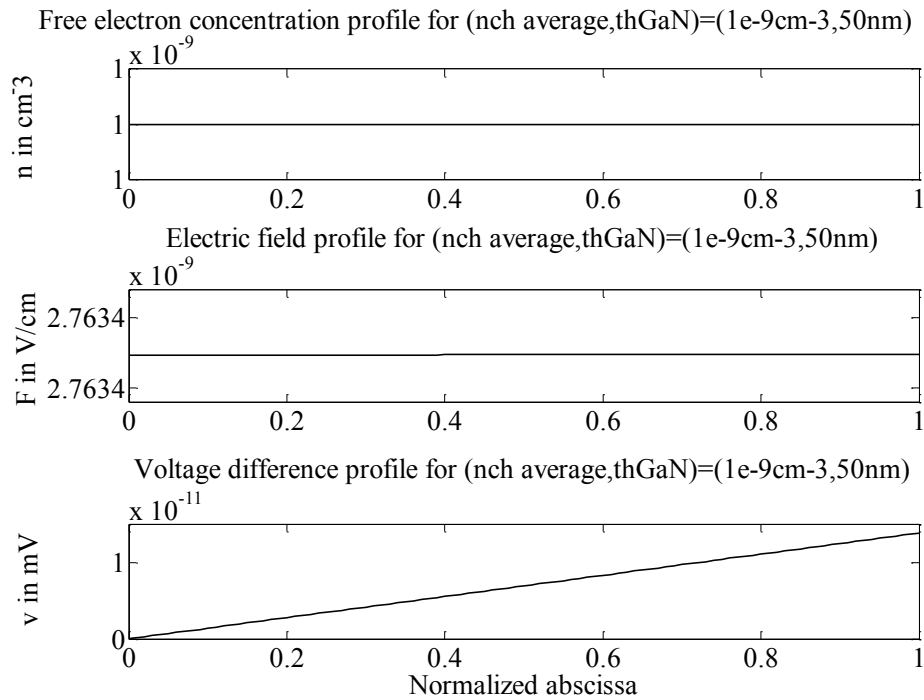


Figure 4-6: Free electron concentration, electric field, and potential drop for $(n_{ch\ ave}, th_{GaN}) = (10^{-9}\text{cm}^{-3}, 50\text{nm})$

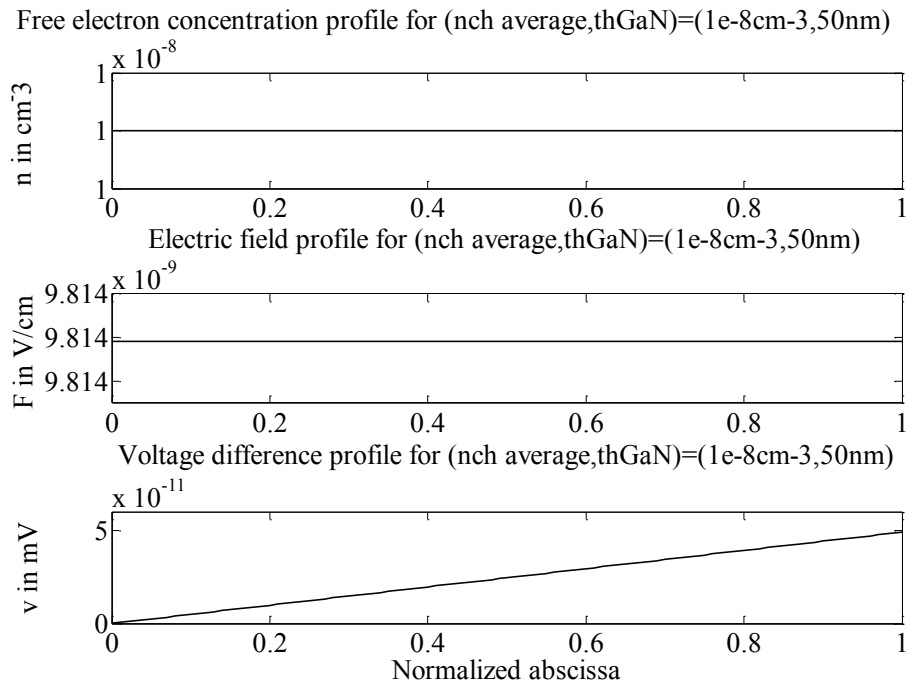


Figure 4-7: Free electron concentration, electric field, and potential drop for $(n_{ch\ ave}, th_{GaN}) = (10^{-8}\text{cm}^{-3}, 50\text{nm})$

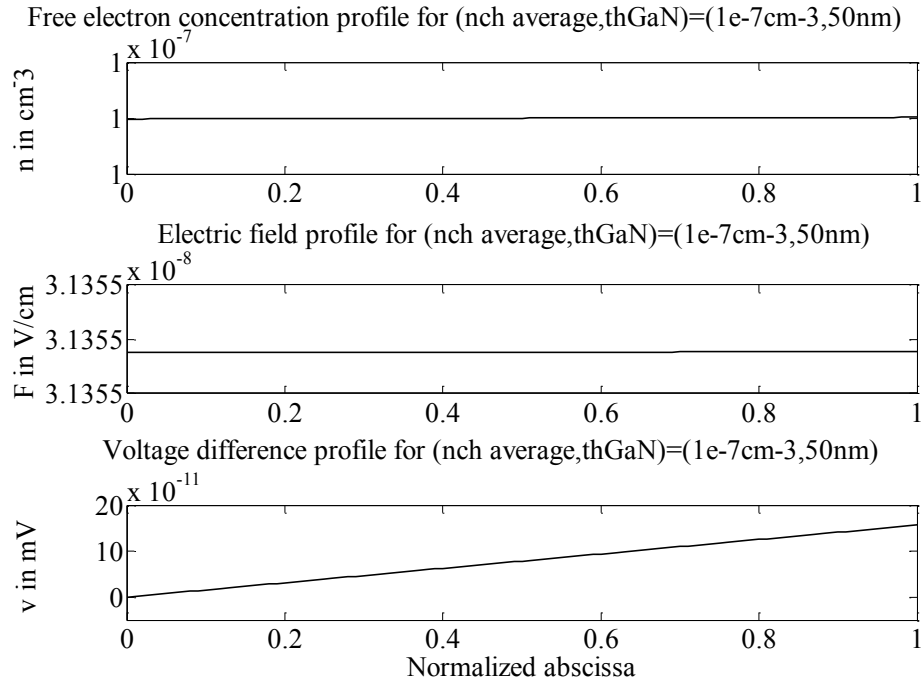


Figure 4-8: Free electron concentration, electric field, and potential drop for $(n_{ch\ ave}, th_{GaN}) = (10^{-7}\text{cm}^{-3}, 50\text{nm})$

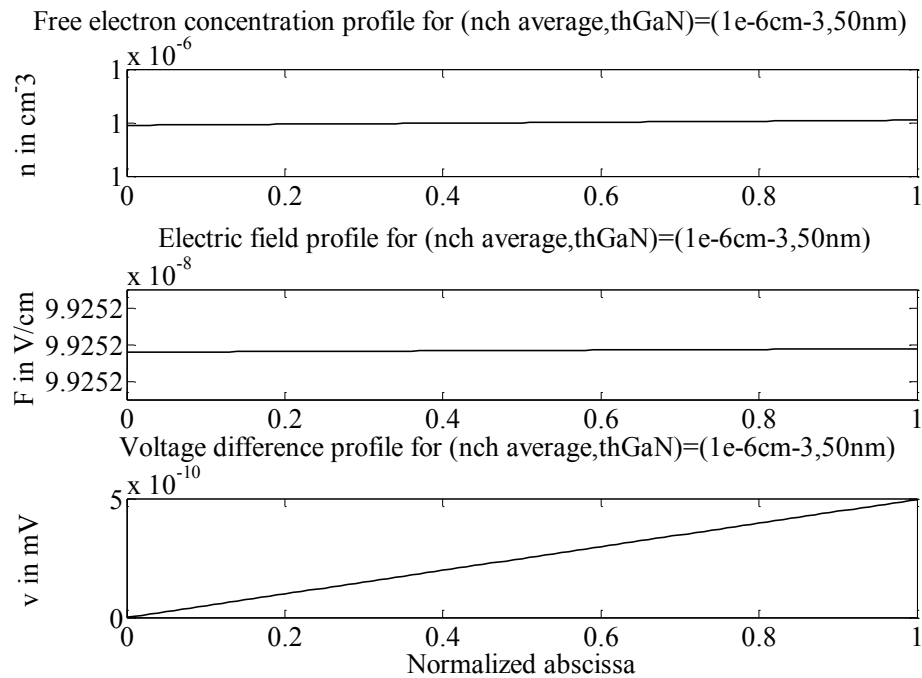


Figure 4-9: Free electron concentration, electric field, and potential drop for $(n_{ch\ ave}, th_{GaN}) = (10^{-6}\text{cm}^{-3}, 50\text{nm})$

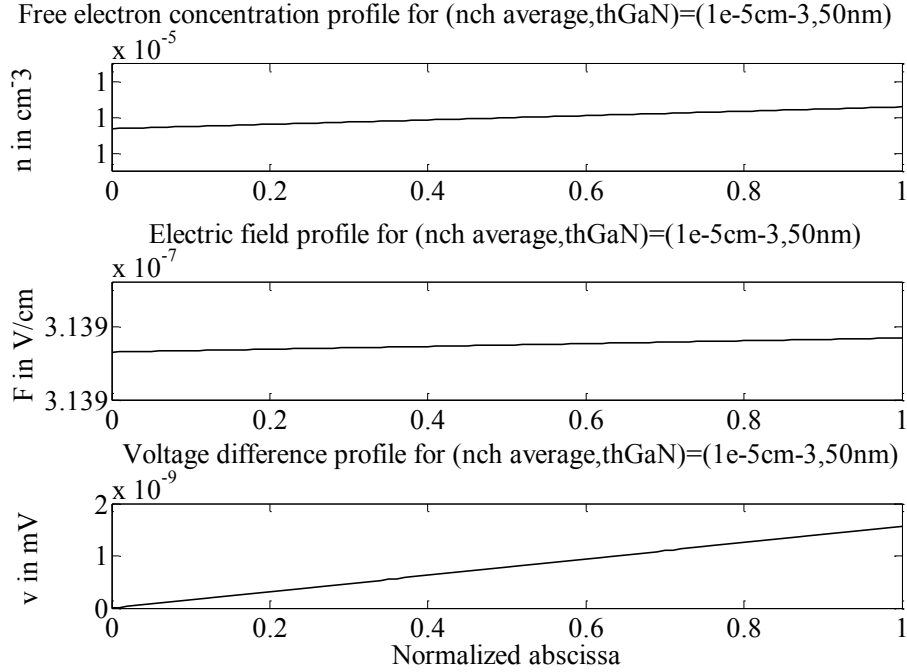


Figure 4-10: Free electron concentration, electric field, and potential drop for $(n_{ch\ ave}, th_{GaN}) = (10^{-5}\text{cm}^{-3}, 50\text{nm})$

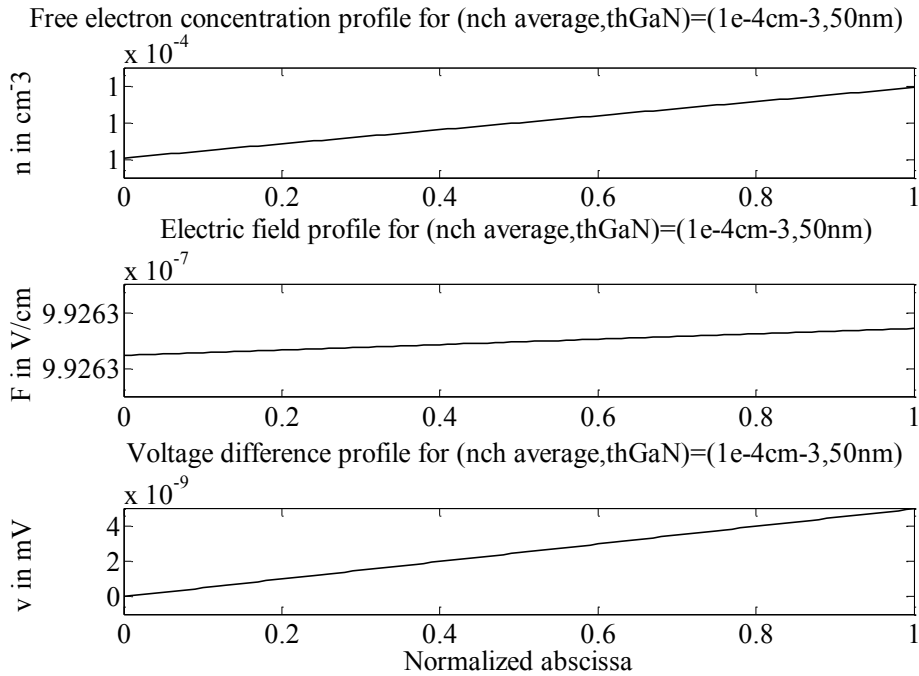


Figure 4-11: Free electron concentration, electric field, and potential drop for $(n_{ch\ ave}, th_{GaN}) = (10^{-4}\text{cm}^{-3}, 50\text{nm})$

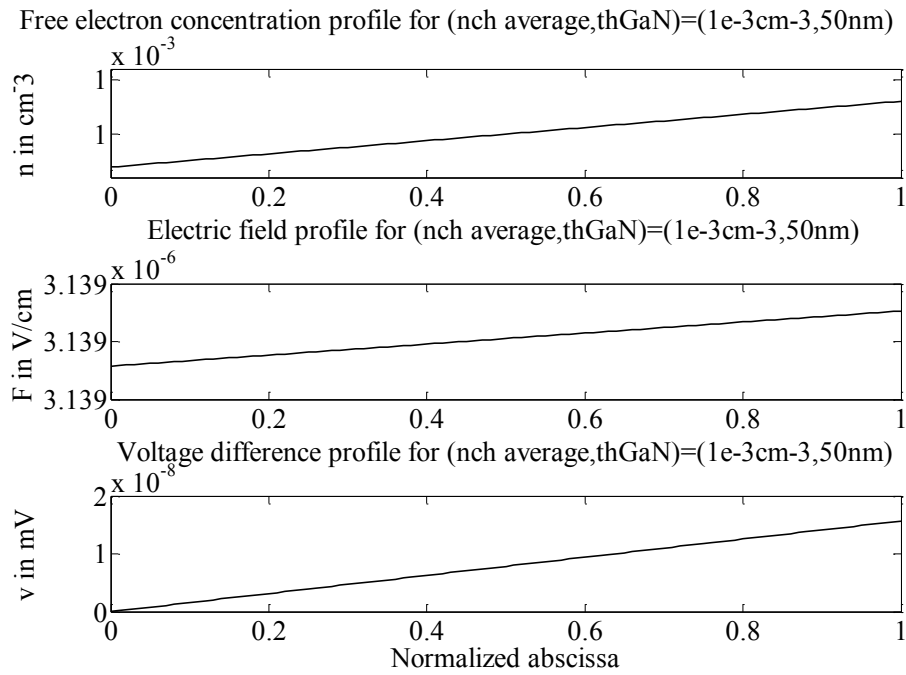


Figure 4-12: Free electron concentration, electric field, and potential drop for $(n_{ch \text{ ave}}, th_{GaN})=(10^{-3} \text{ cm}^{-3}, 50 \text{ nm})$

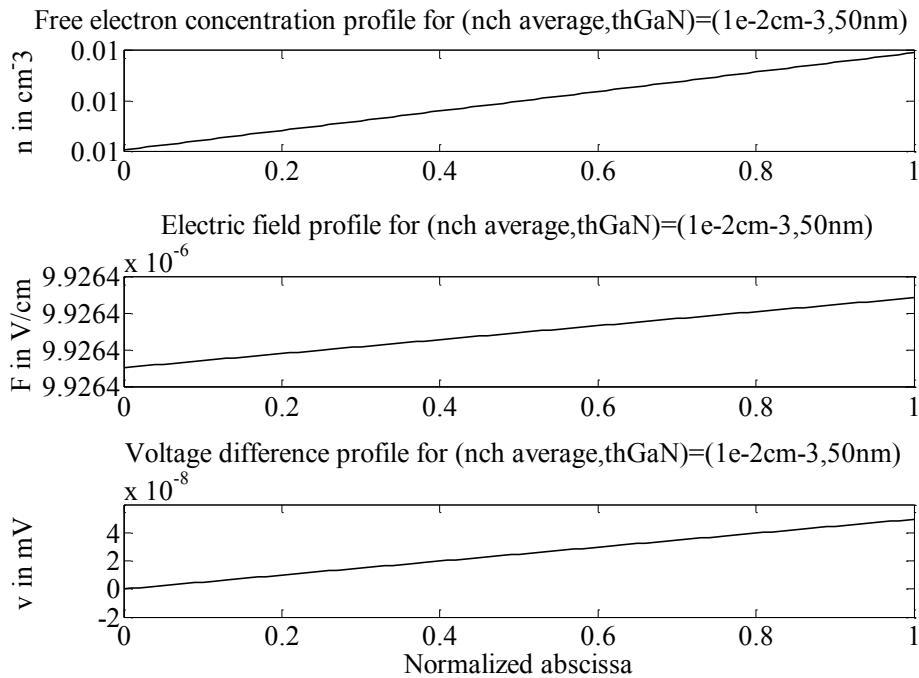


Figure 4-13: Free electron concentration, electric field, and potential drop for $(n_{ch \text{ ave}}, th_{GaN})=(10^{-2} \text{ cm}^{-3}, 50 \text{ nm})$

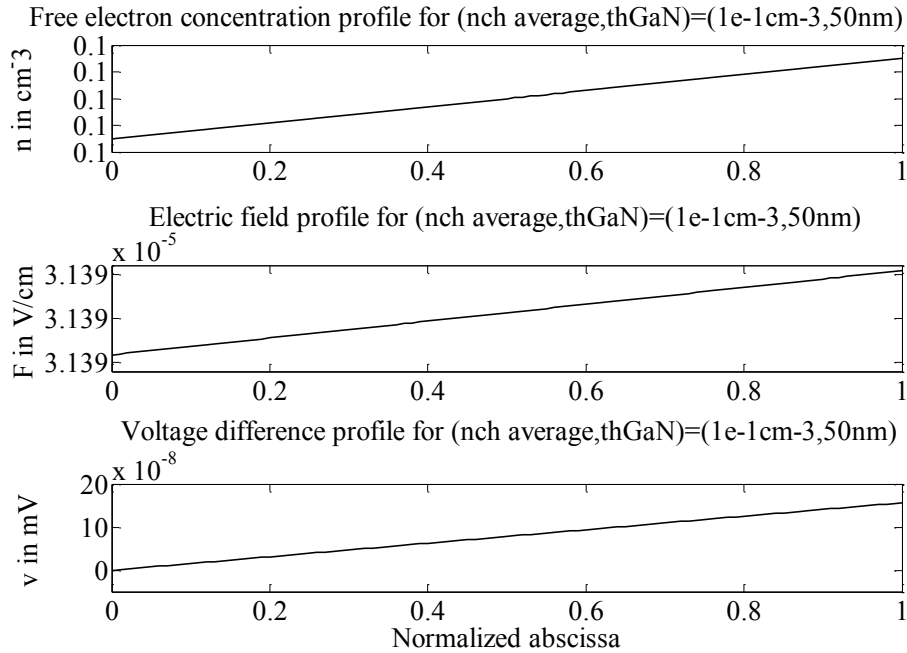


Figure 4-14: Free electron concentration, electric field, and potential drop for $(n_{ch\ ave}, th_{GaN})=(10^{-1}cm^{-3},50nm)$

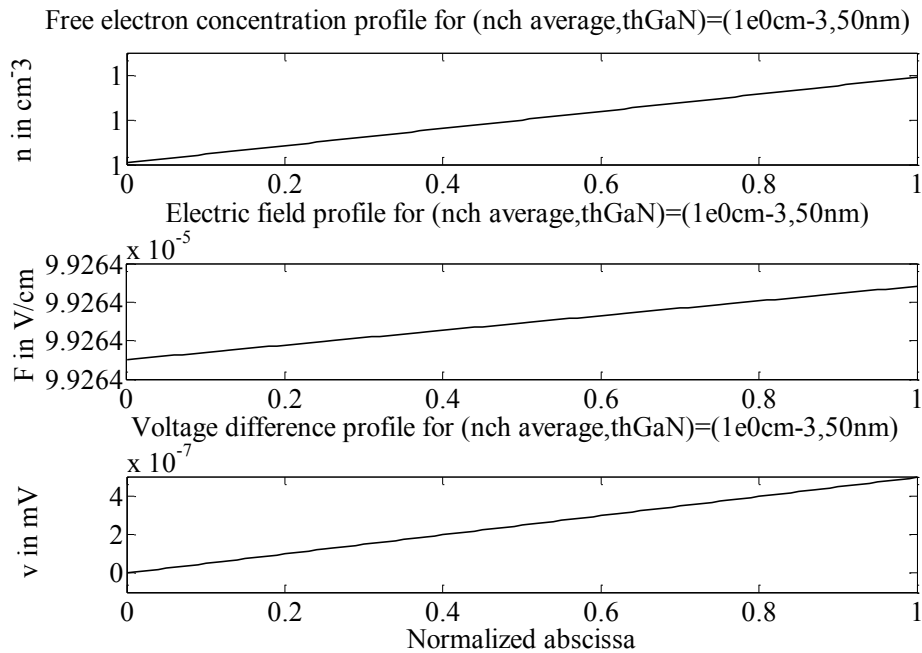


Figure 4-15: Free electron concentration, electric field, and potential drop for $(n_{ch\ ave}, th_{GaN})=(10^0cm^{-3},50nm)$

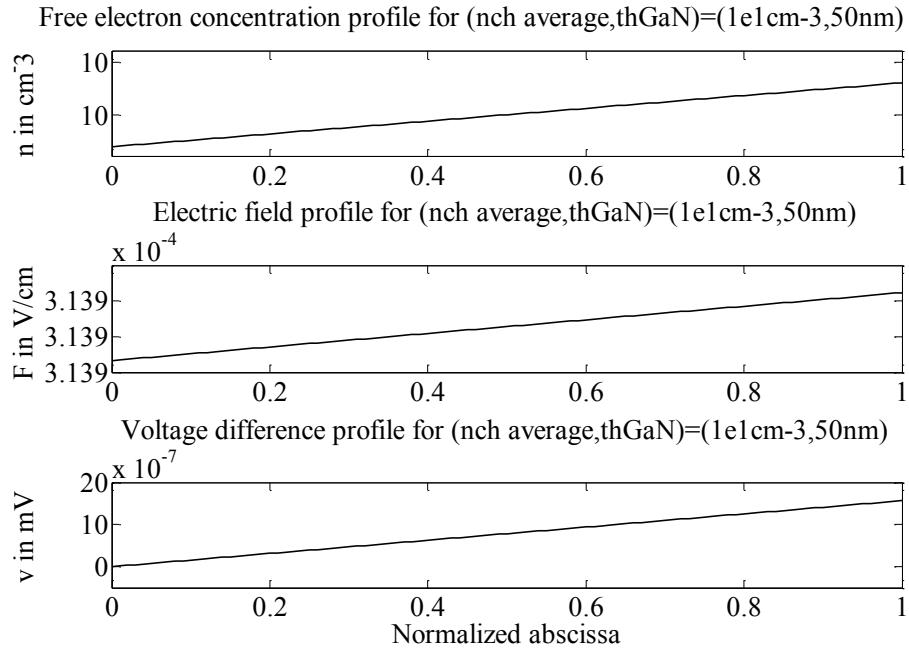


Figure 4-16: Free electron concentration, electric field, and potential drop for $(n_{ch\ ave}, th_{GaN}) = (10^{+1}\ cm^{-3}, 50nm)$

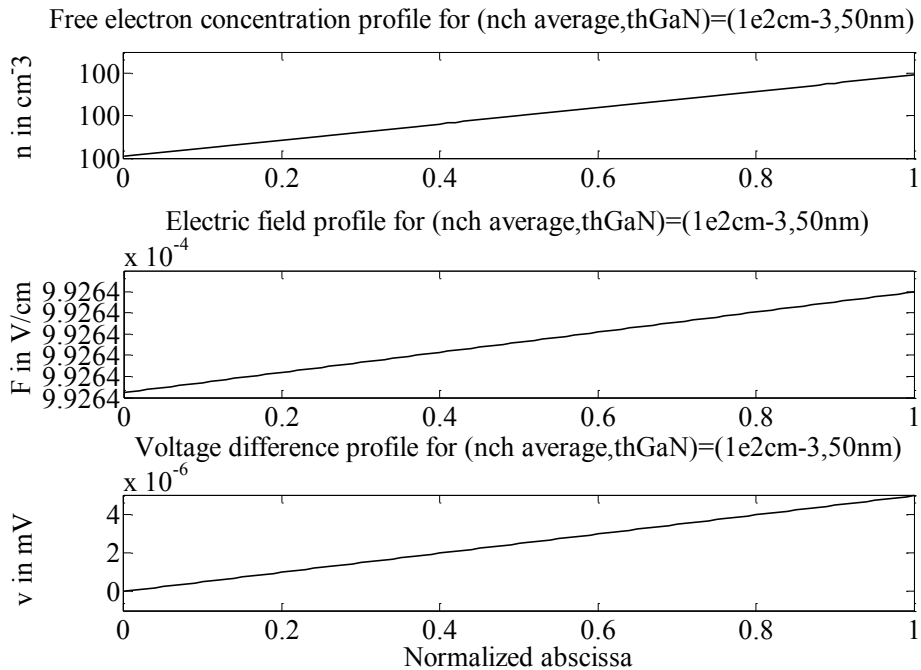


Figure 4-17: Free electron concentration, electric field, and potential drop for $(n_{ch\ ave}, th_{GaN}) = (10^{+2}\ cm^{-3}, 50nm)$

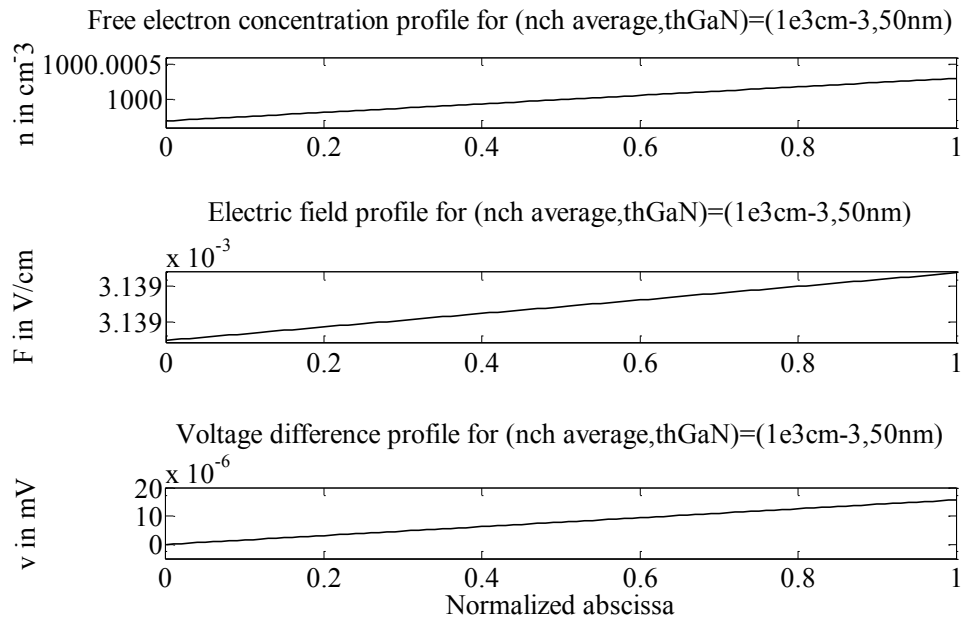


Figure 4-18: Free electron concentration, electric field, and potential drop for $(n_{ch\ ave}, th_{GaN})=(10^{+3}\ cm^{-3}, 50nm)$

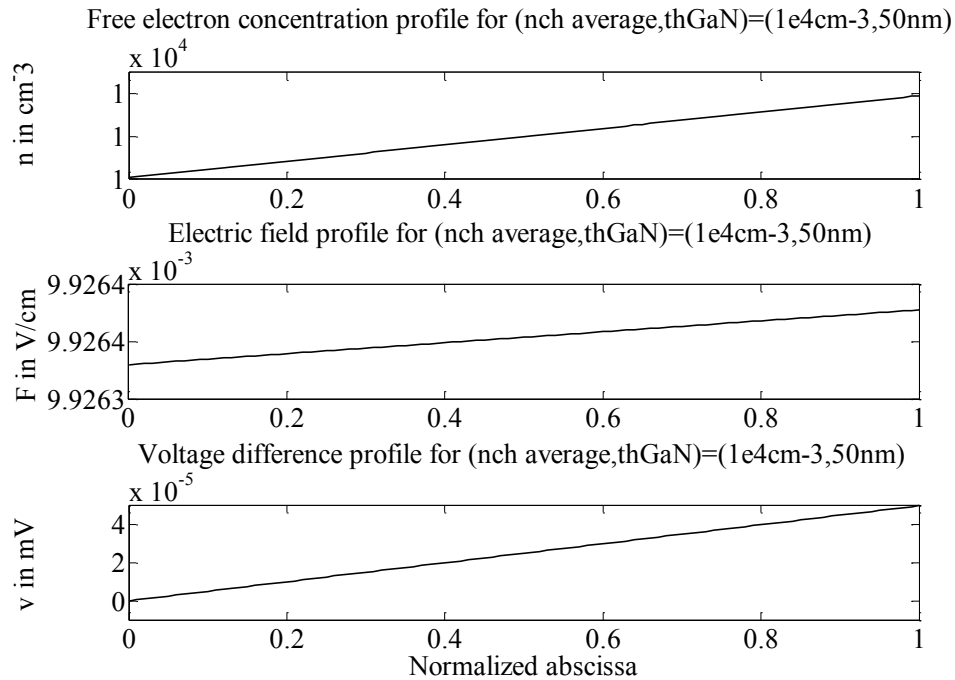


Figure 4-19: Free electron concentration, electric field, and potential drop for $(n_{ch\ ave}, th_{GaN})=(10^{+4}\ cm^{-3}, 50nm)$

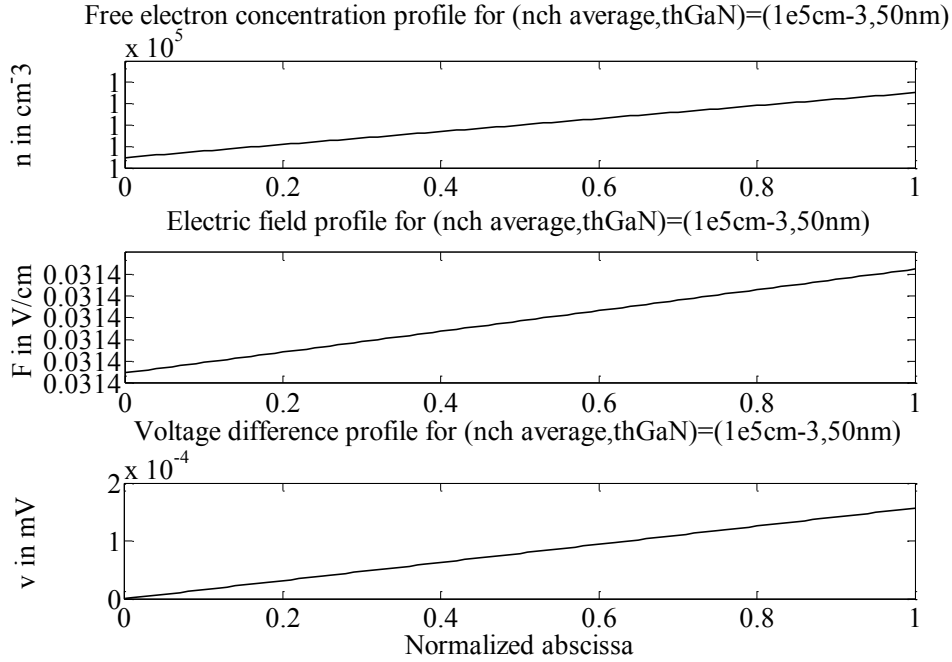


Figure 4-20: Free electron concentration, electric field, and potential drop for $(n_{ch \text{ ave}}, th_{GaN})=(10^{+5} cm^{-3}, 50nm)$

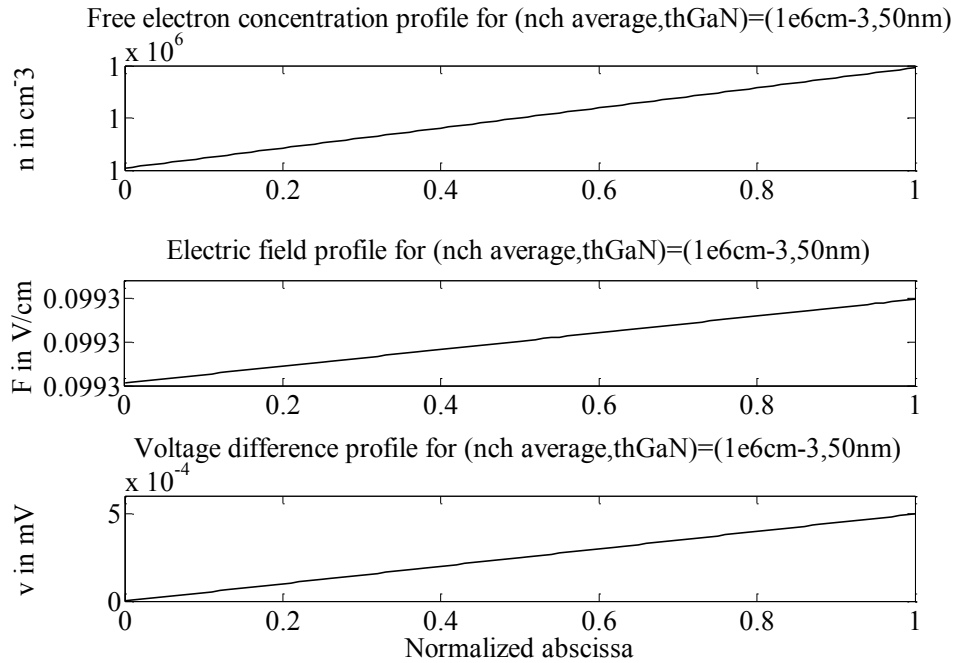


Figure 4-21: Free electron concentration, electric field, and potential drop for $(n_{ch \text{ ave}}, th_{GaN})=(10^{+6} cm^{-3}, 50nm)$

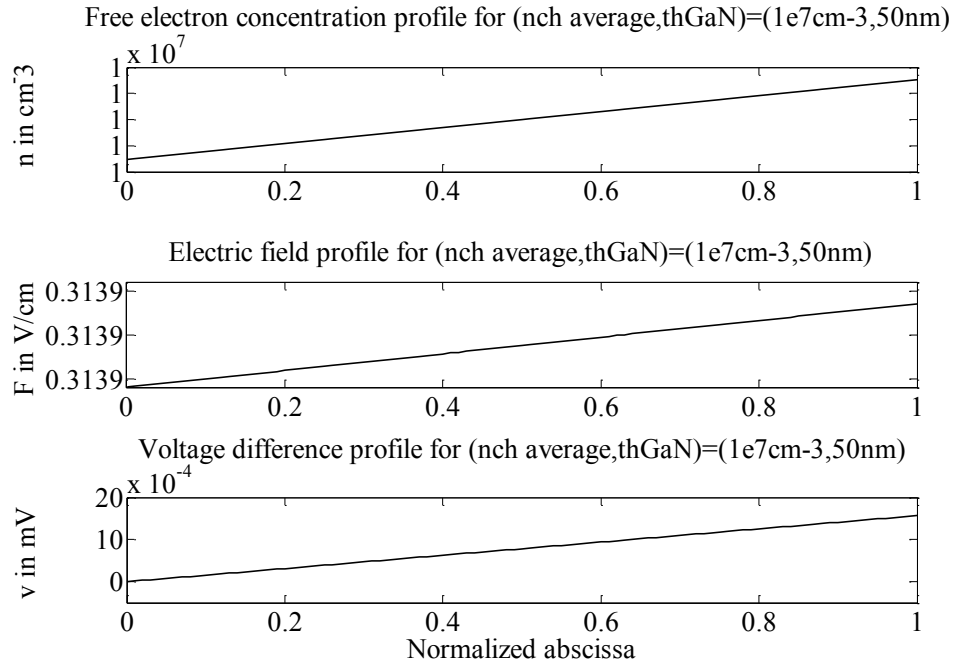


Figure 4-22: Free electron concentration, electric field, and potential drop for $(n_{ch\ ave}, th_{GaN})=(10^{+7} cm^{-3}, 50nm)$

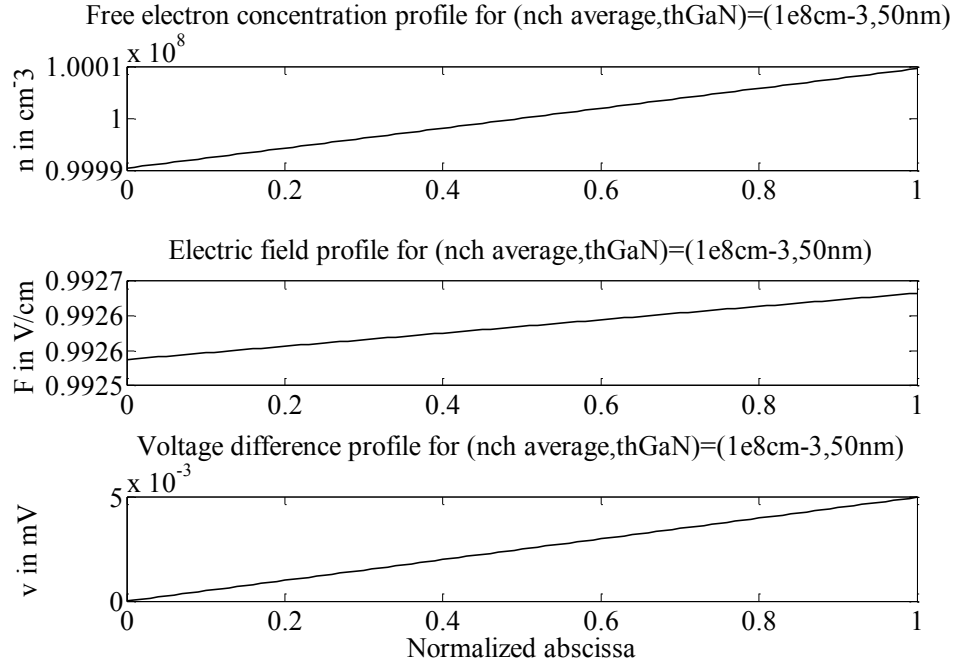


Figure 4-23: Free electron concentration, electric field, and potential drop for $(n_{ch\ ave}, th_{GaN})=(10^{+8} cm^{-3}, 50nm)$

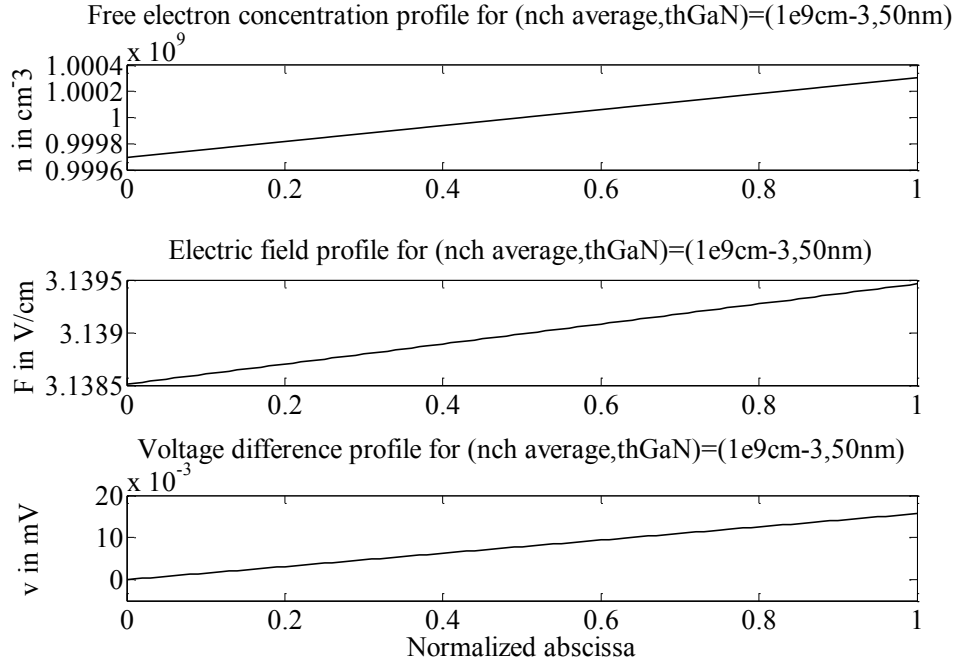


Figure 4-24: Free electron concentration, electric field, and potential drop for $(n_{ch\ ave}, th_{GaN})=(10^{+9} cm^{-3}, 50nm)$

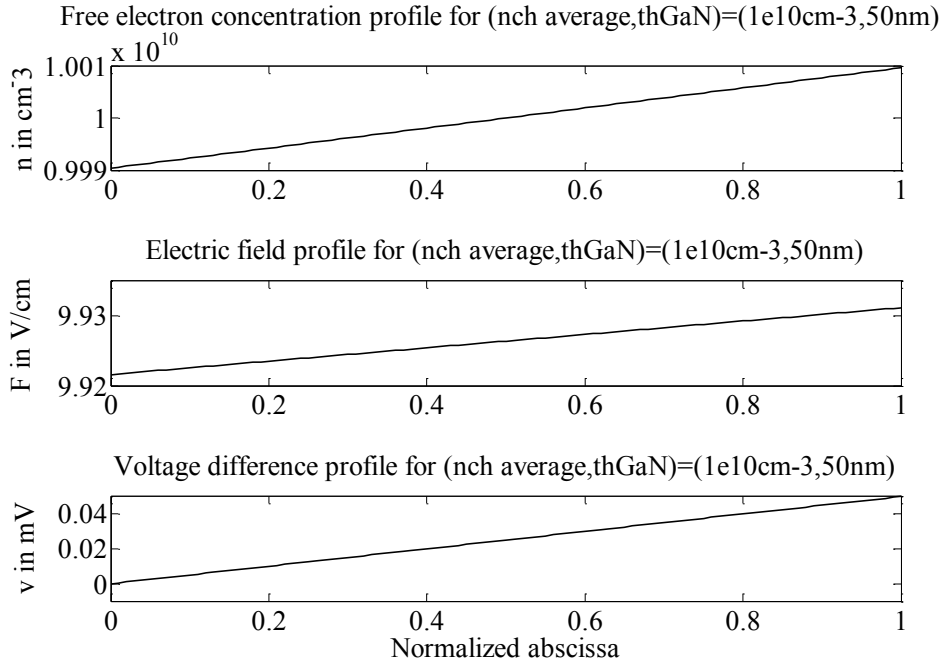


Figure 4-25: Free electron concentration, electric field, and potential drop for $(n_{ch\ ave}, th_{GaN})=(10^{+10} cm^{-3}, 50nm)$

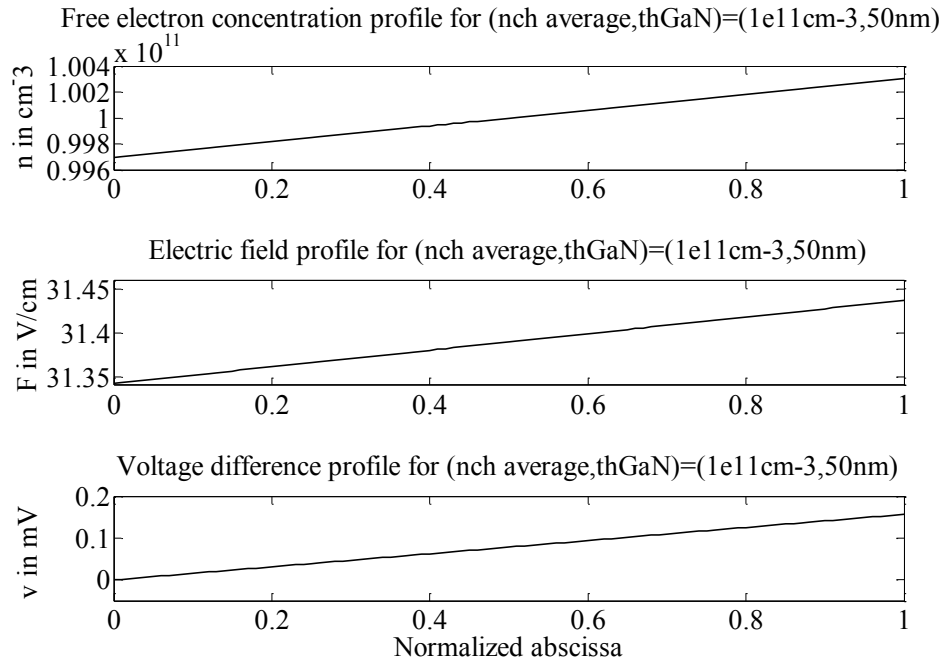


Figure 4-26: Free electron concentration, electric field, and potential drop for $(n_{ch\ ave}, th_{GaN})=(10^{+11}cm^{-3}, 50nm)$

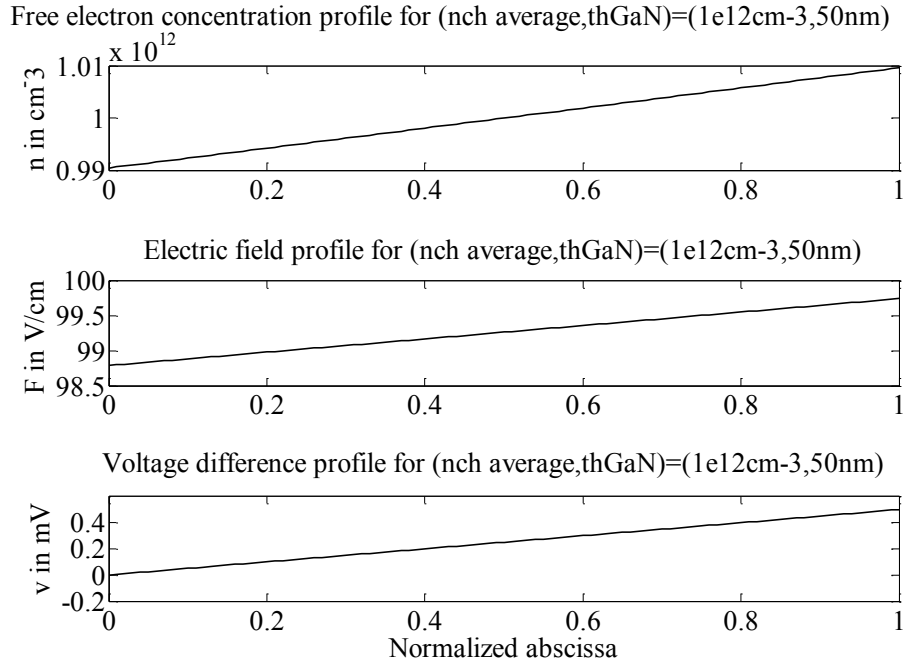


Figure 4-27: Free electron concentration, electric field, and potential drop for $(n_{ch\ ave}, th_{GaN})=(10^{+12}cm^{-3}, 50nm)$

Free electron concentration profile for $(n_{ch\ average}, th_{GaN})=(1e13cm^{-3}, 50nm)$

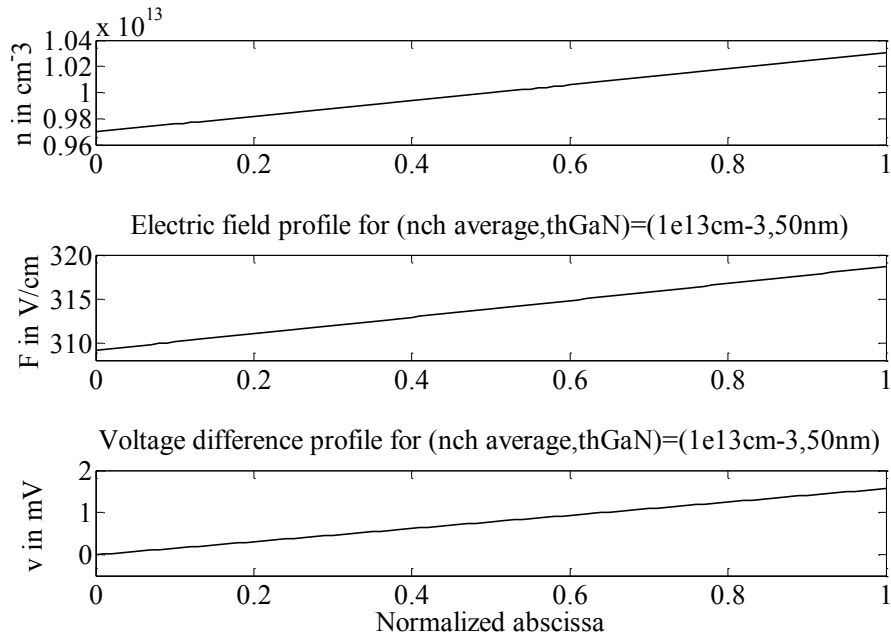


Figure 4-28: Free electron concentration, electric field, and potential drop for $(n_{ch\ ave}, th_{GaN})=(10^{+13}cm^{-3}, 50nm)$

Free electron concentration profile for $(n_{ch\ average}, th_{GaN})=(1e14cm^{-3}, 50nm)$

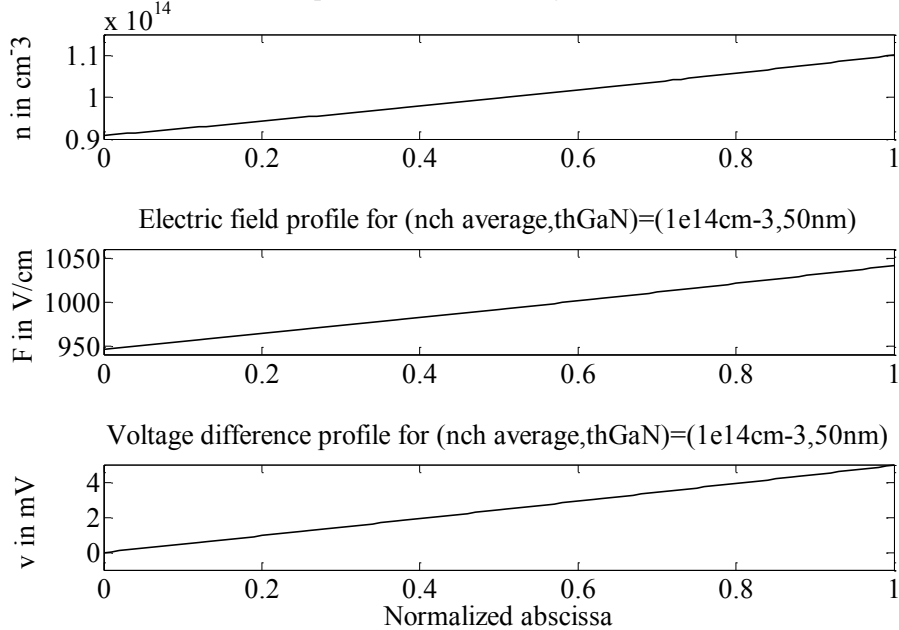


Figure 4-29: Free electron concentration, electric field, and potential drop for $(n_{ch\ ave}, th_{GaN})=(10^{+14}cm^{-3}, 50nm)$

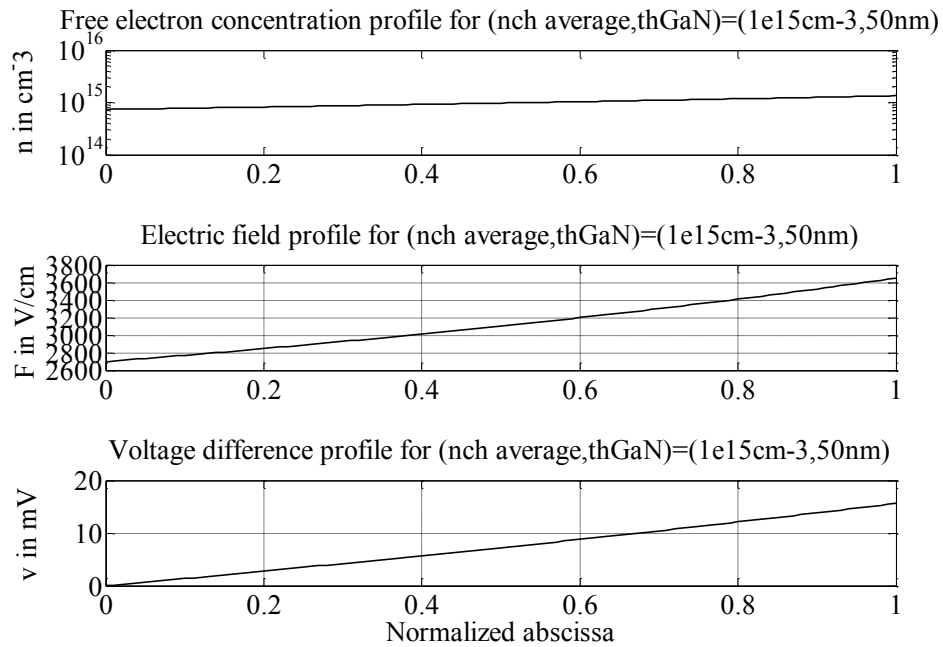


Figure 4-30: Free electron concentration, electric field, and potential drop for $(n_{ch\ ave}, th_{GaN}) = (10^{+15}\ cm^{-3}, 50nm)$

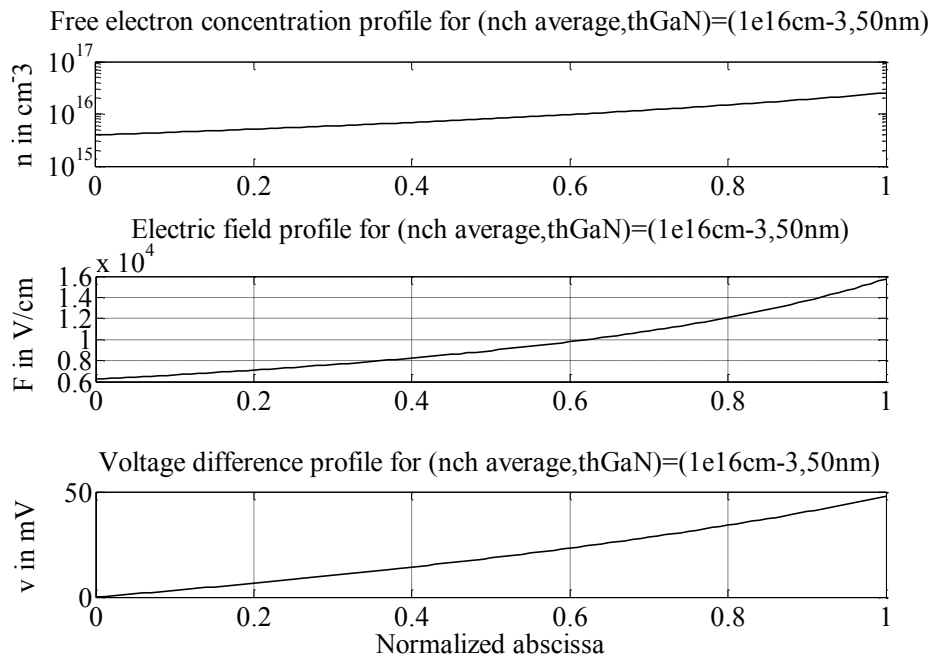


Figure 4-31: Free electrons concentration, electric field, and potential drop for $(n_{ch\ ave}, th_{GaN}) = (10^{+16}\ cm^{-3}, 50nm)$

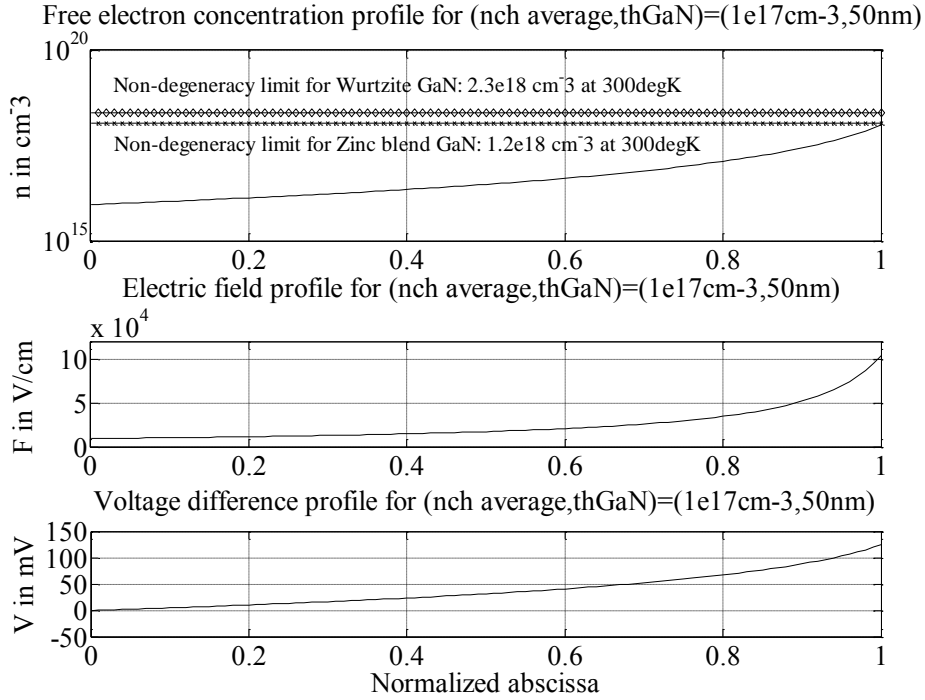


Figure 4-32: Free electron concentration, electric field, and potential drop for $(n_{ch\ ave}, th_{GaN})=(10^{+17}\ cm^{-3}, 50nm)$

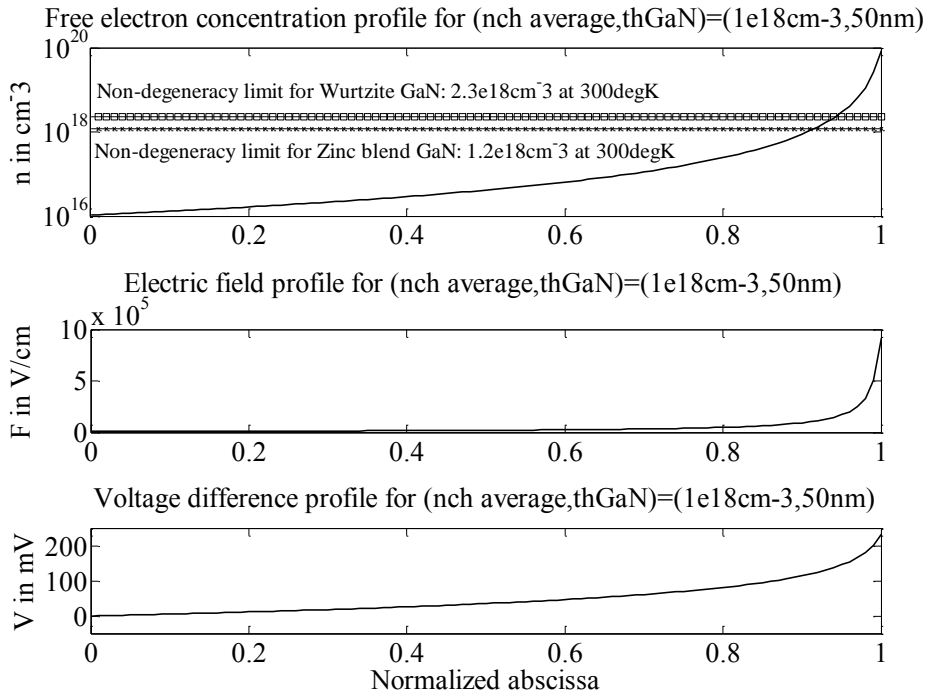


Figure 4-33: Free electron concentration, electric field, and potential drop for $(n_{ch\ ave}, th_{GaN})=(10^{+18}\ cm^{-3}, 50nm)$

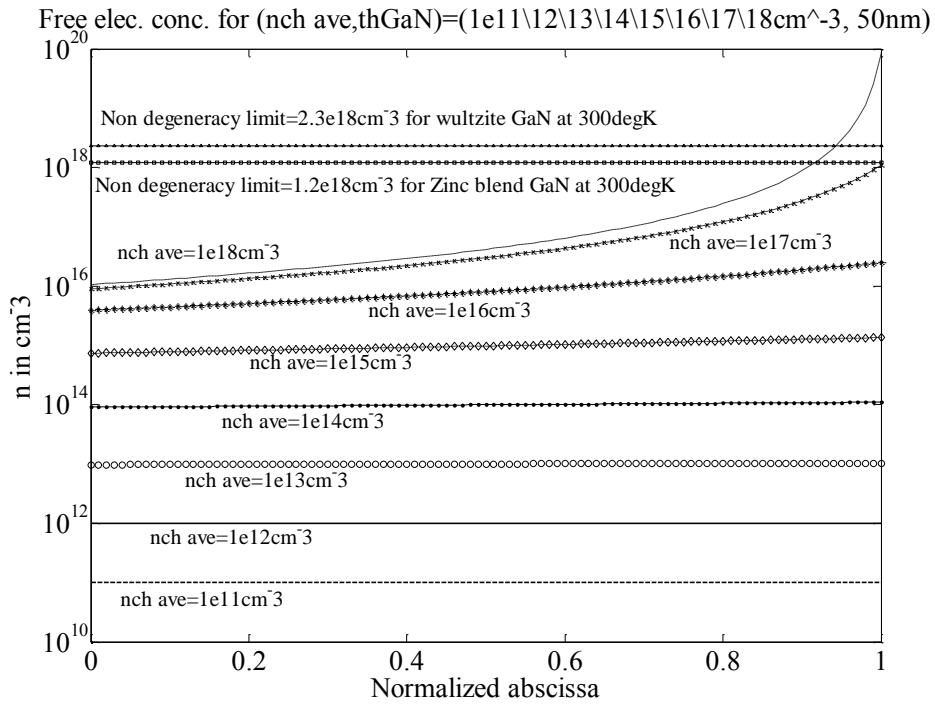


Figure 4-34: Free electron concentration for $(n_{ch\ ave}, th_{GaN}) = (10^{11/12/13/14/15/16/17/18} \text{cm}^{-3}, 50\text{nm})$

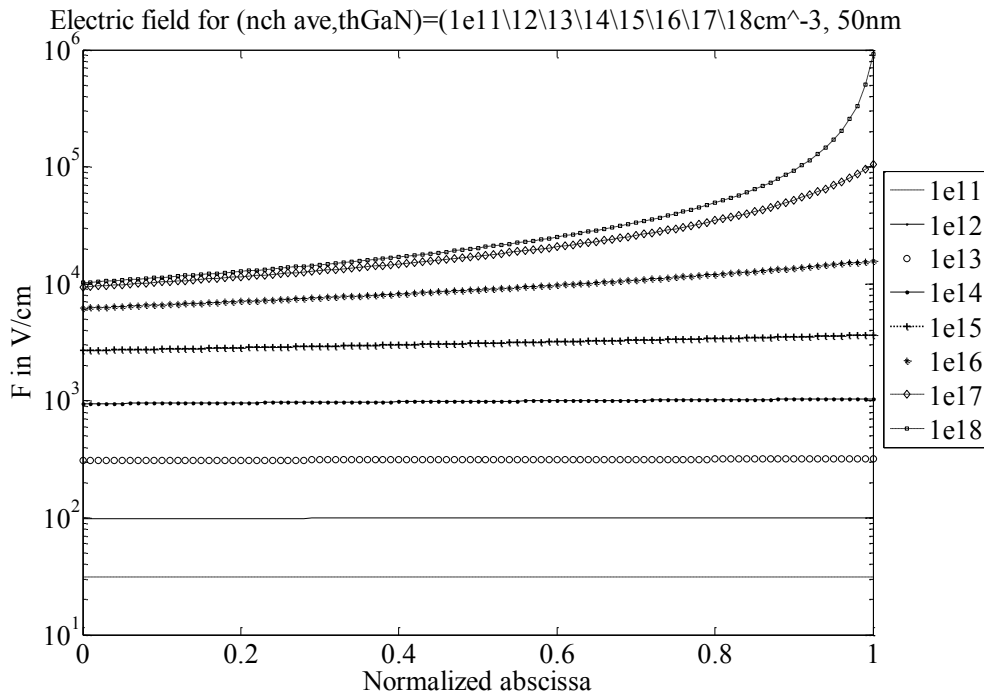


Figure 4-35: Electric field for $(n_{ch\ ave}, th_{GaN}) = (10^{11/12/13/14/15/16/17/18} \text{cm}^{-3}, 50\text{nm})$

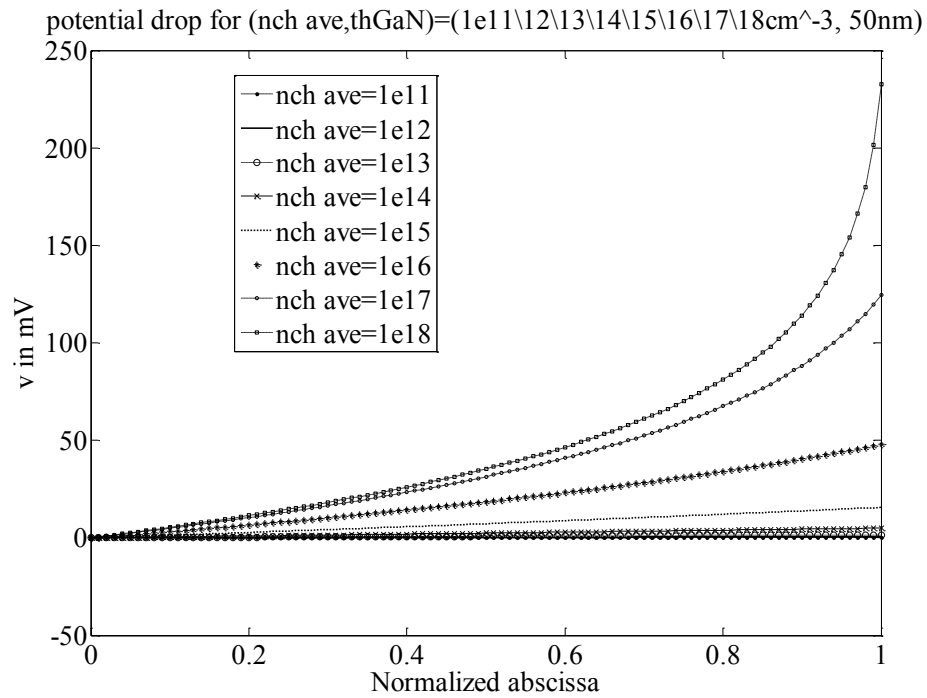


Figure 4-36: Potential drop for $(n_{ch\ ave}, th_{GaN}) = (10^{+11\ 12\ 13\ 14\ 15\ 16\ 17\ 18}\ cm^{-3}, 50nm)$

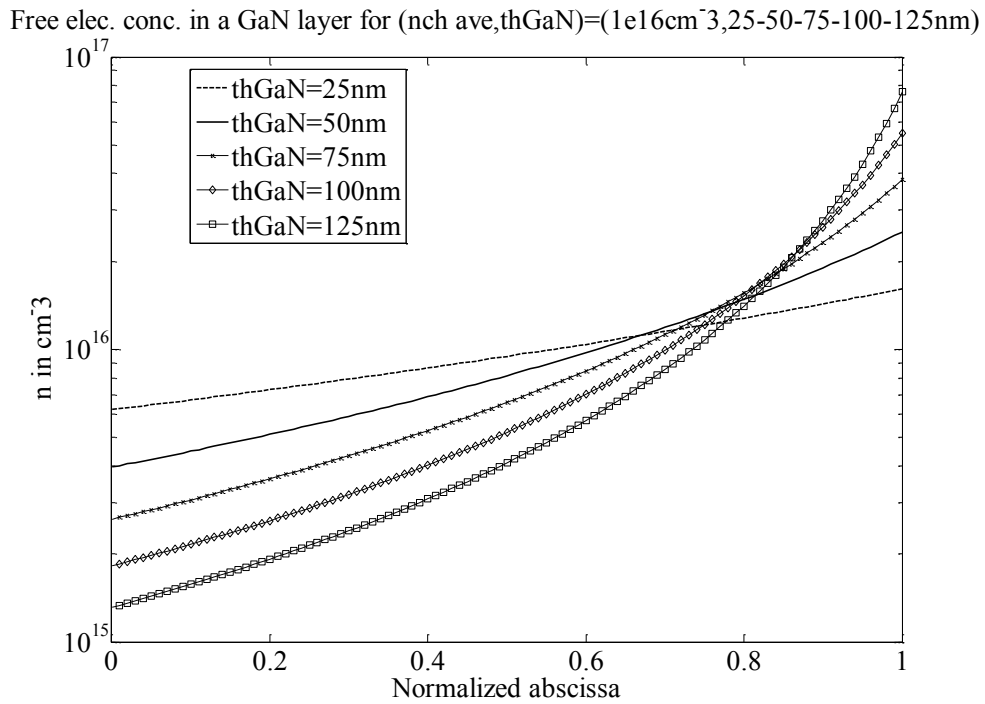


Figure 4-37: Free electron concentration for $(n_{ch\ ave}, th_{GaN}) = (10^{+16}\ cm^{-3}, 25-50-75-100-125nm)$

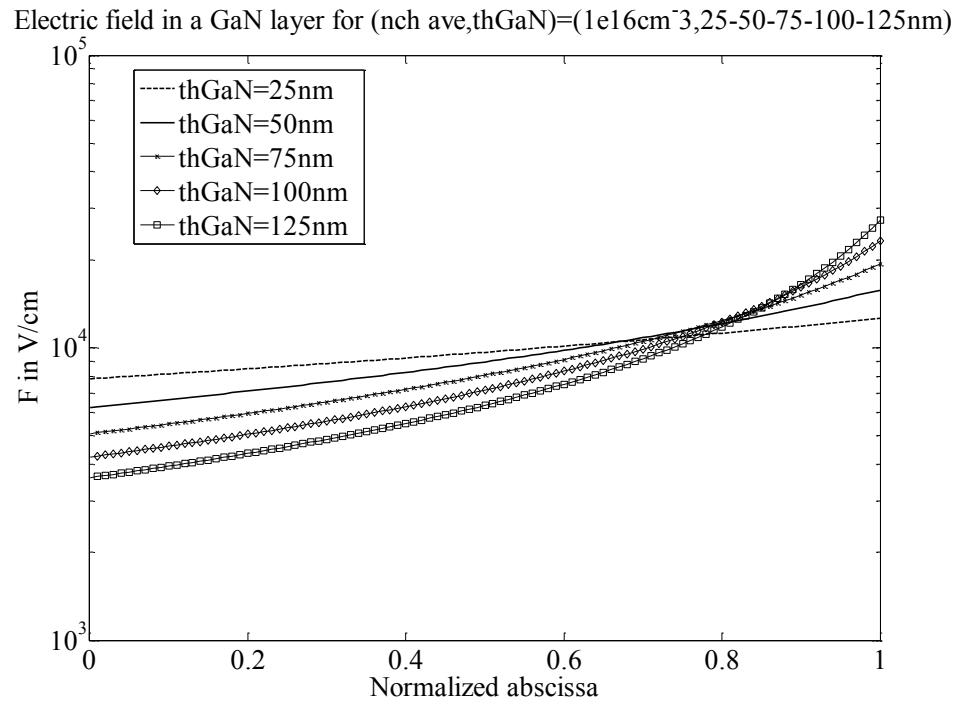


Figure 4-38: Electric field for $(n_{ch\ ave}, th_{GaN})=(10^{+16} cm^{-3}, 25-50-75-100-125nm)$

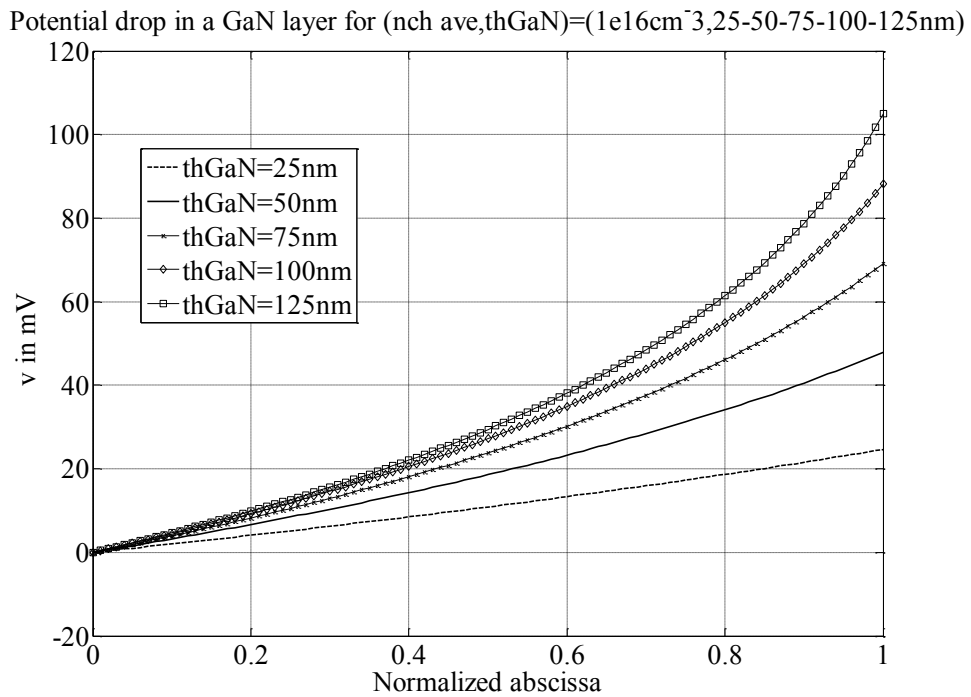


Figure 4-39: Potential drop for $(n_{ch\ ave}, th_{GaN})=(10^{+16} cm^{-3}, 25-50-75-100-125nm)$

Electric field deviation from its initial value for $(n_{ch\ ave}, th_{GaN}) = (1e-9\ to\ 1e18\ cm^{-3}, 50nm)$

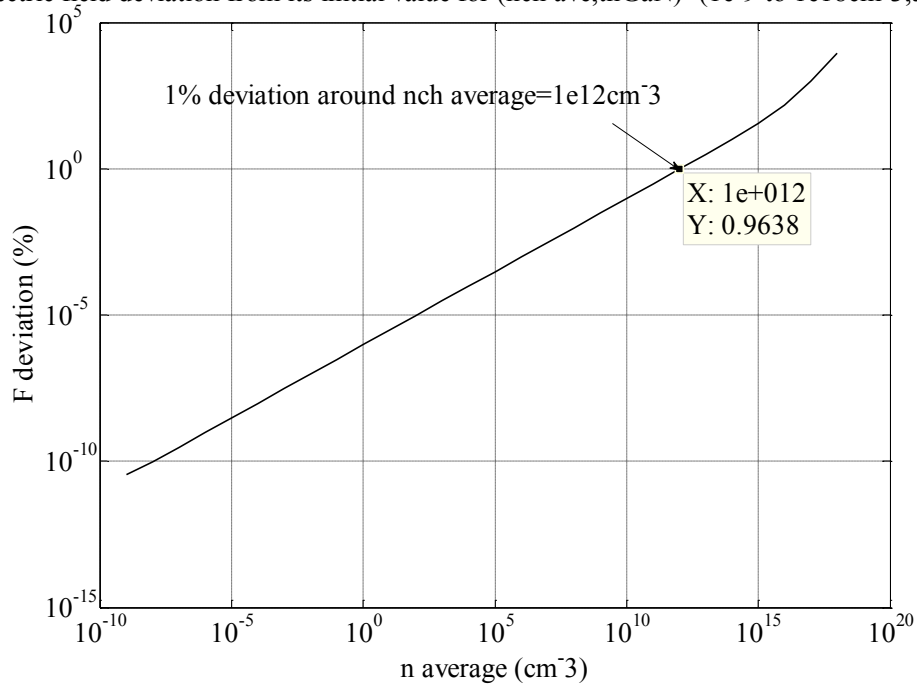


Figure 4-40: Electric field deviation from its initial value for $(n_{ch\ ave}, th_{GaN}) = (10^{-9}\ to\ 10^{+18}\ cm^{-3}, 50nm)$

Table 4-2: Initial and final values of free electron concentration, electric field and potential drop for ($n_{ch\ ave}=10^{-9}$ to 10^{+18} cm^{-3} , $th_{\text{GaN}}=50\text{nm}$)

$\overline{n_{ch}}$ (cm^{-3})	n_0 (cm^{-3})	n_1 (cm^{-3})	F_0 (V/cm)	F_1 (V/cm)	F deviation (%)	Potential drop(mV)
1.00E-09	9.999999999734E-10	1.0000000000027E-09	2.76337909073438E-09	2.76337909073533E-09	3.45E-11	1.38238E-11
1.00E-08	9.999999999052E-09	1.0000000000095E-08	9.81404395890899E-09	9.81404395891851E-09	9.70E-11	4.90639E-11
1.00E-07	9.999999996968E-08	1.0000000000303E-07	3.13545436437578E-08	3.13545436438530E-08	3.04E-10	1.56708E-10
1.00E-06	9.999999990408E-07	1.0000000000959E-06	9.92523394679182E-08	9.92523394688704E-08	9.59E-10	4.96204E-10
1.00E-05	9.999999969680E-06	1.0000000003035E-05	3.13895240032949E-07	3.13895240042471E-07	3.03E-09	1.56965E-09
1.00E-04	9.999999904025E-05	1.0000000009587E-04	9.92633955649096E-07	9.92633955744313E-07	9.59E-09	4.96128E-09
1.00E-03	9.999999697009E-04	1.0000000030368E-03	3.13898736057583E-06	3.13898736152799E-06	3.03E-08	1.57021E-08
1.00E-02	9.999999039504E-03	1.0000000095797E-02	9.92635060767960E-06	9.92635061720128E-06	9.59E-08	4.95937E-08
1.00E-01	9.999996961760E-02	1.0000000302848E-01	3.13898770588764E-05	3.13898771540932E-05	3.03E-07	1.56806E-07
1.00E+00	9.9999990402194E-01	1.0000000958685E+00	9.92635067536585E-05	9.92635077058265E-05	9.59E-07	4.96122E-07
1.00E+01	9.9999969644761E+00	1.00000003031196E+01	3.13898766650983E-04	3.13898776172663E-04	3.03E-06	1.56876E-06
1.00E+02	9.9999904012348E+01	1.0000009585889E+02	9.92635024770342E-04	9.92635119987144E-04	9.59E-06	4.96097E-06
1.00E+03	9.9999696215390E+02	1.00000030288741E+03	3.13898723739904E-03	3.13898818956705E-03	3.03E-05	1.56816E-05
1.00E+04	9.9999040264137E+03	1.0000095872952E+04	9.92634596077951E-03	9.92635548245964E-03	9.59E-05	4.96133E-05
1.00E+05	9.9996967619323E+04	1.00000303433957E+05	3.13898295488105E-02	3.13899247656120E-02	3.03E-04	0.000156958

Table 4-2(cont'd): Initial and final values of free electron concentration, electric field and potential drop for ($n_{ch\ ave}=10^{-9}$ to 10^{+18} cm^{-3} , $th_{GaN}=50nm$)

$\overline{n_{ch}}$ (cm^{-3})	n_0 (cm^{-3})	n_1 (cm^{-3})	F_0 (V/cm)	F_1 (V/cm)	F deviation (%)	Potential drop(mV)
1.00E+06	9.99990411732649E+05	1.00000959638663E+06	9.92630313575180E-02	9.92639835255357E-02	9.59E-04	0.000496367
1.00E+07	9.99969616741041E+06	1.00003028393882E+07	3.13894002748699E-01	3.13903524428361E-01	3.03E-03	0.001568027
1.00E+08	9.99904132559759E+07	1.00009597911338E+08	9.92587490579658E-01	9.92682707385931E-01	9.59E-03	0.004963961
1.00E+09	9.99696356822418E+08	1.00030302853123E+09	3.13851111190354E+00	3.13946327958106E+00	3.03E-02	0.015684092
1.00E+10	9.99040476461449E+09	1.00095893990497E+10	9.92158729760310E+00	9.93110897058344E+00	9.60E-02	0.049606900
1.00E+11	9.96966179384428E+10	1.00303286036085E+11	3.13422253444735E+01	3.14374416620988E+01	3.04E-01	0.156800653
1.00E+12	9.90438849904217E+11	1.00962329469808E+12	9.87878308611460E+01	9.97399846566634E+01	9.64E-01	0.495873594
1.00E+13	9.70089862054568E+12	1.03076088728116E+13	3.09168756287950E+02	3.18690106433404E+02	3.08E+00	1.568353064
1.00E+14	9.08538643499286E+13	1.10059622363878E+14	9.46152885085387E+02	1.04136655379919E+03	1.01E+01	4.959843053
1.00E+15	7.39439185190325E+14	1.35340027927282E+15	2.69923593236704E+03	3.65176436878912E+03	3.53E+01	15.64492511
1.00E+16	3.96168025132385E+15	2.52325298846778E+16	6.24783175594094E+03	1.57677604752943E+04	1.52E+02	47.89018784
1.00E+17	8.99509450114009E+15	1.10460637648494E+18	9.41439640931967E+03	1.04326200005868E+05	1.01E+03	124.4205723
1.00E+18	1.06280564796989E+16	8.62074160429453E+19	1.02333197134016E+04	9.21641304227508E+05	8.91E+03	232.7972326

4.6 Conclusion

A Channel first model was presented; its concept, analysis, and its domain of validity were discussed. Simulation results suggested a way for free electrons, once injected in a thin intrinsic GaN layer, to distribute. These free charge carriers are under the influence of an electric field whose initial value is implicitly dependant on both the average concentration value and the layer thickness. The potential drop across the layer was also computed.

Chapter 5 : Channel model 2 [28]

5.1 Introduction

In chapter 4, the initial value of the electric field is dependent on both the i-GaN layer thickness and the average value of the free electron concentration for Channel model 1. Why emphasize the initial electric field value? This value is (or should be) responsible for the quantum tunneling of electrons of exciton origin into the intrinsic GaN layer. The transmission coefficient expresses the exciton quantity ratio that interacts with the i-GaN/p-type $\text{In}_{0.5}\text{Ga}_{0.5}\text{N}$ heterojunction, and results in electron tunneling. This transmission coefficient is a function of the value of the electric field at the heterojunction [26][27]. Channel model 1 does not provide us with the ability to appreciate the effect of the transmission coefficient variation on the quantity of free charge injected in the GaN layer for the same quantity of excitons created (the potential drop applied across the $\text{In}_{0.5}\text{Ga}_{0.5}\text{N}$ p-n junction is held constant in this case). Note that until now, we did not verify that the electric field initial values given by i-GaN channel model 1 for different inputs $(\overline{n_{ch}}, th_{GaN})$ can produce the electron tunneling [26][27]. This verification will be will performed in chapter 6.

A second channel model is presented in this chapter; this 1-D dimensional model allows control over the electric field initial value. It calculates the free electron concentration, the electric field, and the potential drop profiles for an input $(\overline{n_{ch}}, F_0, th_{GaN})$ instead of only $(\overline{n_{ch}}, th_{GaN})$. The initial value of the electric field in the GaN layer is referred to as F_0 . Figure 5-1 represents a block diagram of the proposed channel model.

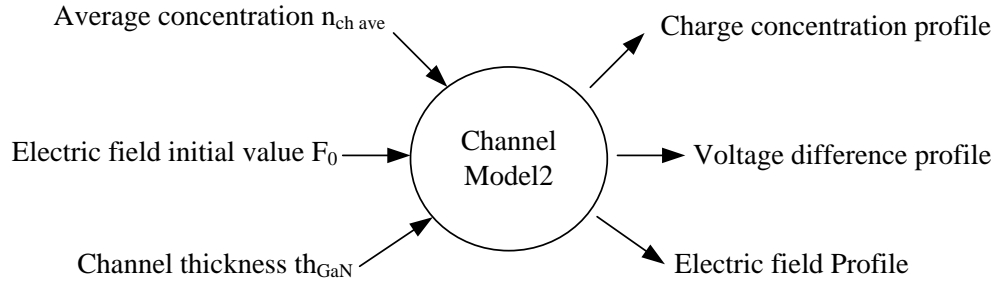


Figure 5-1: Block diagram of i-GaN channel model 2

5.2 Mathematical formulation

Figure 5-2 represents a cross sectional schematic of the i-GaN layer. The final value of the electric field F is referred to as F_1 . The origin for measuring both the potential difference and the distance inside the GaN layer is taken at the side on which F_0 is applied.

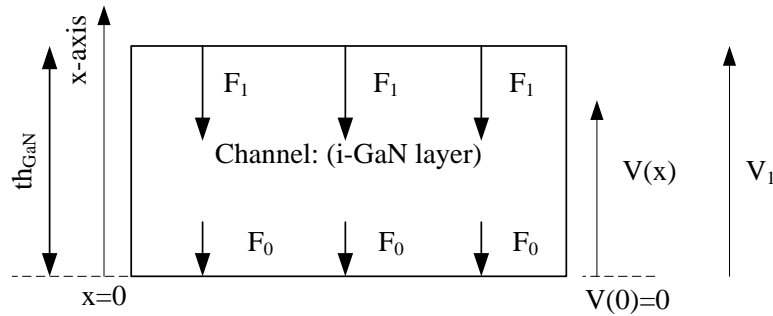


Figure 5-2: A cross-sectional schematics of the intrinsic GaN layer, with the corresponding referenced potential drop, and electric field

The application of the 1-D Poisson equation on the i-GaN channel, as indicated in Figure 5-2, results in the following initial conditions problem [30].

$$\begin{cases} \frac{d^2 v}{dx^2} = \frac{q n_{ch}}{\epsilon_0 \epsilon_{GaN}} \\ v(0) = 0 \\ \frac{dv}{dx}(0) = F_0 \end{cases} ,$$

where $n_{ch} = n_0 \exp\left(\frac{v}{u_T}\right)$. n_{ch} and v represent the free electron concentration, and the potential drop at point x respectively. The value of the free electron concentration at $x = 0$, or at $v = 0$, is referred to as n_0 , this value is generally different from the intrinsic GaN free charge carriers concentration. The solution of this differential equation gives the expression of the potential drop $v(x)$ at a point x ,

$$v(x) = \begin{cases} u_T \ln \left\{ d^2 \operatorname{csch}^2 \left[d \left(\frac{x}{L_d \sqrt{2}} - \frac{\sinh^{-1}(d)}{d} \right) \right] \right\} \\ \text{for } \frac{F_0 L_d}{u_T \sqrt{2}} > 1 \text{ and } x \in \left[0, L_d \sqrt{2} \frac{\sinh^{-1}(d)}{d} \right] \\ u_T \ln \left\{ d^2 \operatorname{sec}^2 \left[d \left(\frac{x}{L_d \sqrt{2}} + \frac{1}{d} \arctan \left(\frac{\sqrt{1-d^2}}{d} \right) \right) \right] \right\} \\ \text{for } 0 < \frac{F_0 L_d}{u_T \sqrt{2}} < 1 \text{ and } x \in \left[0, L_d \sqrt{2} \frac{1}{d} \arctan \left(\frac{d}{\sqrt{1-d^2}} \right) \right] \\ -2u_T \ln \left(1 - \frac{x}{L_d \sqrt{2}} \right) \\ \text{for } \frac{F_0 L_d}{u_T \sqrt{2}} = 1 \text{ and } x \in [0, L_d \sqrt{2}] \end{cases},$$

where

$$L_d = \left(\frac{\epsilon_0 \epsilon_{GaN} u_T}{q n_0} \right)^{1/2} \text{ and } d = \begin{cases} \left[-1 + \left(\frac{L_d F_0}{u_T \sqrt{2}} \right)^2 \right]^{1/2} \text{ for } \frac{F_0 L_d}{u_T \sqrt{2}} > 1 \\ \left[1 - \left(\frac{L_d F_0}{u_T \sqrt{2}} \right)^2 \right]^{1/2} \text{ for } 0 < \frac{F_0 L_d}{u_T \sqrt{2}} < 1 \end{cases}$$

L_d represents a normalizing length, and d is a dimensionless positive constant. A closer look at the case corresponding to $\frac{F_0 L_d}{u_T \sqrt{2}} = 1$ shows that the initial value n_0 of free electron concentration is solely determined by the electric field initial value F_0 . In other words, regardless of the value of the average concentration $\overline{n_{ch}}$, the initial value n_0 is pinned. This is incorrect since, two different values of the average concentration lead to two different initial values under the same conditions. This case is, thus, discarded.

From now on, we refer to:

$$\frac{F_0 L_d}{u_T \sqrt{2}} > 1 \quad \text{and} \quad th_{GaN} \in \left[0, L_d \sqrt{2} \frac{\sinh^{-1}(d)}{d} \right] \quad \text{as case 1,}$$

and to

$$0 < \frac{F_0 L_d}{u_T \sqrt{2}} < 1 \quad \text{and} \quad th_{GaN} \in \left[0, L_d \sqrt{2} \frac{1}{d} \arctan \left(\frac{d}{\sqrt{1-d^2}} \right) \right] \quad \text{as case 2}$$

The free electron concentration n_{ch} , the potential drop v , and the electric field F at any point λ in the i-GaN layer are derived.

$$\begin{cases} n_{ch} = n_0 d^2 \operatorname{csch}^2 \left[d \left(\lambda \frac{th_{GaN}}{L_d \sqrt{2}} - \frac{\sinh^{-1}(d)}{d} \right) \right] \\ v = u_T \ln \left\{ d^2 \operatorname{csch}^2 \left[d \left(\frac{th_{GaN}}{L_d \sqrt{2}} \lambda - \frac{\sinh^{-1}(d)}{d} \right) \right] \right\} \\ F = - \frac{u_T d \sqrt{2}}{L_d} \operatorname{cotanh} \left[d \left(\lambda \frac{th_{GaN}}{L_d \sqrt{2}} - \frac{\sinh^{-1}(d)}{d} \right) \right] \end{cases} \quad \text{case 1} \quad (5-1)$$

$$\begin{cases} n_{ch} = n_0 d^2 \operatorname{sec}^2 \left[d \left(\frac{th_{GaN}}{L_d \sqrt{2}} \lambda + \frac{1}{d} \arctan \left(\frac{\sqrt{1-d^2}}{d} \right) \right) \right] \\ v = u_T \ln \left\{ d^2 \operatorname{sec}^2 \left[d \left(\frac{th_{GaN}}{L_d \sqrt{2}} \lambda + \frac{1}{d} \arctan \left(\frac{\sqrt{1-d^2}}{d} \right) \right) \right] \right\} \\ F = \frac{u_T d \sqrt{2}}{L_d} \tan \left[d \left(\lambda \frac{th_{GaN}}{L_d \sqrt{2}} + \frac{1}{d} \arctan \left(\frac{\sqrt{1-d^2}}{d} \right) \right) \right] \end{cases} \quad \text{case 2} \quad (5-2)$$

where $\lambda \in [0,1]$

The quantity λ is the normalized abscissa, it is defined as

$$\begin{cases} \lambda = \frac{x}{th_{GaN}} \\ x \in [0, th_{GaN}] \end{cases}$$

The free electron concentration, the potential drop, and the electric field are functions of four variables $(\lambda, \bar{n}_{ch}, F_0, th_{GaN})$. The average concentration \bar{n}_{ch} is used to compute the initial value n_0 which is obtained by solving, for an appropriate choice of the unknown, the following equation;

$$\int_0^1 n_{ch}(\lambda, \bar{n}_{ch}, th_{GaN}, F_0) \partial \lambda = \bar{n}_{ch} \quad (5-3)$$

Substituting the free electron concentration n_{ch} by its expression obtained from the first equation in set 5-1 or 5-2, according to the case considered, in equation 5-3, we obtain;

$$n_0 = \frac{\bar{n}_{ch} th_{GaN}}{L_d \sqrt{2}} \left\{ -\sqrt{1+d^2} + d + \frac{2d}{-1 + \exp\left\{\sqrt{2} \frac{th_{GaN} \cdot d}{L_d}\right\}} \right\} \quad \text{case 1} \quad (5-4),$$

and

$$n_0 = \frac{\bar{n}_{ch} th_{GaN}}{L_d \sqrt{2} \left\{ d \cdot \tan\left[\frac{th_{GaN} \cdot d}{L_d \sqrt{2}} + \arctan\left(\frac{\sqrt{1-d^2}}{d}\right)\right] - \sqrt{1-d^2} \right\}} \quad \text{case 2} \quad (5-5)$$

Using the two following bijections

$$\left\{ \begin{array}{l} X \rightarrow Z = a \frac{\sqrt{-1+X^2}}{X} \\ X \in]1, +\infty[\text{ and } Z \in]0, a[, \quad a \in \mathbb{R}_+^* \end{array} \right. \quad \text{case 1,}$$

and

$$\left\{ \begin{array}{l} X \rightarrow Z = \frac{1}{2} a \frac{\sqrt{1-X^2}}{X} \\ X \in]0, 1[\text{ and } Z \in]0, +\infty[, \quad a \in \mathbb{R}_+^* \end{array} \right. \quad \text{case 2,}$$

the following variable change is justified

$$X = \frac{L_d F_0}{u_T \sqrt{2}}, Z = \frac{F_0 th_{GaN}}{u_T} \frac{\left[-1 + \left(\frac{L_d F_0}{u_T \sqrt{2}}\right)^2\right]^{1/2}}{\left(\frac{L_d F_0}{u_T \sqrt{2}}\right)}, a = \frac{F_0 th_{GaN}}{u_T} \quad \text{case 1,}$$

and

$$X = \frac{L_d F_0}{u_T \sqrt{2}}, Z = \frac{F_0 th_{GaN}}{2u_T} \frac{\left[1 - \left(\frac{L_d F_0}{u_T \sqrt{2}}\right)^2\right]^{1/2}}{\left(\frac{L_d F_0}{u_T \sqrt{2}}\right)}, a = \frac{F_0 th_{GaN}}{u_T} \quad \text{case 2}$$

Expressions 5-4 and 5-5 can be put into the forms

$$Z = \ln \left[1 + \frac{Z}{-\frac{b}{2a}(Z-a)(Z+\frac{a(b+1)}{b})} \right], \quad Z \in]0, a[\quad \text{case 1} \quad (5-6)$$

$$Z = \arctan \left[\frac{2Z}{\frac{4b}{a}Z^2 + a(b+1)} \right], \quad Z \in \left[0, \arctan \left(\frac{d}{\sqrt{1-d^2}} \right) \right] \left(\subset \left[0, \frac{\pi}{2} \right] \right) \quad \text{case 2} \quad (5-7),$$

where
$$a = \frac{F_0 th_{GaN}}{u_T}, \quad b = \frac{\varepsilon_0 \varepsilon_{GaN} F_0}{q \bar{n}_{ch} th_{GaN}}$$

Equation 5-3, put into forms 5-6 or 5-7, is solved numerically for the unknown Z using an iterative method. Appendices B and C present the proof that equations 5-6 and 5-7 have unique solutions, different from the trivial one $Z = 0$, if constants (a, b) satisfy one of the mutually exclusive following conditions (one condition for each equation).

Condition1: $a(b+1) > 2$ case 1

Condition2: $a(b+1) < 2$ case 2

Constants (a, b) are expressed in terms of the electric field initial value F_0 , the average value of free electron concentration \bar{n}_{ch} , and the i-GaN layer thickness th_{GaN} . The product $a(b+1)$ is directly obtained from the input $(\bar{n}_{ch}, th_{GaN}, F_0)$, and indicates which case (1 or 2) is taken.

Suppose that equation 5-3, put under form 5-6 or 5-7 has a solution Z_0 , then the initial value of free electron concentration n_0 is computed using reciprocals of bijections introduced earlier to justify the variable change. It is given as;

$$n_0 = \frac{\varepsilon_0 \varepsilon_{GaN} F_0^2}{2q u_T} \left[1 - \left(\frac{u_T}{F_0 th_{GaN}} Z_0 \right)^2 \right] \quad \text{case 1} \quad (5-8),$$

or

$$n_0 = \frac{\epsilon_0 \epsilon_{GaN} F_0^2}{2q u_T} \left[1 + \left(\frac{2u_T}{F_0 t h_{GaN}} Z_0 \right)^2 \right] \quad \text{case 2} \quad (5-9)$$

For an input $(\bar{n}_{ch}, F_0, th_{GaN})$ that satisfies condition 1(2), equation 5-3, put into form 5-6 (5-7), is solved for the unknown Z . The free electron concentration initial value n_0 is evaluated using 5-8(5-9). The free electron concentration, the potential drop, and the electric field profiles can be computed using equation set 5-1(5-2). Figure 5-3 represents the solution flowchart used to calculate output (n_{ch}, v, F) starting from input $(\bar{n}_{ch}, F_0, th_{GaN})$,

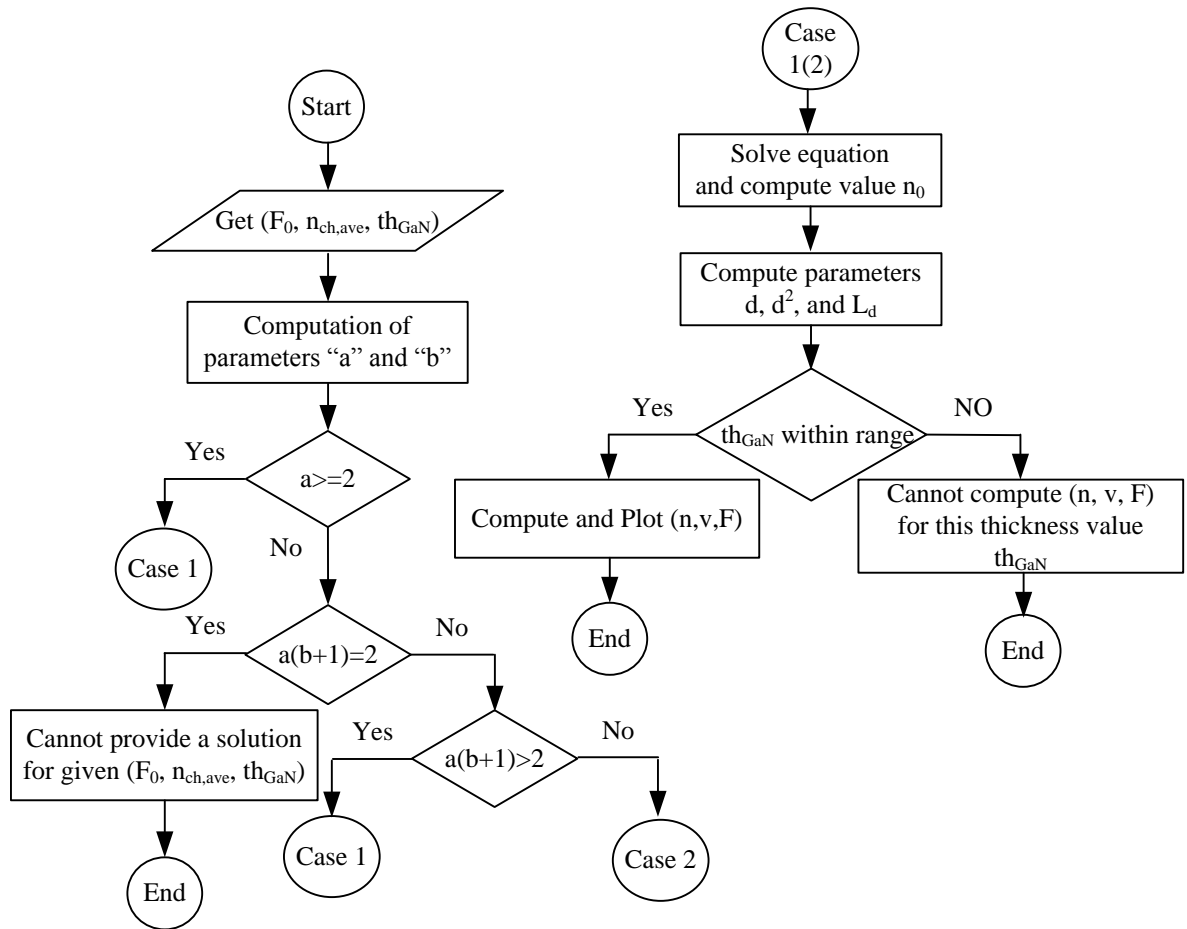


Figure 5-3: Solution flowchart for intrinsic GaN channel model 2

Once the initial value n_0 is computed, the free electron concentration final value n_1 , the voltage drop V across the GaN layer, and the electric field final F_1 can be computed using equations set 5-1 or 5-2 for $\lambda = 1$.

$$\left\{ \begin{array}{l} n_1 = n_0 d^2 \operatorname{csch}^2 \left[d \left(\frac{th_{GaN}}{L_d \sqrt{2}} - \frac{\sinh^{-1}(d)}{d} \right) \right] \\ V = u_T \ln \left\{ d^2 \operatorname{csch}^2 \left[d \left(\frac{th_{GaN}}{L_d \sqrt{2}} - \frac{\sinh^{-1}(d)}{d} \right) \right] \right\} \\ F_1 = - \frac{u_T d \sqrt{2}}{L_d} \operatorname{cotanh} \left[d \left(\lambda \frac{th_{GaN}}{L_d \sqrt{2}} - \frac{\sinh^{-1}(d)}{d} \right) \right] \end{array} \right. \quad \text{case 1} \quad (5-10)$$

$$\left\{ \begin{array}{l} n_1 = n_0 d^2 \operatorname{sec}^2 \left[d \left(\frac{th_{GaN}}{L_d \sqrt{2}} + \frac{1}{d} \arctan \left(\frac{\sqrt{1-d^2}}{d} \right) \right) \right] \\ V = u_T \ln \left\{ d^2 \operatorname{sec}^2 \left[d \left(\frac{th_{GaN}}{L_d \sqrt{2}} + \frac{1}{d} \arctan \left(\frac{\sqrt{1-d^2}}{d} \right) \right) \right] \right\} \\ F_1 = \frac{u_T d \sqrt{2}}{L_d} \tan \left[d \left(\frac{th_{GaN}}{L_d \sqrt{2}} + \frac{1}{d} \arctan \left(\frac{\sqrt{1-d^2}}{d} \right) \right) \right] \end{array} \right. \quad \text{case 2} \quad (5-11)$$

where $\lambda \in [0,1]$

All the coefficients in the expression of the free electron concentration n_{ch} (first equation in equations set 5-1 or 5-2) can be computed once the initial value n_0 is calculated. A numerical integration of n_{ch} over the interval $[0,1]$ is performed with respect to the variable λ . The result should be equal to the average value $\overline{n_{ch}}$. This numerical integration verifies the correctness of the value n_0 obtained previously. The initial value of the electric field is also recomputed using third equation in equations set 5-1 or 5-2 for the value $\lambda = 0$.

5.3 Simulation results and Discussion

For a given i-GaN layer thickness, here we considered $th_{GaN} = 50\text{nm}$ as in [1]. Constants a and b depend on both the electric field initial value F_0 and the free electron concentration average value $\overline{n_{ch}}$. To emphasize the difference between case 1 and case 2, consider the following practical situations. First, the i-GaN layer is heavily charged, and under the influence of an electric field whose initial value is low.

Second, the i-GaN layer is lightly charged, and under the influence of an electric field whose initial value is high. The first situation satisfies condition 2 and thus falls under case 2, while the second satisfies condition 1 and thus falls under case 1. Condition 1 is always satisfied if constant $a \geq 2$. This corresponds to situations where $F_0 \geq 1.04 * 10^4$ V/cm at room temperature for an i-GaN layer thickness of 50nm, regardless of the charge density value.

Figures 5-4 to 5-30 show the charge density distribution, the electric field, and the potential drop across an i-GaN layer of thickness 50nm for free carriers concentration typical average values in the range $[10^9 \text{cm}^{-3}, 10^{17} \text{cm}^{-3}]$ under the influence of an electric field whose two initial values are chosen to be weak enough so that all these input $(\bar{n}_{ch}, F_0, th_{GaN})$ values satisfy condition 2. For all typical values of the average concentration, and although the electric field initial value increased by one order of magnitude each time, no noticeable differences in the charge density and potential drop were observed. If we take the example where $\bar{n}_{ch} = 10^{13} \text{cm}^{-3}$, the initial value $n_0 = 9.9969 * 10^{12} \text{cm}^{-3}$ for $F_0 = 10^{-2} \text{V/cm}$, and $n_0 = 9.9968 * 10^{12} \text{cm}^{-3}$ for $F_0 = 10^{-1} \text{V/cm}$ (see figure 5-8 and table 5-1), this comes from the fact that the electric field initial values are too small to have noticeable distinct effects on the charge density distribution. Table 5-1 contains initial and final values of both the free electron concentration and the electric field, and also the potential drop across this layer. Although, the initial electric field is an input, it has been computed for verification purposes. For the potential difference across the i-GaN layer, its values start in the range of tenths of fV; $v = 0.5 \text{fV}$ for $(\bar{n}_{ch}, F_0, th_{GaN}) = (10^9 \text{cm}^{-3}, 10^{-10} \text{V/cm}, 50 \text{nm})$ to reach almost a hundred of mV; $v = 97.4 \text{mV}$ for $(\bar{n}_{ch}, F_0, th_{GaN}) = (10^{17} \text{cm}^{-3}, 10^{-1} \text{V/cm}, 50 \text{nm})$. The electric field final value ranges from $F_1 \approx 10^{-10} \text{V/cm}$ with a deviation of $9.52 * 10^{-10} \%$ from its initial value for an input $(\bar{n}_{ch}, F_0, th_{GaN}) = (10^9 \text{cm}^{-3}, 10^{-10} \text{V/cm}, 50 \text{nm})$ to $F_1 = 9.5 * 10^{+4} \text{V/cm}$ with a deviation of $9.52 * 10^{+7} \%$ from its initial value for an input $(\bar{n}_{ch}, F_0, th_{GaN}) = (10^{17} \text{cm}^{-3}, 10^{-1} \text{V/cm}, 50 \text{nm})$.

Figures 5-31 to 5-50 show the charge density distribution, the electric field, and the potential drop across an i-GaN layer of thickness 50nm for free charge carriers concentration typical average values in the range $[10^0 \text{cm}^{-3}, 10^{18} \text{cm}^{-3}]$ under the influence of an electric field whose two initial values are chosen to be high enough so that all these input $(\bar{n}_{ch}, F_0, th_{GaN})$ values satisfy condition 1.

Table 5-2 contains initial and final values of both the free electron concentration and the electric field, and also the potential drop across this layer for the same input typical values $(\bar{n}_{ch}, F_0, th_{GaN})$, where $th_{GaN} = 50\text{nm}$. When the electric field initial value is high, it pushes free charge carriers away from the corresponding i-GaN layer side, increasing the charge depletion. On the other side, an accumulation region is created. Both the depletion and the accumulation SCRs are enforced as the electric field initial value keeps getting higher. For strong initial fields, a change by one order of magnitude can result in a dramatic difference in the charge distribution profile, as well as for the potential drop across the i-GaN layer. For an average concentration value of 10^{18}cm^{-3} , see figures 5-31, 5-32 and table 5-2, the initial concentration density changes by almost six orders of magnitude from $1.09 \cdot 10^{+16}\text{cm}^{-3}$ for $F_0 = 10^{+4}\text{V/cm}$ to $1.35 \cdot 10^{+10}\text{cm}^{-3}$ for $F_0 = 10^{+5}\text{V/cm}$. The potential drop across the i-GaN layer varies from 235mV for $F_0 = 10^{+4}\text{V/cm}$ to 590mV for $F_0 = 10^{+5}\text{V/cm}$. The potential drop values across the i-GaN layer start from a few millivolts; $v = 2.5\text{mV}$ for an input $(\bar{n}_{ch}, F_0, th_{GaN}) = (10^0\text{cm}^{-3}, 10^{+3}\text{V/cm}, 50\text{nm})$, to reach hundreds of milli-volts; $v = 590\text{mV}$ for $(\bar{n}_{ch}, F_0, th_{GaN}) = (10^{+18}\text{cm}^{-3}, 10^{+5}\text{V/cm}, 50\text{nm})$. Although, the initial electric field is an input, it has been computed for verification purposes.

Another trend is noticed; for a given value of the initial electric field, the charge density distribution gets steeper as the average concentration value increases when the GaN layer thickness is kept constant. The concentration density varies from $9.49 \cdot 10^{+13}\text{cm}^{-3}$ to $1.06 \cdot 10^{+14}\text{cm}^{-3}$ for $\bar{n}_{ch} = 10^{+14}\text{cm}^{-3}$ and from $2.09 \cdot 10^{+16}\text{cm}^{-3}$ to $9.50 \cdot 10^{+17}\text{cm}^{-3}$ for $\bar{n}_{ch} = 10^{+17}\text{cm}^{-3}$ under the same condition of $F_0 = 5 \cdot 10^{+2}\text{V/cm}$ (see Figure 5-51). In fact Gauss's law, applied to the i-GaN layer, shows that the difference between final and initial values of the electric field is proportional to the total net charge encapsulated by this layer, an increase in the average concentration leads to a higher total charge which in turn increases the final value of the electric field if its initial value is kept constant. So, as the difference between the electric field final and initial values increases, the charge distribution gets steeper and the potential difference increases. Figure 5-52 illustrates the effects of varying the initial value of the electric field together with the average concentration on charge density distribution (see Figure 5-52a), on electric field (see Figure 5-52b), and on potential drop profiles (see Figure 5-52c) for the same GaN thickness of 50nm.

To this point, the i-GaN layer thickness was kept constant. The analysis however, allows the consideration of different thickness values. Changing the thickness allows the determination of its maximum value before breakdown for predetermined conditions of operation. For an average concentration $\overline{n_{ch}}=10^{16}\text{cm}^{-3}$ and an electric field initial value $F_0 =10^4\text{V/cm}$, the charge density distribution varies from $5.52*10^{15}\text{cm}^{-3}$ to a final value of $1.75*10^{16}\text{cm}^{-3}$ for a thickness of 25nm and from $1.83*10^{14}\text{cm}^{-3}$ to $1.06*10^{17}\text{cm}^{-3}$ for a thickness of 125nm (see Figure 5-53a). The potential drop across the GaN layer varies from 29.82mV for 25nm to 164.60mV for 125nm (see Figure 5-53c). The electric field final value is around $1.48*10^4\text{V/cm}$ for 25nm and $3.38*10^4\text{V/cm}$ for 125nm (see Figure 5-53b). An increase in the electric field final value is expected: for constant average concentration and electric field initial values, an increase of the i-GaN layer thickness results in an increase of the total net charge in the GaN layer and thus of the electric field final value according to Gauss's law. If $\overline{n_{ch}}$ and F_0 are kept constant, then the electric field final values F_1 and F_2 corresponding to the i-GaN layer thicknesses th_1 , th_2 respectively, satisfy the following proportionality (derived from Gauss's law).

$$\frac{F_1 - F_0}{F_2 - F_0} = \frac{th_1}{th_2} \quad (5-10)$$

Values $F_0=10^4\text{V/cm}$, $F_1=1.48*10^4\text{V/cm}$, $F_2=3.38*10^4\text{V/cm}$, $th_1=25\text{nm}$, and $th_2=125\text{nm}$ satisfy proportionality 5-10.

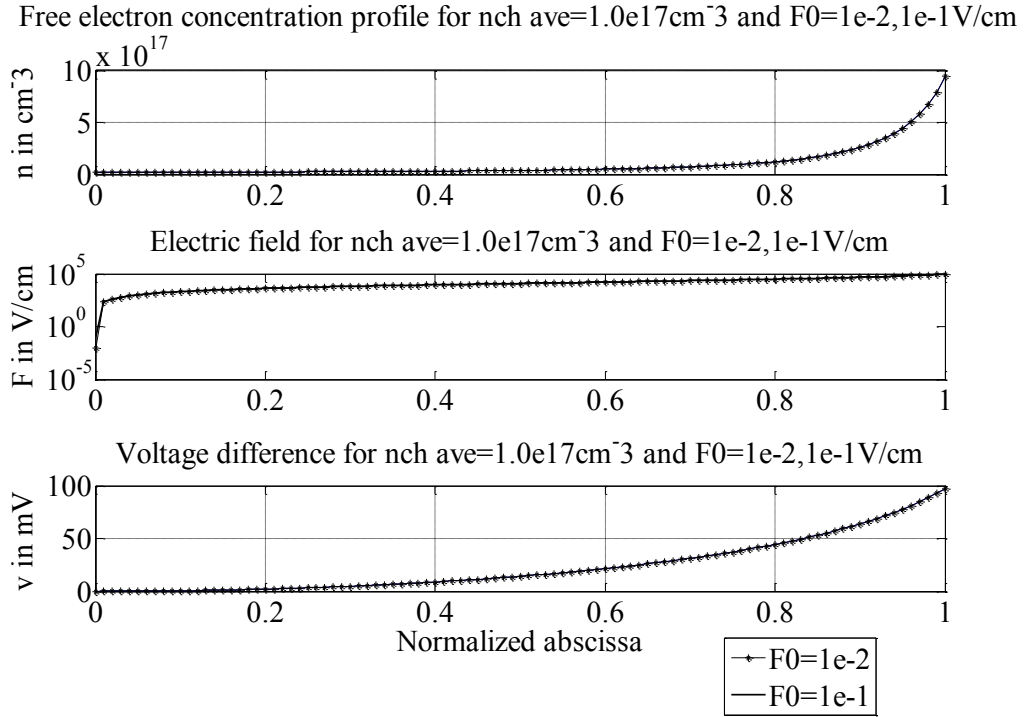


Figure 5-4: (n_{ch}, F, v) for input $(n_{ch\ ave}, th_{GaN})=(10^{+17}cm^{-3}, 10^{-2}\backslash 10^{-1}V/cm, 50nm)$

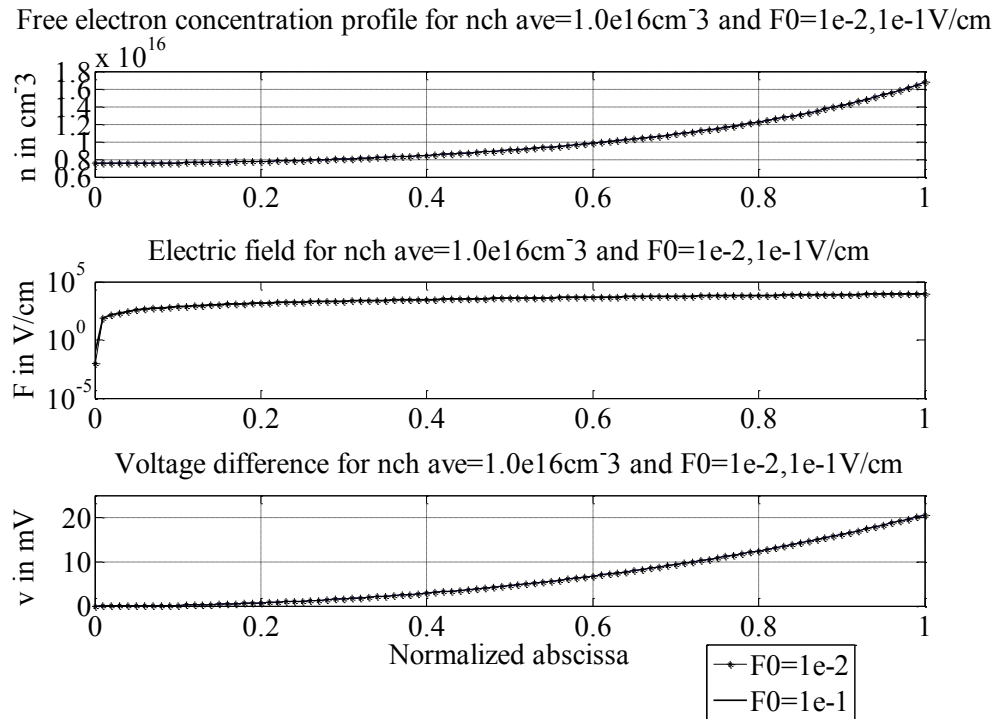


Figure 5-5: (n_{ch}, F, v) for input $(n_{ch\ ave}, th_{GaN})=(10^{+16}cm^{-3}, 10^{-2}\backslash 10^{-1}V/cm, 50nm)$

Free electron concentration profile for $n_{ch\ ave}=1.0e15cm^{-3}$ and $F0=1e-2,1e-1V/cm$

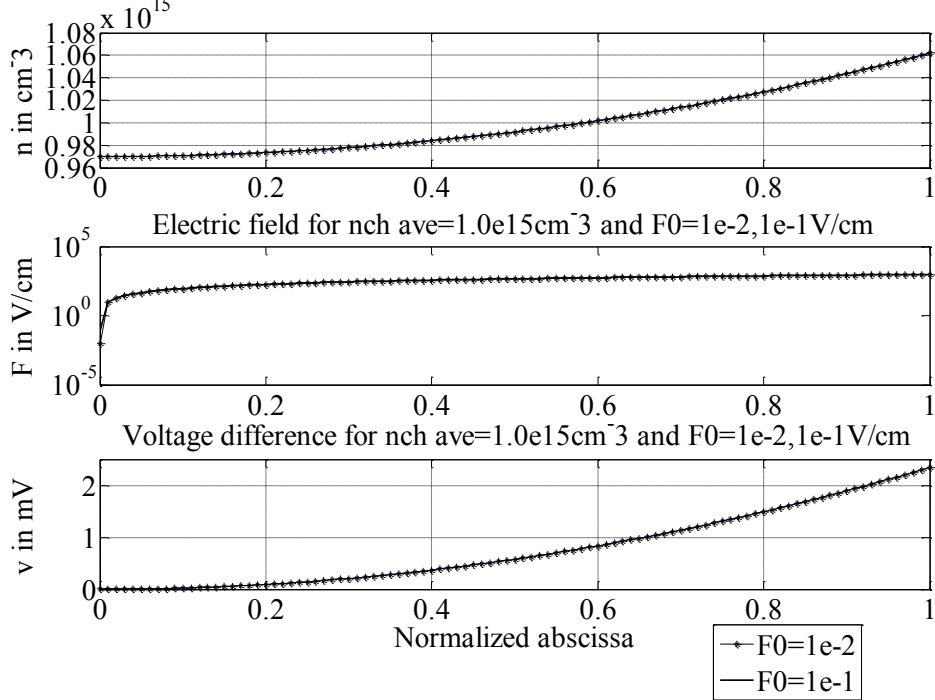


Figure 5-6: (n_{ch}, F, v) for input $(n_{ch\ ave}, th_{GaN})=(10^{+15}cm^{-3}, 10^{-2}\backslash 10^{-1}V/cm, 50nm)$

Free electron concentration profile for $n_{ch\ ave}=1.0e14cm^{-3}$ and $F0=1e-2,1e-1V/cm$

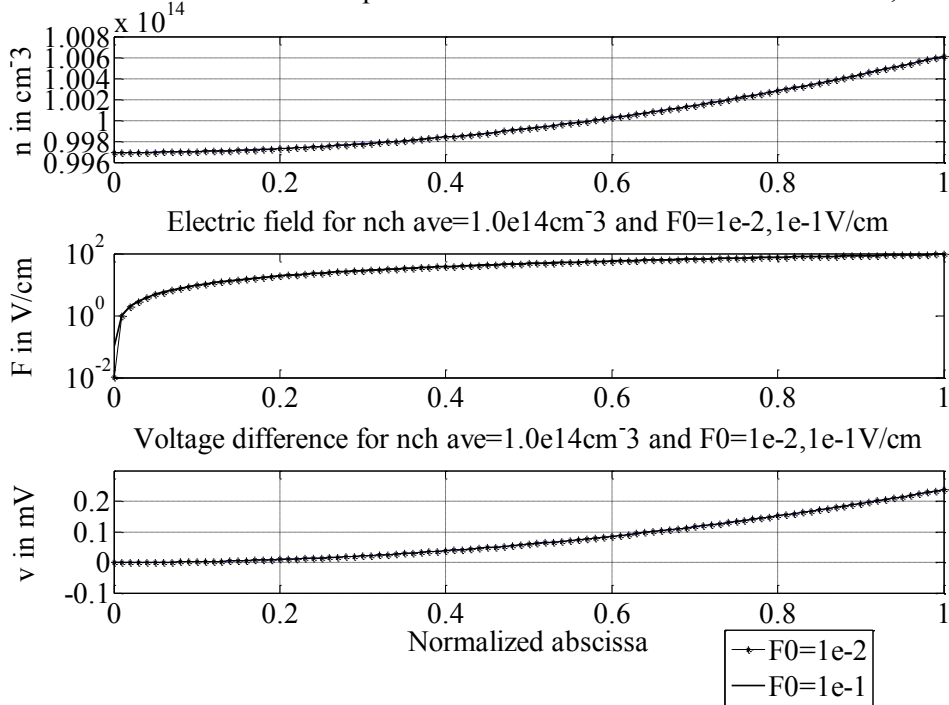


Figure 5-7: (n_{ch}, F, v) for input $(n_{ch\ ave}, th_{GaN})=(10^{+14}cm^{-3}, 10^{-2}\backslash 10^{-1}V/cm, 50nm)$

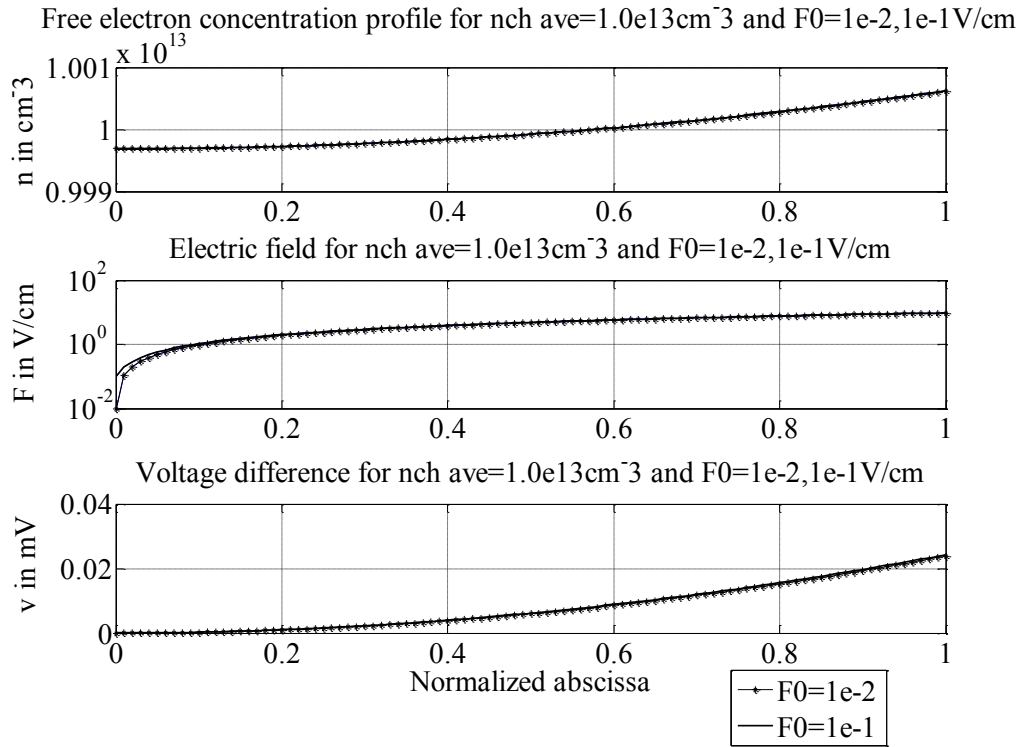


Figure 5-8: (n_{ch}, F, v) for input $(n_{ch\ ave}, th_{GaN})=(10^{+13}\text{cm}^{-3}, 10^{-2}\backslash 10^{-1}\text{V/cm}, 50\text{nm})$

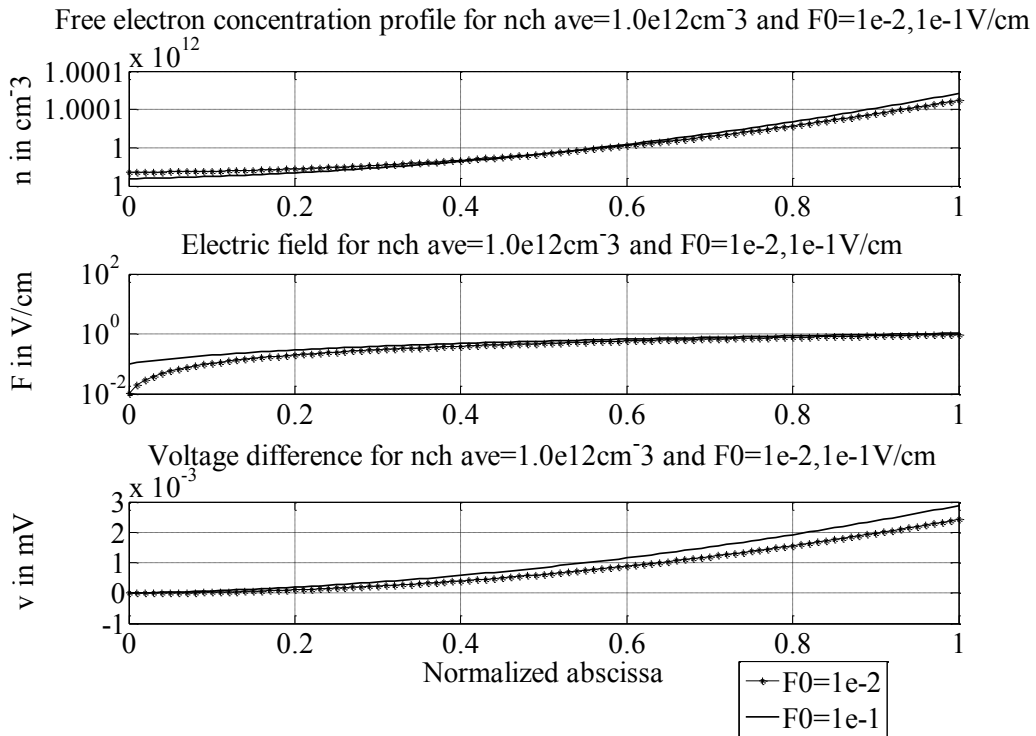


Figure 5-9: (n_{ch}, F, v) for input $(n_{ch\ ave}, th_{GaN})=(10^{+12}\text{cm}^{-3}, 10^{-2}\backslash 10^{-1}\text{V/cm}, 50\text{nm})$

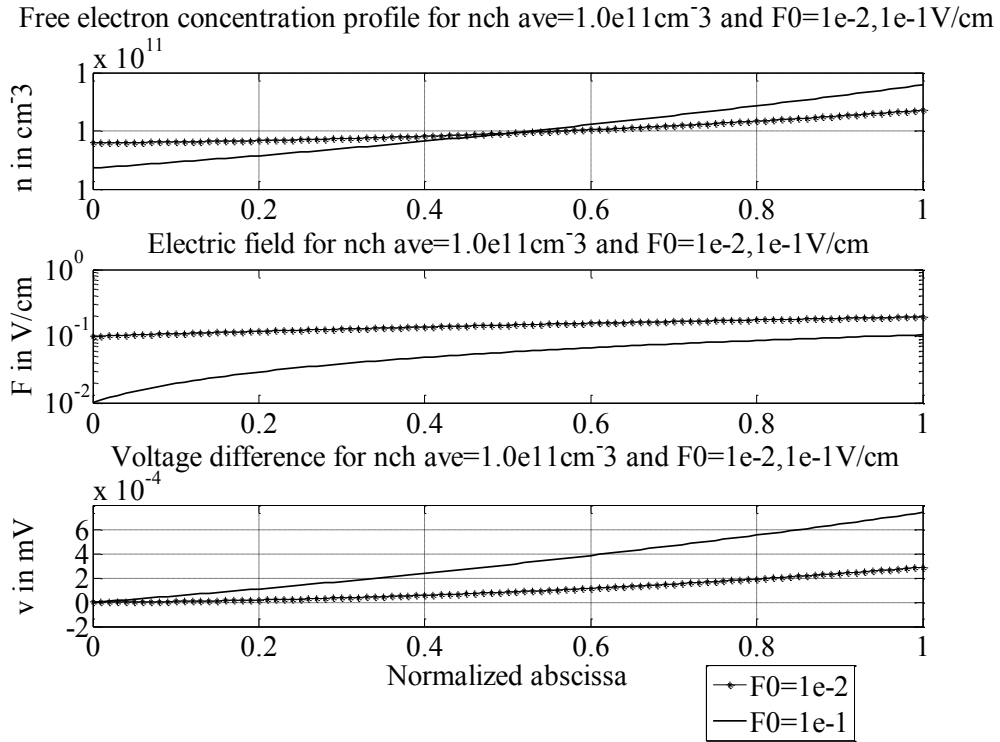


Figure 5-10: (n_{ch}, F, v) for input $(n_{ch\ ave}, th_{GaN})=(10^{+11}\text{cm}^{-3}, 10^{-2}\backslash 10^{-1}\text{V/cm}, 50\text{nm})$

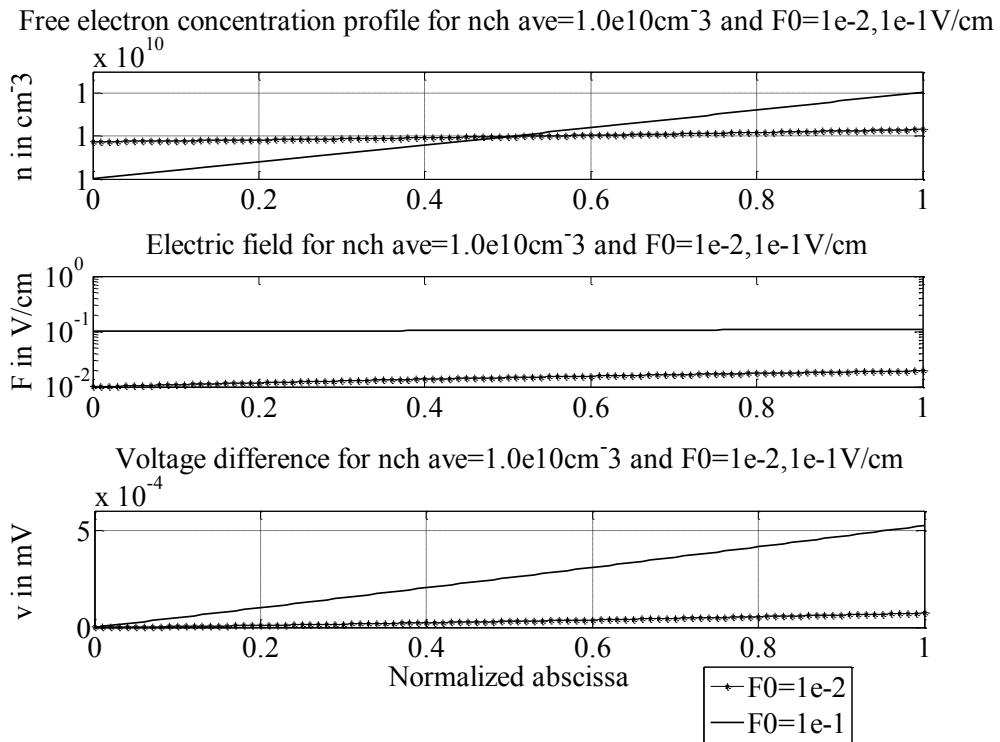


Figure 5-11: (n_{ch}, F, v) for input $(n_{ch\ ave}, th_{GaN})=(10^{+10}\text{cm}^{-3}, 10^{-2}\backslash 10^{-1}\text{V/cm}, 50\text{nm})$

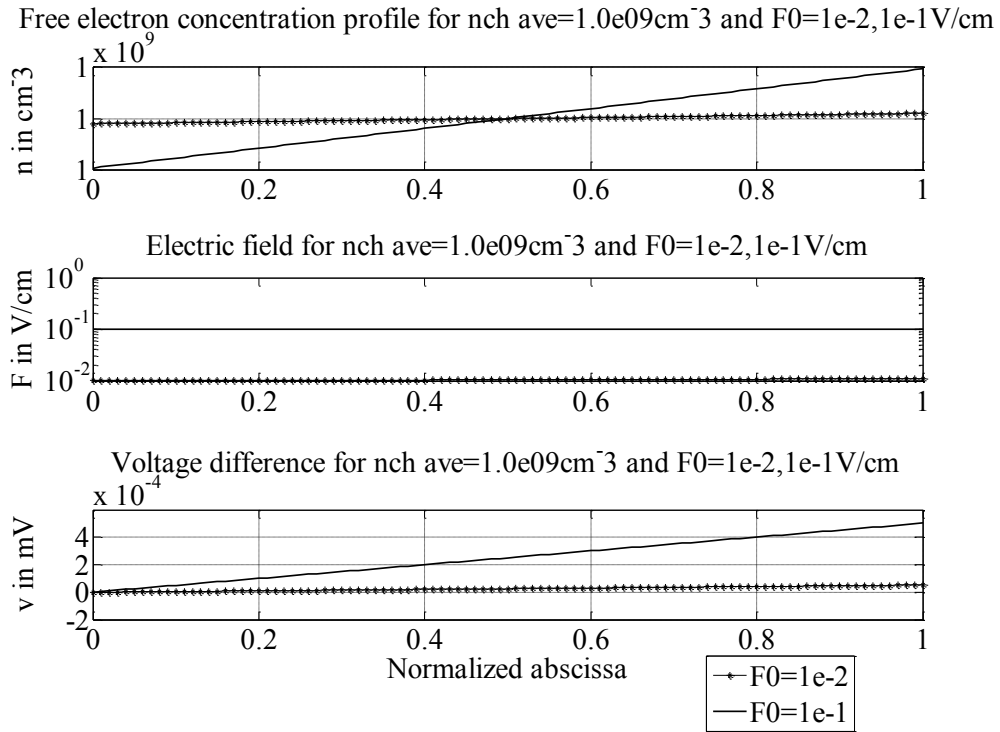


Figure 5-12: (n_{ch}, F, v) for input $(n_{ch\ ave}, th_{GaN})=(10^{+9}\text{cm}^{-3}, 10^{-2}\backslash 10^{-1}\text{V/cm}, 50\text{nm})$

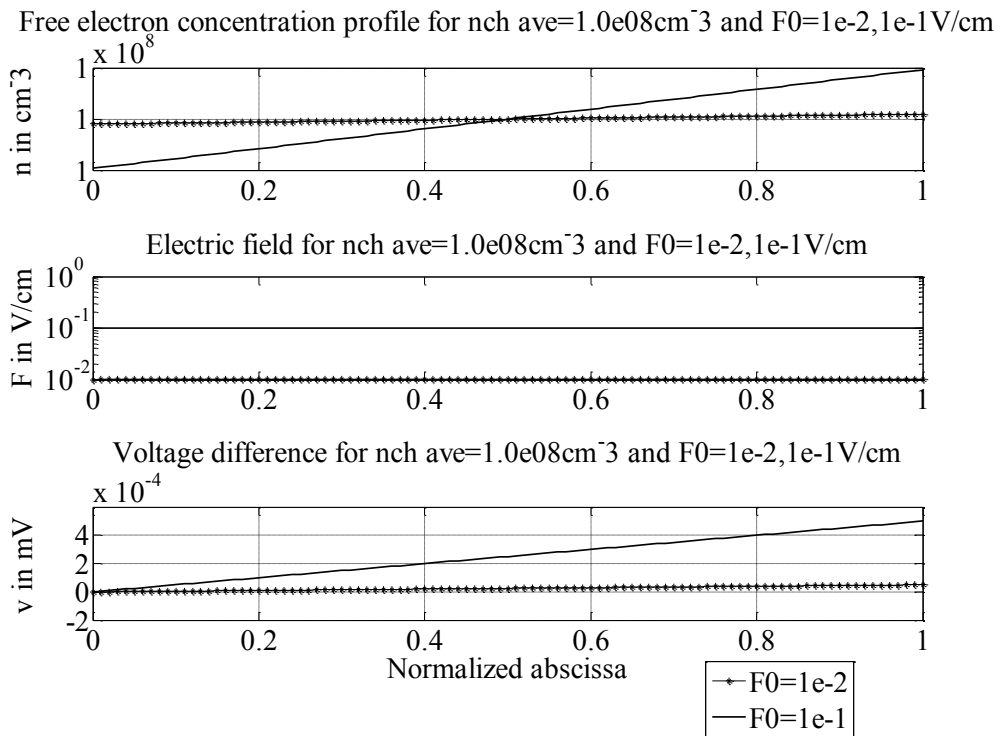


Figure 5-13: (n_{ch}, F, v) for input $(n_{ch\ ave}, th_{GaN})=(10^{+8}\text{cm}^{-3}, 10^{-2}\backslash 10^{-1}\text{V/cm}, 50\text{nm})$

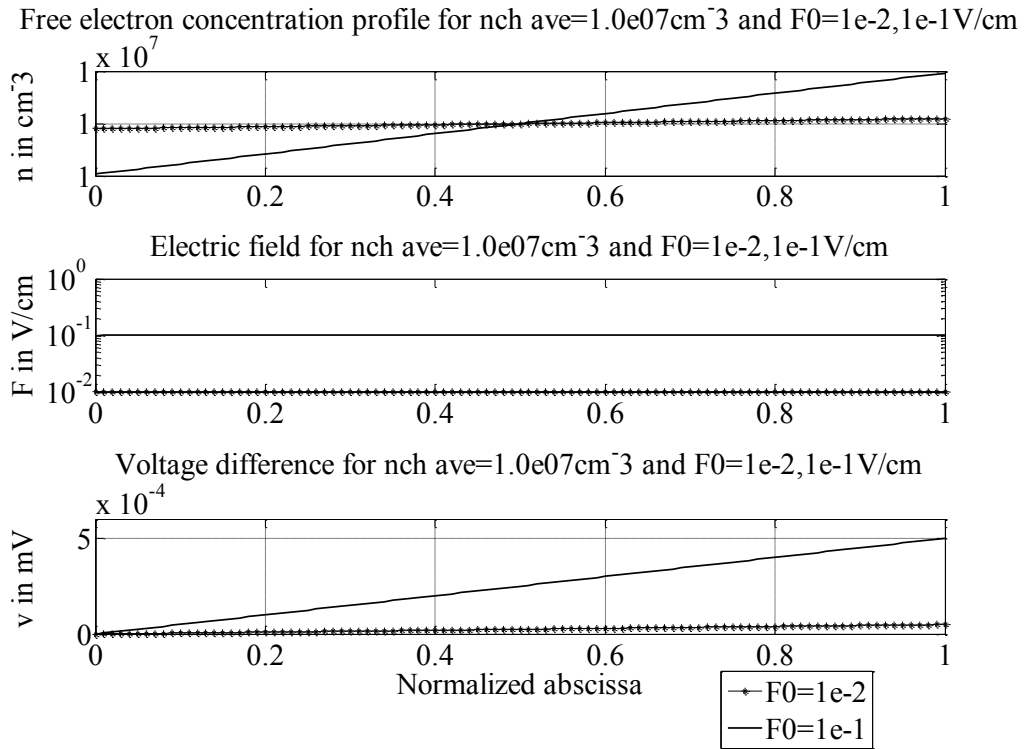


Figure 5-14: (n_{ch}, F, v) for input $(n_{ch\ ave}, th_{GaN})=(10^{+7}cm^{-3}, 10^{-2}\backslash 10^{-1}V/cm, 50nm)$

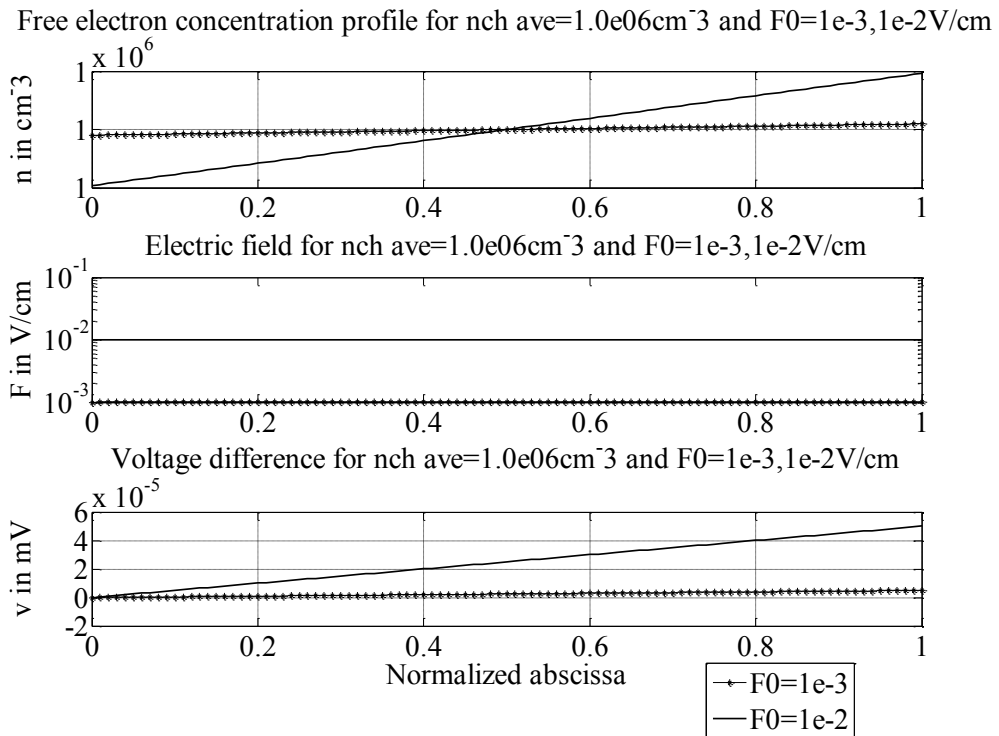


Figure 5-15: (n_{ch}, F, v) for input $(n_{ch\ ave}, th_{GaN})=(10^{+6}cm^{-3}, 10^{-3}\backslash 10^{-2}V/cm, 50nm)$

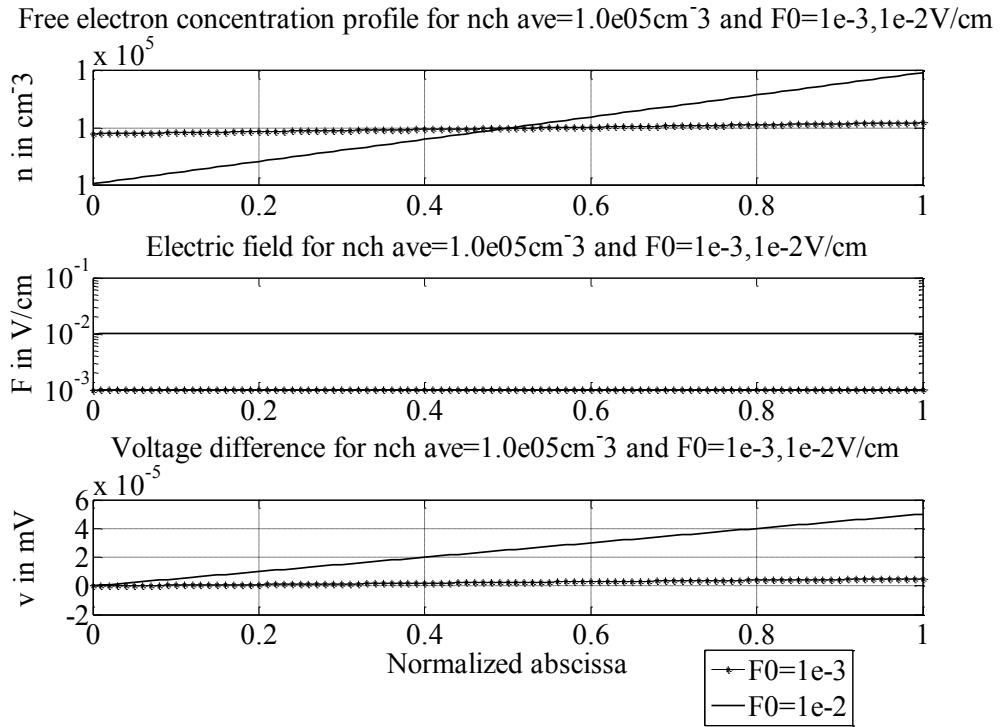


Figure 5-16: (n_{ch}, F, v) for input $(n_{ch\ ave}, th_{GaN})=(10^{+5}\text{cm}^{-3}, 10^{-3}\backslash 10^{-2}\text{V/cm}, 50\text{nm})$

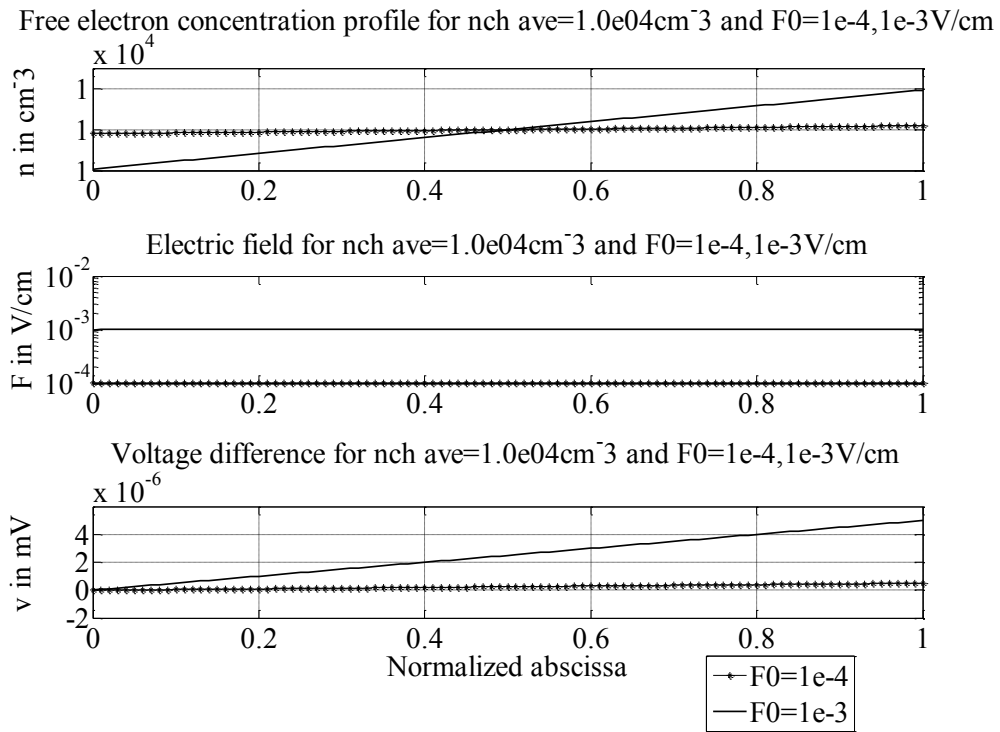


Figure 5-17: (n_{ch}, F, v) for input $(n_{ch\ ave}, th_{GaN})=(10^{+4}\text{cm}^{-3}, 10^{-4}\backslash 10^{-3}\text{V/cm}, 50\text{nm})$

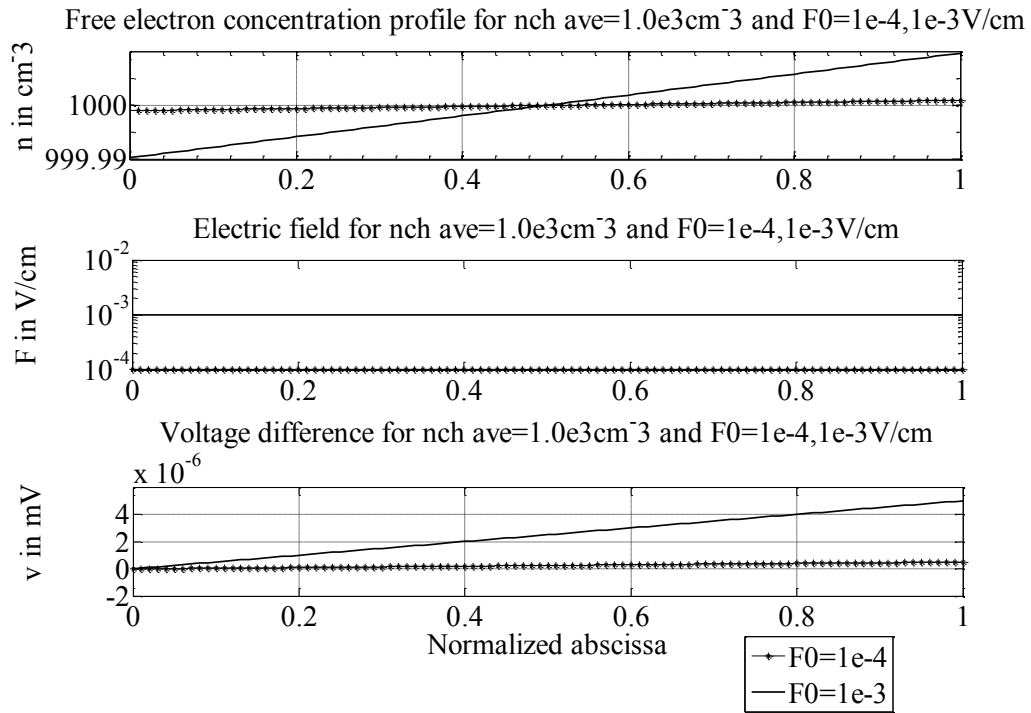


Figure 5-18: (n_{ch}, F, v) for input $(n_{ch\ ave}, th_{GaN})=(10^{+3}\text{cm}^{-3}, 10^{-4}\backslash 10^{-3}\text{V/cm}, 50\text{nm})$

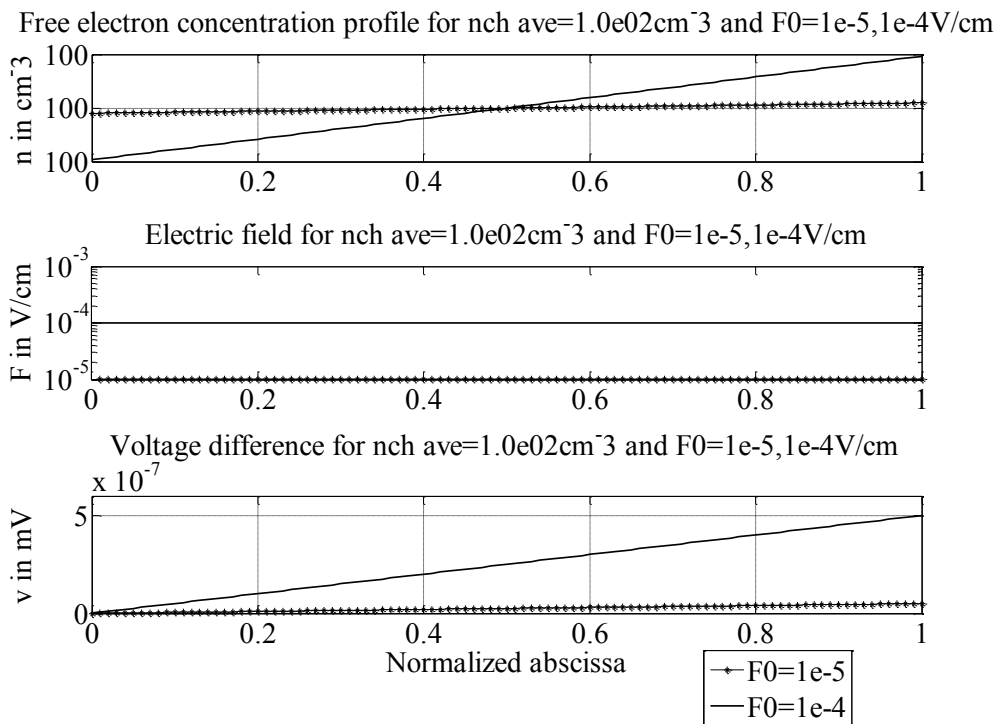


Figure 5-19: (n_{ch}, F, v) for input $(n_{ch\ ave}, th_{GaN})=(10^{+2}\text{cm}^{-3}, 10^{-5}\backslash 10^{-4}\text{V/cm}, 50\text{nm})$

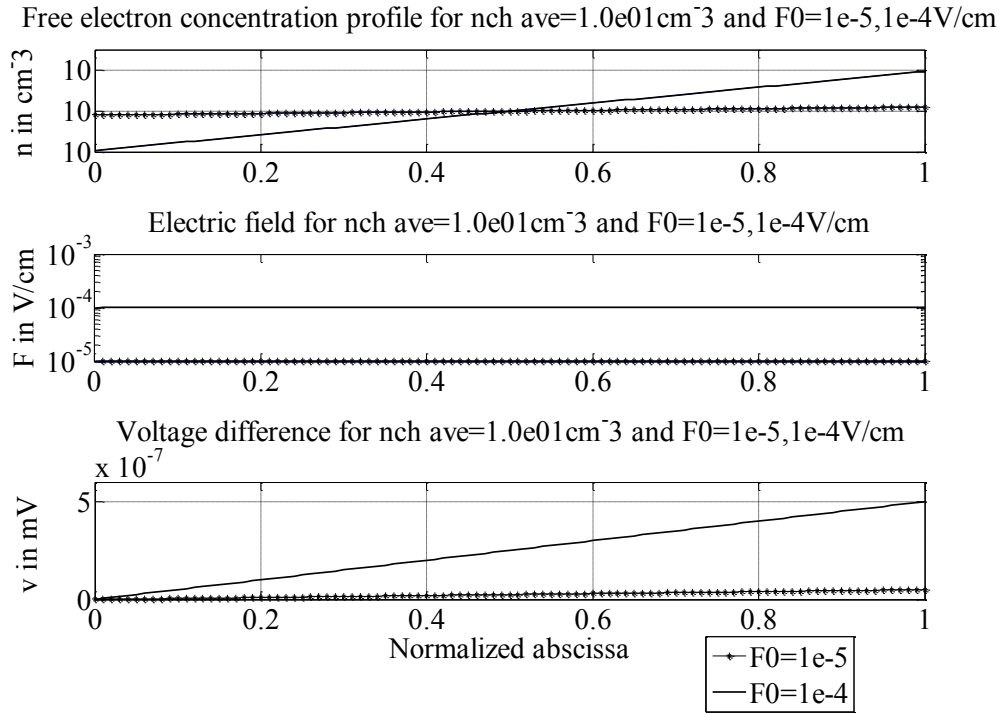


Figure 5-20: (n_{ch}, F, v) for input $(n_{ch\ ave}, th_{GaN})=(10^{+1}cm^{-3}, 10^{-5}10^{-4}V/cm, 50nm)$

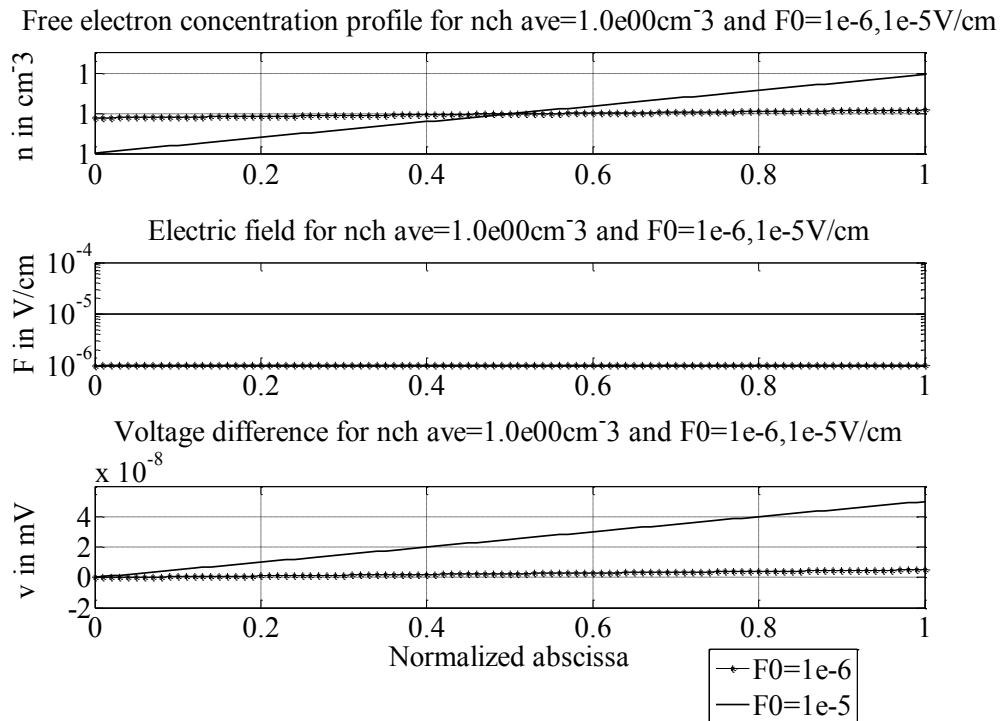


Figure 5-21: (n_{ch}, F, v) for input $(n_{ch\ ave}, th_{GaN})=(1cm^{-3}, 10^{-6}10^{-5}V/cm, 50nm)$

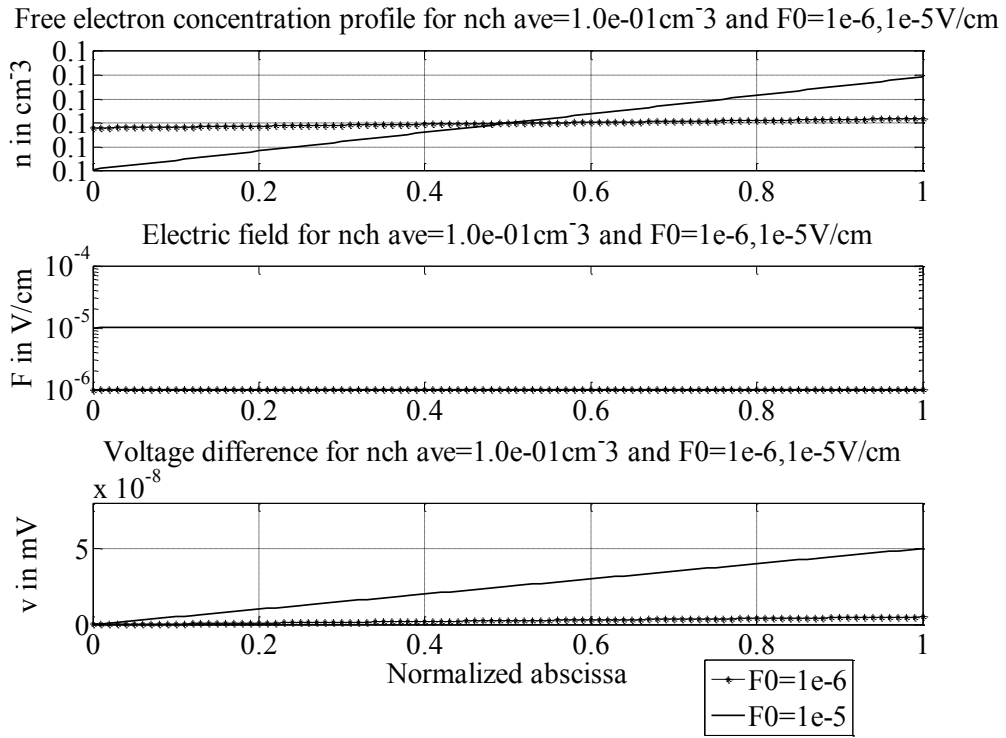


Figure 5-22: (n_{ch}, F, v) for input $(n_{ch\ ave}, th_{GaN})=(10^{-1}\text{cm}^{-3}, 10^{-6}\backslash 10^{-5}\text{V/cm}, 50\text{nm})$

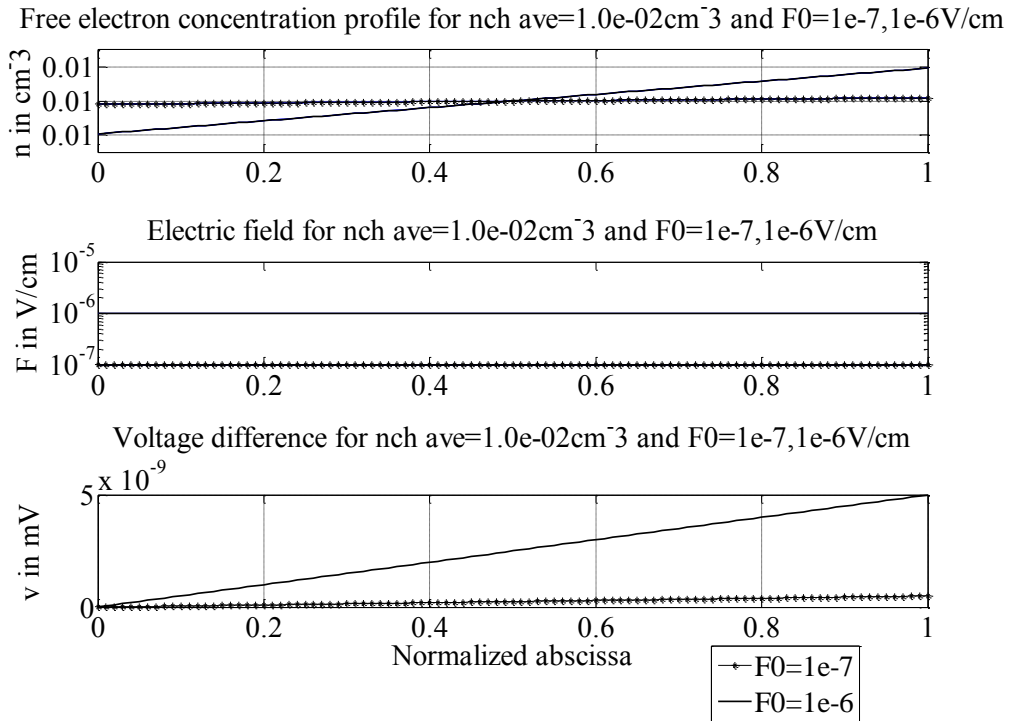


Figure 5-23: (n_{ch}, F, v) for input $(n_{ch\ ave}, th_{GaN})=(10^{-2}\text{cm}^{-3}, 10^{-7}\backslash 10^{-6}\text{V/cm}, 50\text{nm})$

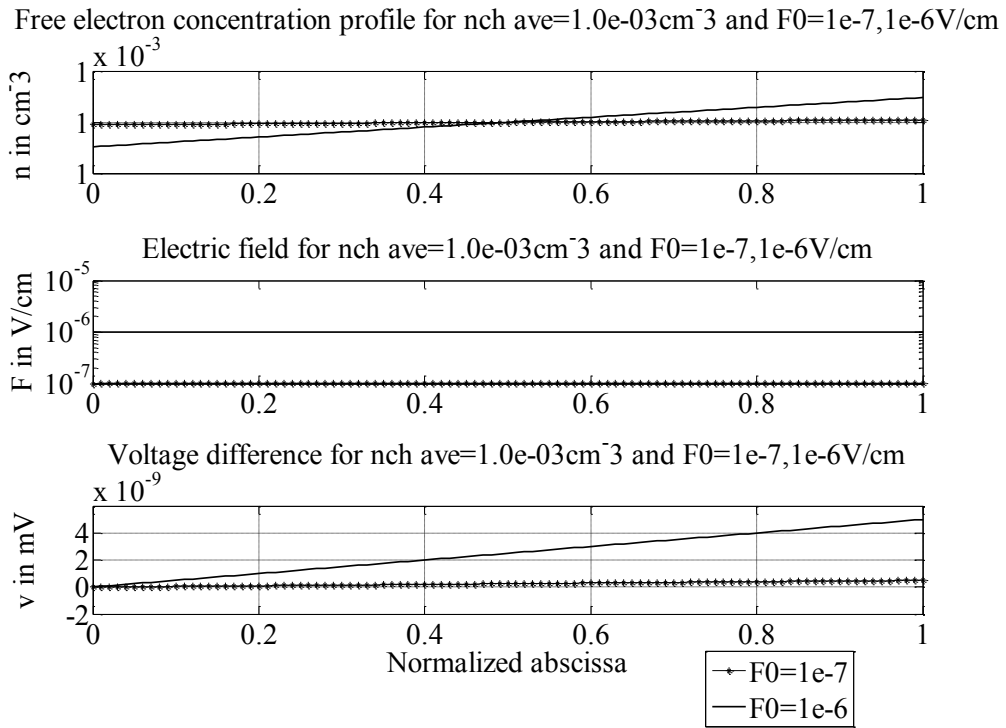


Figure 5-24: (n_{ch}, F, v) for input $(n_{ch\ ave}, th_{GaN})=(10^{-3}cm^{-3}, 10^{-7}\backslash 10^{-6}V/cm, 50nm)$

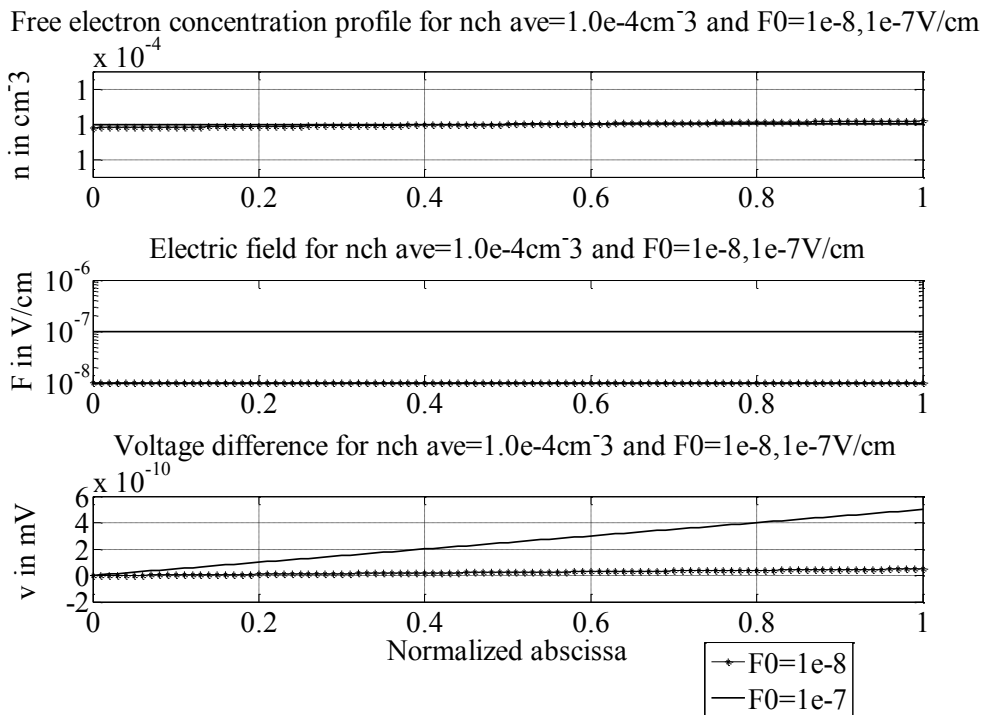


Figure 5-25: (n_{ch}, F, v) for input $(n_{ch\ ave}, th_{GaN})=(10^{-4}cm^{-3}, 10^{-8}\backslash 10^{-7}V/cm, 50nm)$

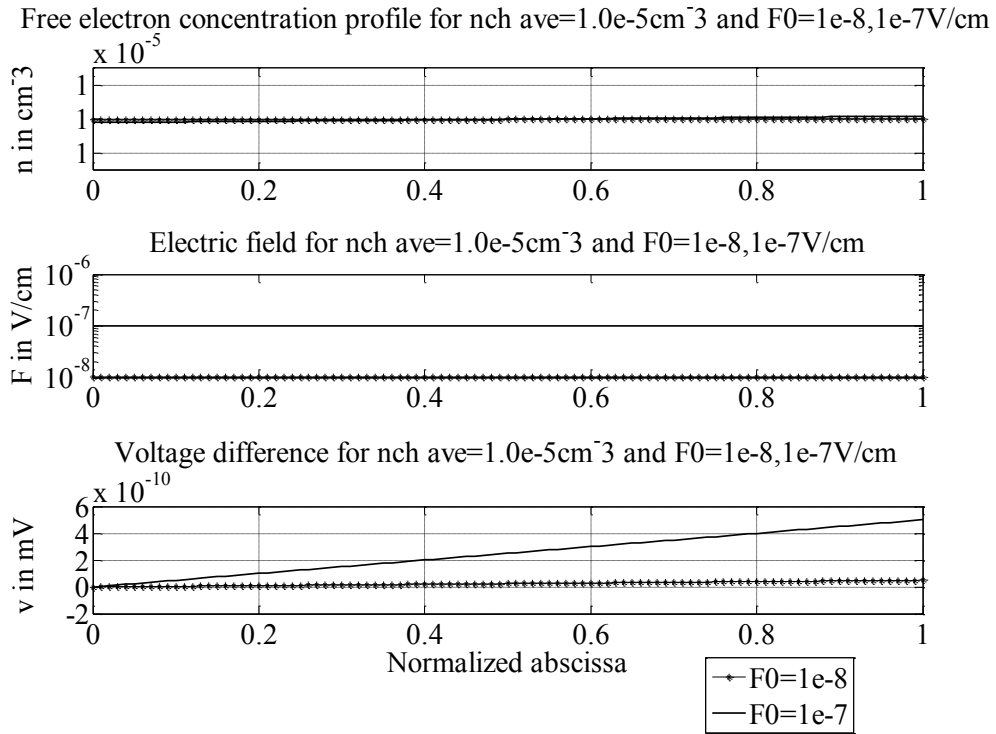


Figure 5-26: (n_{ch}, F, v) for input $(n_{ch\ ave}, th_{GaN})=(10^{-5}\text{cm}^{-3}, 10^{-8}\text{V/cm}, 50\text{nm})$

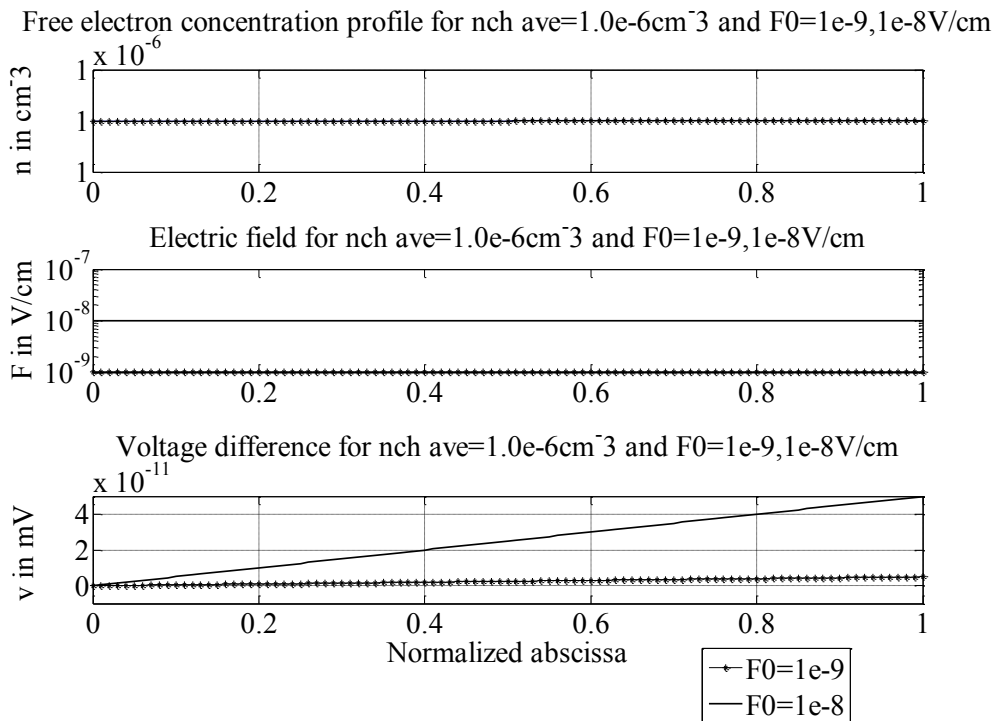


Figure 5-27: (n_{ch}, F, v) for input $(n_{ch\ ave}, th_{GaN})=(10^{-6}\text{cm}^{-3}, 10^{-9}\text{V/cm}, 50\text{nm})$

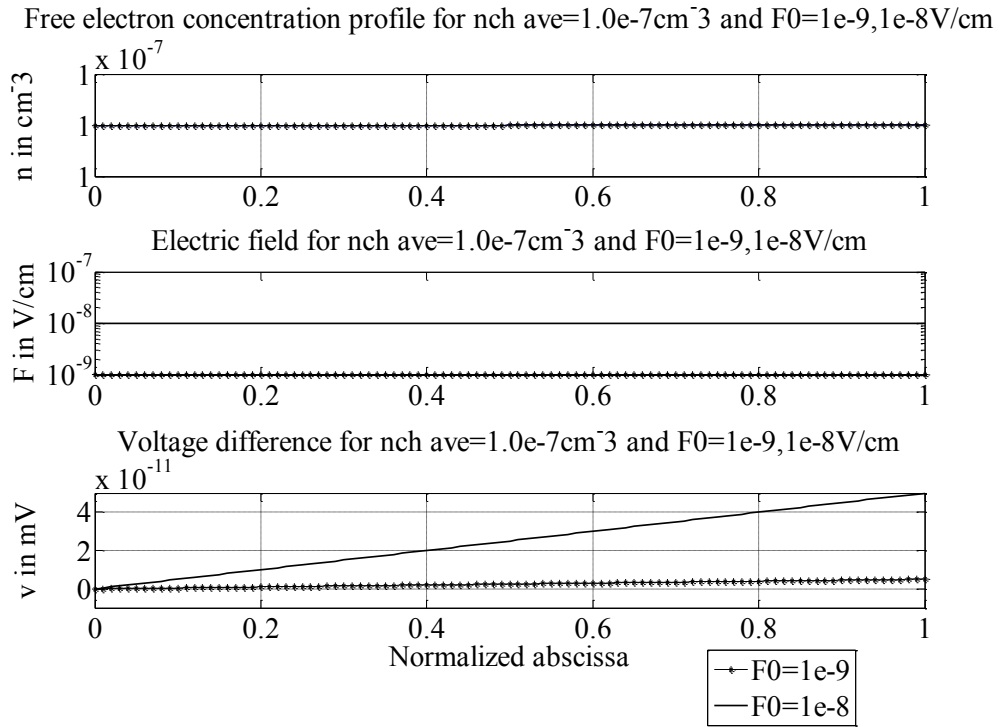


Figure 5-28: (n_{ch}, F, v) for input $(n_{ch\ ave}, th_{GaN})=(10^{-7}cm^{-3}, 10^{-9}\backslash 10^{-8}V/cm, 50nm)$

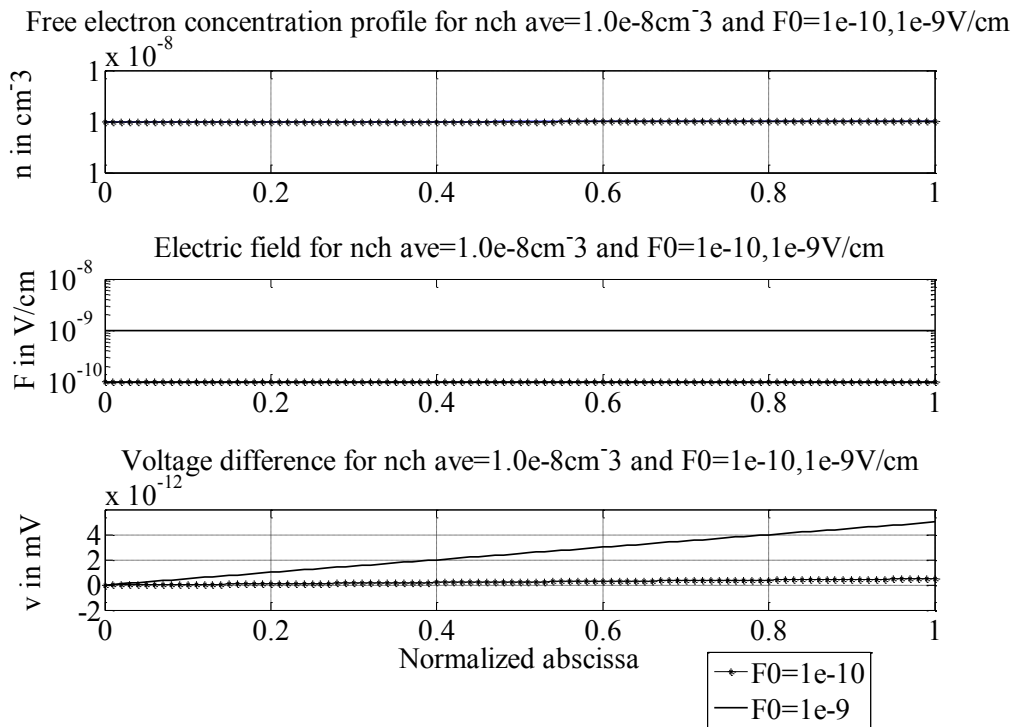


Figure 5-29: (n_{ch}, F, v) for input $(n_{ch\ ave}, th_{GaN})=(10^{-8}cm^{-3}, 10^{-10}\backslash 10^{-9}V/cm, 50nm)$

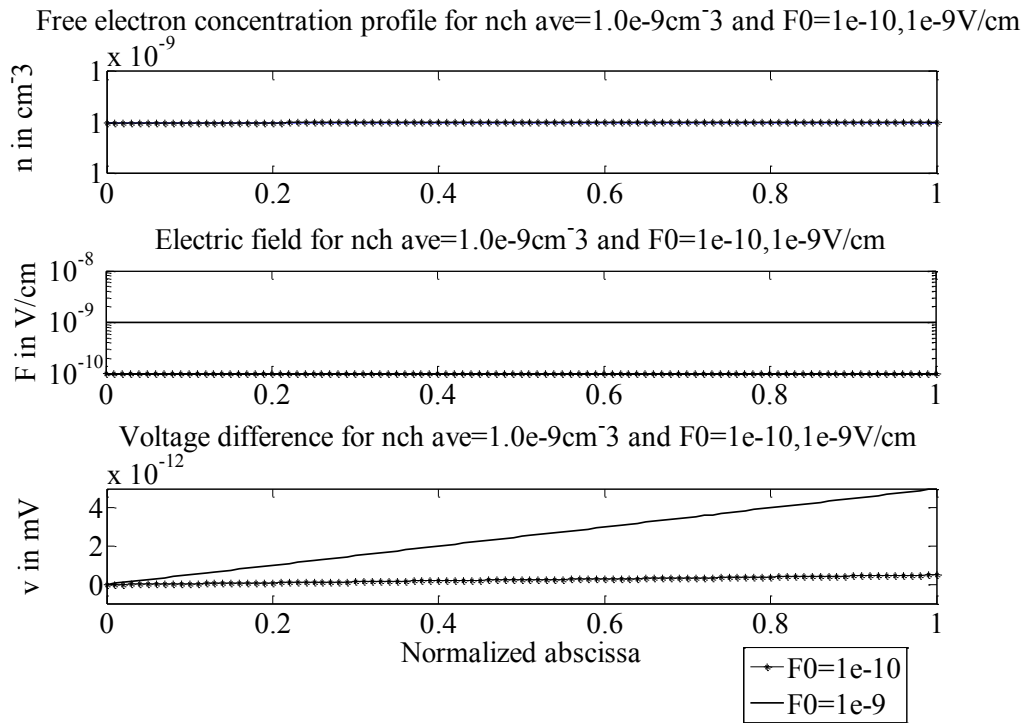


Figure 5-30: (n_{ch}, F, v) for input $(n_{ch\ ave}, th_{GaN})=(10^{-9}cm^{-3}, 10^{-10}\backslash 10^{-9}V/cm, 50nm)$

Table 5-1: Initial and final values for the free electron concentration, and the electric field, and the voltage drop across GaN layer of 50nm thickness (weak initial field)

$\overline{n_{ch}}$ (cm ⁻³)	F_0 (V/cm)	n_0 (cm ⁻³)	n_1 (cm ⁻³)	F_0 (computed) (V/cm)	F_1 (V/cm)	$F_deviation$ (%)	v (mV)
1.00E-09	1.00E-10	9.9999999999994E-10	1.0000000000001E-09	1.0000000000000E-10	1.0000000000953E-10	9.52E-10	5.05398702466815E-13
1.00E-09	1.00E-09	9.9999999999903E-10	1.0000000000010E-09	1.0000000000000E-09	1.0000000000095E-09	9.52E-11	5.00229852100633E-12
1.00E-08	1.00E-10	9.999999999990E-09	1.0000000000001E-08	1.0000000000006E-10	1.0000000009530E-10	9.52E-09	4.99655535393328E-13
1.00E-08	1.00E-09	9.9999999999903E-09	1.0000000000010E-08	9.999999999998E-10	1.0000000000952E-09	9.52E-10	4.99081218685936E-12
1.00E-07	1.00E-09	9.9999999999904E-08	1.0000000000010E-07	1.0000000000001E-09	1.0000000009525E-09	9.52E-09	4.99655535393285E-12
1.00E-07	1.00E-08	9.99999999999037E-08	1.0000000000097E-07	1.0000000000000E-08	1.000000000952E-08	9.52E-10	4.99942693746524E-11
1.00E-06	1.00E-09	9.9999999999903E-07	1.0000000000010E-06	1.0000000000001E-09	1.0000000095239E-09	9.52E-08	5.00229852100633E-12
1.00E-06	1.00E-08	9.99999999999033E-07	1.0000000000097E-06	1.0000000000000E-08	1.000000009524E-08	9.52E-09	4.99942693746524E-11
1.00E-05	1.00E-08	9.99999999999033E-06	1.0000000000097E-05	1.0000000000002E-08	1.0000000095239E-08	9.52E-08	5.00000125417259E-11
1.00E-05	1.00E-07	9.999999999990334E-06	1.00000000000967E-05	1.0000000000000E-07	1.000000009524E-07	9.52E-09	5.00005868579983E-10
1.00E-04	1.00E-08	9.99999999999034E-05	1.0000000000097E-04	1.0000000000013E-08	1.0000000952388E-08	9.52E-07	5.00000125417259E-11
1.00E-04	1.00E-07	9.999999999990334E-05	1.00000000000967E-04	9.999999999999E-08	1.0000000095237E-07	9.52E-08	5.00005868579983E-10
1.00E-03	1.00E-07	9.999999999990338E-04	1.00000000000967E-03	9.999999999990E-08	1.0000000952374E-07	9.52E-07	5.00005868579983E-10
1.00E-03	1.00E-06	9.9999999999903344E-04	1.00000000009666E-03	1.0000000000000E-06	1.000000095238E-06	9.52E-08	4.99999551052707E-09

Table 5-1 (cont'd): Initial and final values for the free electron concentration, and the electric field, and the voltage drop across GaN layer of 50nm thickness (weak initial field)

$\overline{n_{ch}}$ (cm ⁻³)	F_0 (V/cm)	n_0 (cm ⁻³)	n_1 (cm ⁻³)	F_0 (computed) (V/cm)	F_1 (V/cm)	$F_deviation$ (%)	v (mV)
1.00E-02	1.00E-07	9.9999999990334E-03	1.0000000000967E-02	1.0000000000015E-07	1.00000009523766E-07	9.52E-06	5.00000125412909E-10
1.00E-02	1.00E-06	9.9999999903343E-03	1.00000000009665E-02	9.999999999998E-07	1.0000000952375E-06	9.52E-07	4.99998976735999E-09
1.00E-01	1.00E-06	9.9999999903344E-02	1.00000000009666E-01	9.999999999977E-07	1.00000009523748E-06	9.52E-06	5.00000699686121E-09
1.00E-01	1.00E-05	9.9999999033440E-02	1.00000000096656E-01	1.0000000000000E-05	1.0000000952375E-05	9.52E-07	5.0000010071121E-08
1.00E+00	1.00E-06	9.9999999903359E-01	1.0000000009667E+00	9.999999999875E-07	1.00000095237494E-06	9.52E-05	4.99999551052707E-09
1.00E+00	1.00E-05	9.9999999033455E-01	1.00000000096657E+00	1.0000000000000E-05	1.0000009523751E-05	9.52E-06	5.0000010071121E-08
1.00E+01	1.00E-05	9.9999999033438E+00	1.00000000096656E+01	1.0000000000003E-05	1.00000095237509E-05	9.52E-05	5.00000182366133E-08
1.00E+01	1.00E-04	9.99999990334396E+00	1.00000000966560E+01	1.0000000000000E-04	1.0000009523751E-04	9.52E-06	5.00000022951102E-07
1.00E+02	1.00E-05	9.9999999033436E+01	1.00000000096657E+02	9.999999999751E-06	1.00000952375038E-05	9.52E-04	5.00002422201287E-08
1.00E+02	1.00E-04	9.99999990334390E+01	1.00000000966560E+02	9.999999999998E-05	1.00000095237506E-04	9.52E-05	5.00000241191446E-07
1.00E+03	1.00E-04	9.99999990334374E+02	1.00000000966566E+03	1.0000000000001E-04	1.00000952375065E-04	9.52E-04	5.00002383392723E-07
1.00E+03	1.00E-03	9.99999903343980E+02	1.00000009665606E+03	1.0000000000000E-03	1.00000095237506E-03	9.52E-05	5.00000238472691E-06
1.00E+04	1.00E-04	9.99999990334084E+03	1.00000000966620E+04	1.0000000000009E-04	1.00009523750643E-04	9.52E-03	5.00023811148660E-07

Table 5-1 (cont'd): Initial and final values for the free electron concentration and the electric field, and the voltage drop across GaN layer of 50nm thickness (weak initial field)

\bar{n}_{ch} (cm ⁻³)	F_0 (V/cm)	n_0 (cm ⁻³)	n_1 (cm ⁻³)	F_0 (computed) (V/cm)	F_1 (V/cm)	$F_deviation$ (%)	v (mV)
1.00E+04	1.00E-03	9.99999903343705E+03	1.00000009665661E+04	1.00000000000000E-03	1.00000952375064E-03	9.52E-04	5.00002380673596E-06
1.00E+05	1.00E-03	9.99999903340940E+04	1.00000009666213E+05	1.00000000000002E-03	1.00009523750636E-03	9.52E-03	5.00023810148754E-06
1.00E+05	1.00E-02	9.99999033437327E+04	1.00000096656638E+05	1.00000000000000E-02	1.00000952375063E-02	9.52E-04	5.00002380934381E-05
1.00E+06	1.00E-03	9.99999903313468E+05	1.00000009671751E+06	9.9999999999739E-04	1.00095237506314E-03	9.52E-02	5.00238093413999E-06
1.00E+06	1.00E-02	9.99999033409706E+05	1.00000096662160E+06	1.00000000000000E-02	1.00009523750634E-02	9.52E-03	5.00023809338487E-05
1.00E+07	1.00E-02	9.99999033133503E+06	1.00000096717388E+07	1.00000000000002E-02	1.00095237506343E-02	9.52E-02	5.00238093666611E-05
1.00E+07	1.00E-01	9.99990334125097E+06	1.00000966624408E+07	1.00000000000000E-01	1.00009523750634E-01	9.52E-03	5.00023809300184E-04
1.00E+08	1.00E-02	9.99999030371973E+07	1.00000097269709E+08	9.9999999999961E-03	1.00952375063402E-02	9.52E-01	5.02380936880660E-05
1.00E+08	1.00E-01	9.99990331363520E+07	1.00000967176725E+08	9.9999999999999E-02	1.00095237506340E-01	9.52E-02	5.00238092994736E-04
1.00E+09	1.00E-02	9.99999002756171E+08	1.00000102792877E+09	1.00000000000126E-02	1.09523750634181E-02	9.52E+00	5.23809368504191E-05
1.00E+09	1.00E-01	9.99990303747961E+08	1.00000972699917E+09	1.00000000000000E-01	1.00952375063406E-01	9.52E-01	5.02380929951735E-04
1.00E+10	1.00E-02	9.99998726598238E+09	1.00000158024565E+10	1.00000000002515E-02	1.95237506343070E-02	9.52E+01	7.38093652685331E-05
1.00E+10	1.00E-01	9.99990027592431E+09	1.00001027931846E+10	1.0000000000010E-01	1.09523750634066E-01	9.52E+00	5.23809296224358E-04
1.00E+11	1.00E-02	9.99995965025661E+10	1.00000710342118E+11	1.00000000015384E-02	1.05237506342094E-01	9.52E+02	2.88093323865519E-04
1.00E+11	1.00E-01	9.99987266043880E+10	1.00001580251801E+11	1.0000000000028E-01	1.95237506340584E-01	9.52E+01	7.38092633458408E-04

Table 5-1 (cont'd): Initial and final values for the free electron concentration and the electric field, and the voltage drop across GaN layer of 50nm thickness (weak initial field)

\bar{n}_{ch} (cm ⁻³)	F_0 (V/cm)	n_0 (cm ⁻³)	n_1 (cm ⁻³)	F_0 (computed) (V/cm)	F_1 (V/cm)	$F_deviation$ (%)	v (mV)
1.00E+12	1.00E-02	9.99968349970994E+11	1.00006233584762E+12	1.00000000190377E-02	9.62375063424593E-01	9.52E+03	2.43090036331983E-03
1.00E+12	1.00E-01	9.99959651229436E+11	1.00007103518467E+12	9.9999999989261E-02	1.05237506340448E+00	9.52E+02	2.88089345933737E-03
1.00E+13	1.00E-02	9.99692266522992E+12	1.00061472721057E+13	9.9999989141552E-03	9.53375063394685E+00	9.52E+04	2.38557164982275E-02
1.00E+13	1.00E-01	9.99683570183255E+12	1.00062342894946E+13	9.9999999751378E-02	9.62375063403065E+00	9.52E+03	2.43056474675537E-02
1.00E+14	1.00E-02	9.96938130162913E+13	1.00614533896031E+14	1.00000000913163E-02	9.52475063406475E+01	9.52E+05	2.37778851165481E-01
1.00E+14	1.00E-01	9.96929457797583E+13	1.00615406467358E+14	1.00000000010331E-01	9.53375063405658E+01	9.52E+04	2.38228161618813E-01
1.00E+15	1.00E-02	9.70054907509055E+14	1.06210959739941E+15	9.99997713082546E-03	9.52385063380514E+02	9.52E+06	2.34490686564022E+00
1.00E+15	1.00E-01	9.70046470506161E+14	1.06211855847989E+15	9.9999996647913E-02	9.52475063405186E+02	9.52E+05	2.34535004843799E+00
1.00E+16	1.00E-02	7.56371402058978E+15	1.67690090296758E+16	1.00000823361356E-02	9.52376063423807E+03	9.52E+07	2.05928810346977E+01
1.00E+16	1.00E-01	7.56364902744476E+15	1.67691180168784E+16	9.9999800148333E-02	9.52385063401124E+03	9.52E+06	2.05932713905800E+01
1.00E+17	1.00E-02	2.18419143094493E+16	9.42369675140983E+17	9.99971935197382E-03	9.52375163284544E+04	9.52E+08	9.73702392038633E+01
1.00E+17	1.00E-01	2.18417474010874E+16	9.42371248305366E+17	1.00000037098578E-01	9.52376063421568E+04	9.52E+07	9.73704800335524E+01

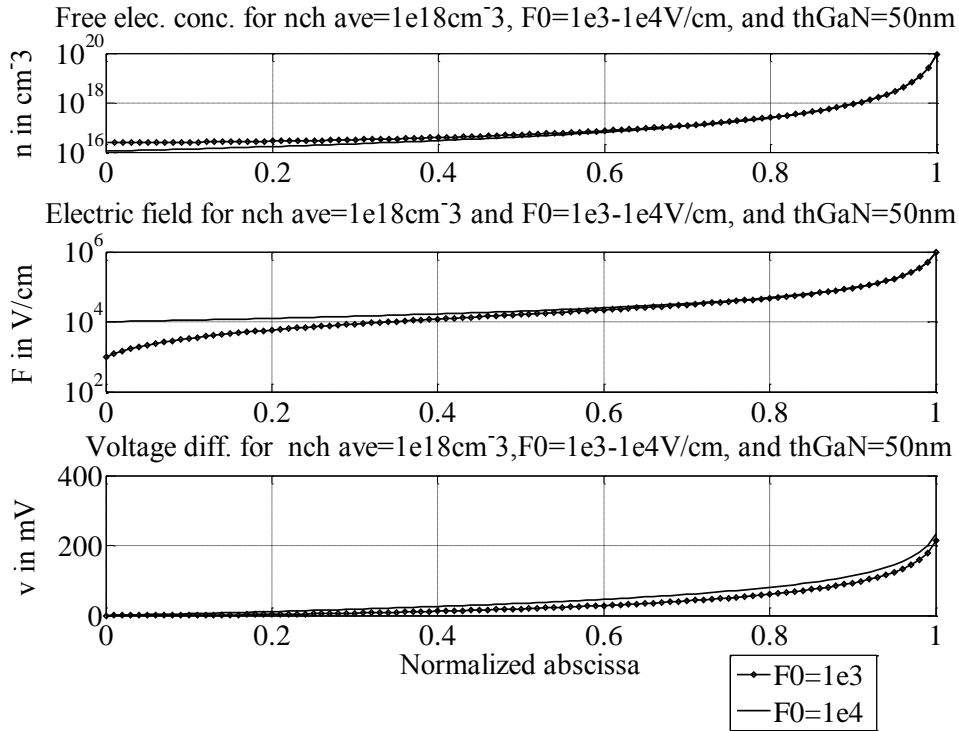


Figure 5-31: (n_{ch}, F, v) for input $(n_{ch\ ave}, th_{GaN}) = (10^{+18} \text{ cm}^{-3}, 5 \cdot 10^{+3} \setminus 10^{+4} \text{ V/cm}, 50 \text{ nm})$

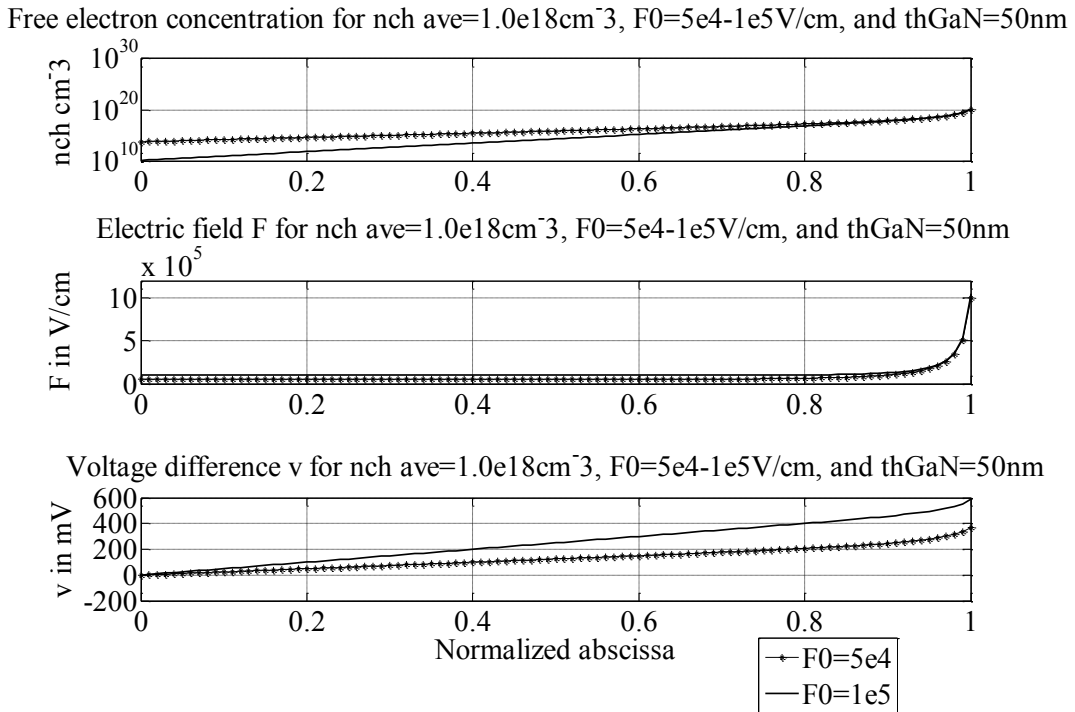
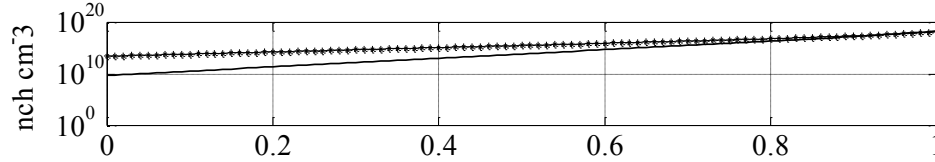
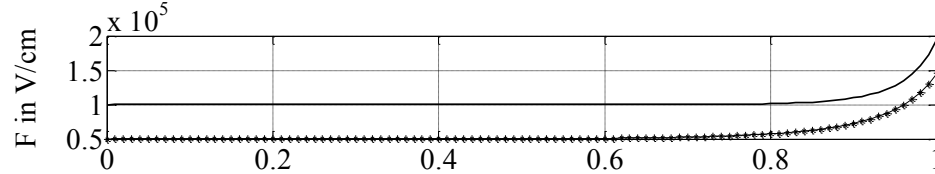


Figure 5-32: (n_{ch}, F, v) for input $(n_{ch\ ave}, th_{GaN}) = (10^{+18} \text{ cm}^{-3}, 5 \cdot 10^{+4} \setminus 10^{+5} \text{ V/cm}, 50 \text{ nm})$

Free electron concentration for $n_{ch\ ave}=1.0e17cm^{-3}$, $F_0=5e4-1e5V/cm$, and $th_{GaN}=50nm$



Electric field F for $n_{ch\ ave}=1.0e17cm^{-3}$, $F_0=5e4-1e5V/cm$, and $th_{GaN}=50nm$



Voltage difference v for $n_{ch\ ave}=1.0e17cm^{-3}$, $F_0=5e4-1e5V/cm$, and $th_{GaN}=50nm$

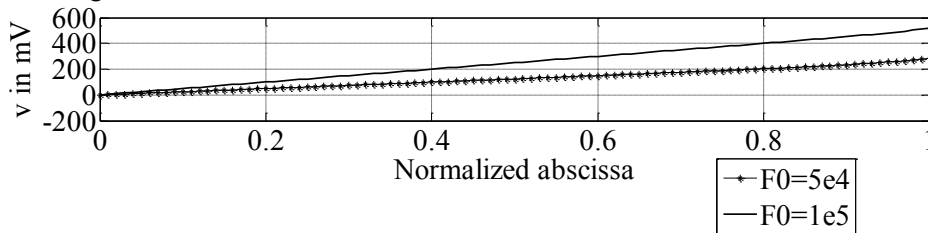
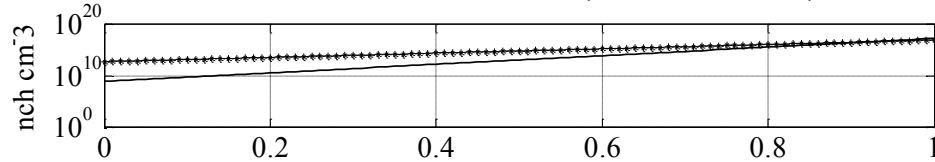
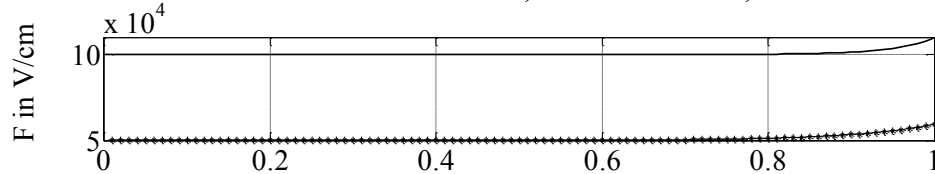


Figure 5-33: (n_{ch}, F, v) for input $(n_{ch\ ave}, th_{GaN})=(10^{+17}cm^{-3}, 5*10^{+4}\backslash 10^{+5}V/cm, 50nm)$

Free electron concentration for $n_{ch\ ave}=1.0e16cm^{-3}$, $F_0=5e4-1e5V/cm$, and $th_{GaN}=50nm$



Electric field F for $n_{ch\ ave}=1.0e16cm^{-3}$, $F_0=5e4-1e5V/cm$, and $th_{GaN}=50nm$



Voltage difference v for $n_{ch\ ave}=1.0e16cm^{-3}$, $F_0=5e4-1e5V/cm$, and $th_{GaN}=50nm$

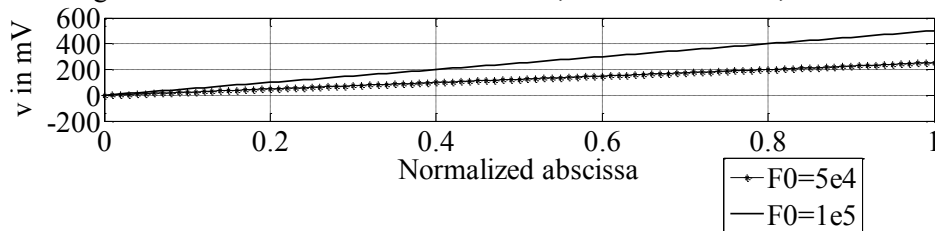
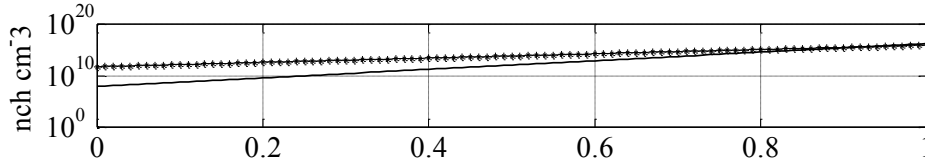
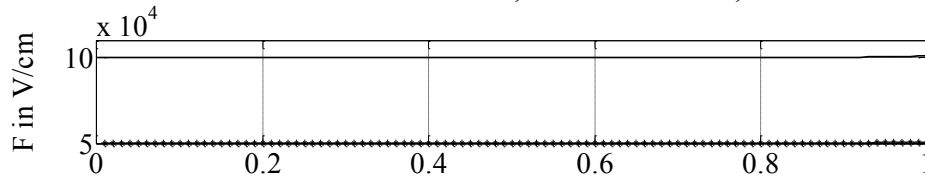


Figure 5-34: (n_{ch}, F, v) for input $(n_{ch\ ave}, th_{GaN})=(10^{+16}cm^{-3}, 5*10^{+4}\backslash 10^{+5}V/cm, 50nm)$

Free electron concentration for $n_{ch\ ave}=1.0e15cm^{-3}$, $F_0=5e4-1e5V/cm$, and $th_{GaN}=50nm$



Electric field F for $n_{ch\ ave}=1.0e15cm^{-3}$, $F_0=5e4-1e5V/cm$, and $th_{GaN}=50nm$



Voltage difference v for $n_{ch\ ave}=1.0e15cm^{-3}$, $F_0=5e4-1e5V/cm$, and $th_{GaN}=50nm$

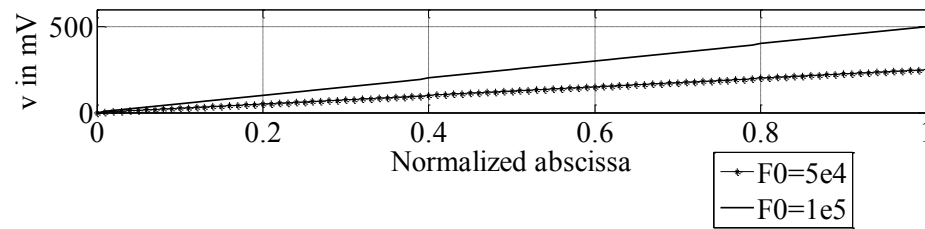
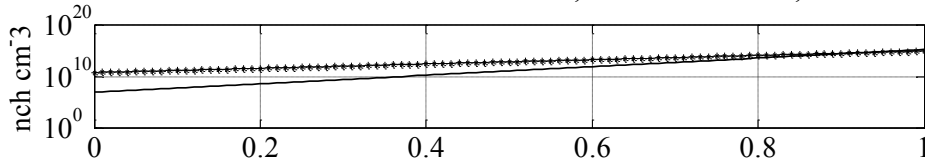
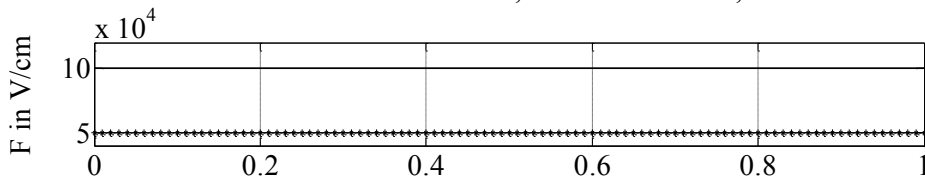


Figure 5-35: (n_{ch}, F, v) for input $(n_{ch\ ave}, th_{GaN})=(10^{+15}cm^{-3}, 5*10^{+4}\backslash 10^{+5}V/cm, 50nm)$

Free electron concentration for $n_{ch\ ave}=1.0e14cm^{-3}$, $F_0=5e4-1e5V/cm$, and $th_{GaN}=50nm$



Electric field F for $n_{ch\ ave}=1.0e14cm^{-3}$, $F_0=5e4-1e5V/cm$, and $th_{GaN}=50nm$



Voltage difference v for $n_{ch\ ave}=1.0e14cm^{-3}$, $F_0=5e4-1e5V/cm$, and $th_{GaN}=50nm$

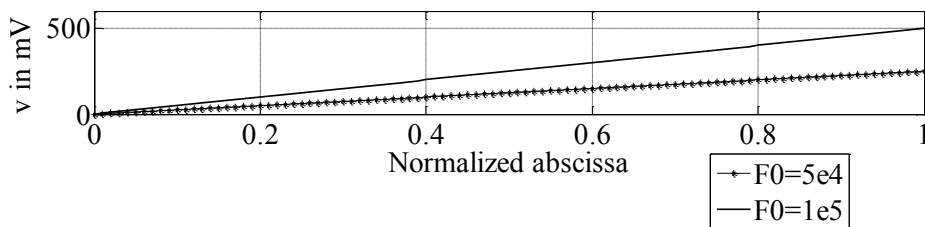
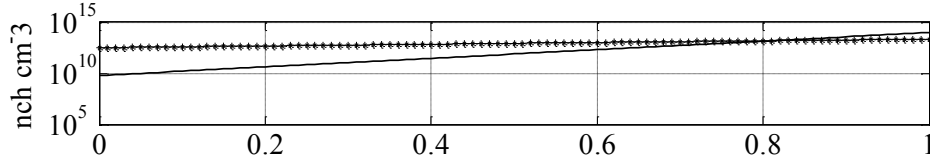
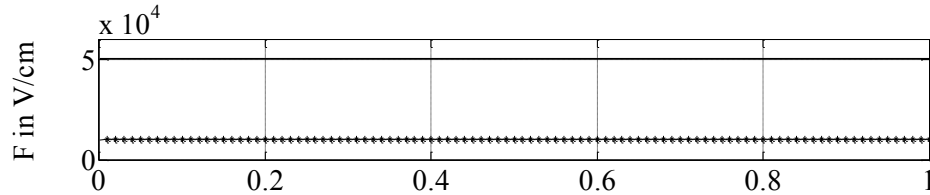


Figure 5-36: (n_{ch}, F, v) for input $(n_{ch\ ave}, th_{GaN})=(10^{+14}cm^{-3}, 5*10^{+4}\backslash 10^{+5}V/cm, 50nm)$

Free electron concentration for $n_{ch\ ave}=1.0e13cm^{-3}$, $F_0=1e4-5e4V/cm$, and $th_{GaN}=50nm$



Electric field F for $n_{ch\ ave}=1.0e13cm^{-3}$, $F_0=1e4-5e4V/cm$, and $th_{GaN}=50nm$



Voltage difference v for $n_{ch\ ave}=1.0e13cm^{-3}$, $F_0=1e4-5e4V/cm$, and $th_{GaN}=50nm$

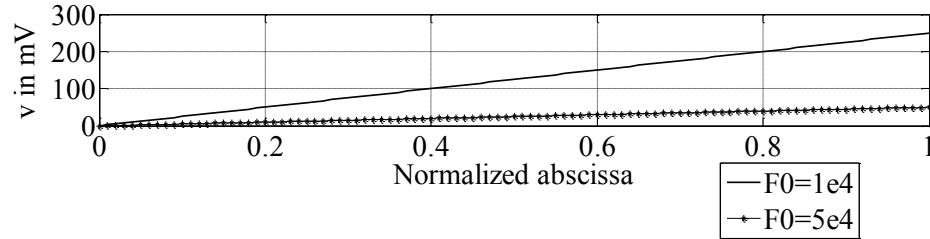
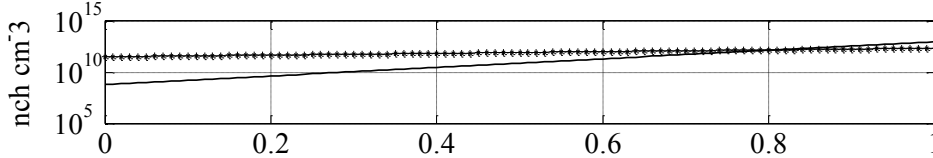
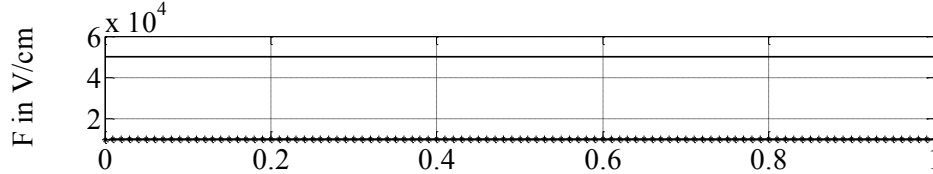


Figure 5-37: (n_{ch}, F, v) for input $(n_{ch\ ave}, th_{GaN})=(10^{+13}cm^{-3}, 10^+4\ 5*10^+4V/cm, 50nm)$

Free electron concentration for $n_{ch\ ave}=1.0e12cm^{-3}$, $F_0=1e4-5e4V/cm$, and $th_{GaN}=50nm$



Electric field F for $n_{ch\ ave}=1.0e12cm^{-3}$, $F_0=1e4-5e4V/cm$, and $th_{GaN}=50nm$



Voltage difference v for $n_{ch\ ave}=1.0e12cm^{-3}$, $F_0=1e4-5e4V/cm$, and $th_{GaN}=50nm$

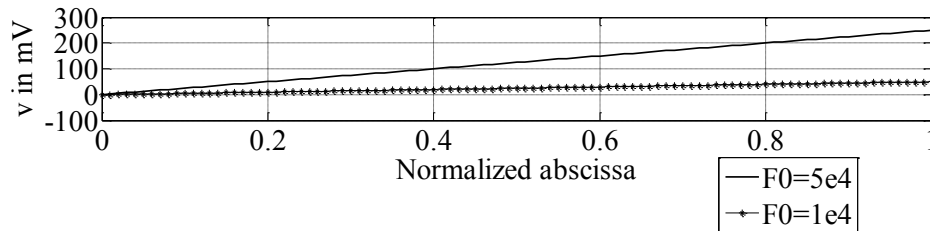
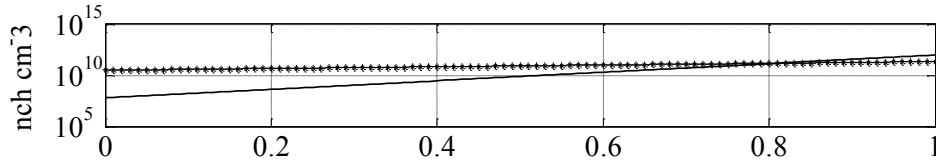
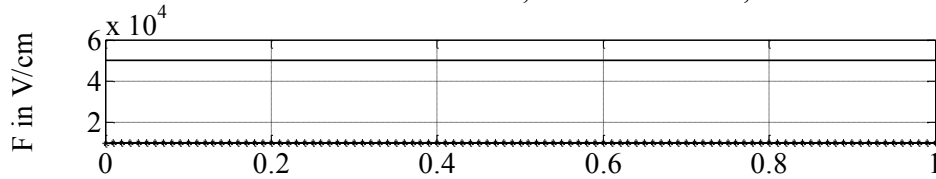


Figure 5-38: (n_{ch}, F, v) for input $(n_{ch\ ave}, th_{GaN})=(10^{+12}cm^{-3}, 10^+4\ 5*10^+4V/cm, 50nm)$

Free electron concentration for $n_{ch\ ave}=1.0e11\text{cm}^{-3}$, $F_0=1e4-5e4\text{V/cm}$, and $th_{GaN}=50\text{nm}$



Electric field F for $n_{ch\ ave}=1.0e11\text{cm}^{-3}$, $F_0=1e4-5e4\text{V/cm}$, and $th_{GaN}=50\text{nm}$



Voltage difference v for $n_{ch\ ave}=1.0e11\text{cm}^{-3}$, $F_0=1e4-5e4\text{V/cm}$, and $th_{GaN}=50\text{nm}$

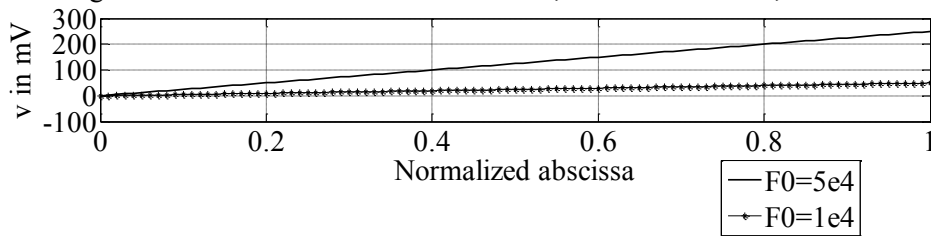
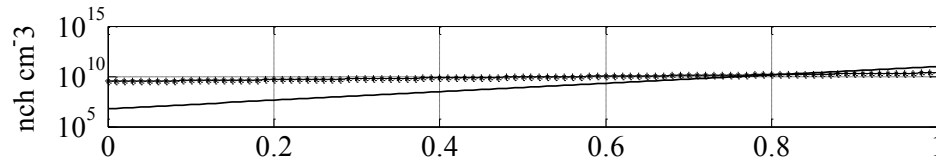
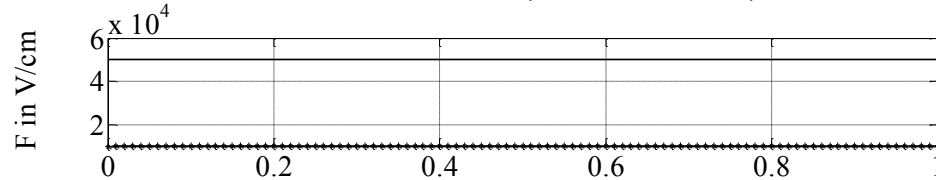


Figure 5-39: (n_{ch}, F, v) for input $(n_{ch\ ave}, th_{GaN})=(10^{+11}\text{cm}^{-3}, 10^4\sqrt{5}\cdot 10^{+4}\text{V/cm}, 50\text{nm})$

Free electron concentration for $n_{ch\ ave}=1.0e10\text{cm}^{-3}$, $F_0=1e4-5e4\text{V/cm}$, and $th_{GaN}=50\text{nm}$



Electric field F for $n_{ch\ ave}=1.0e10\text{cm}^{-3}$, $F_0=1e4-5e4\text{V/cm}$, and $th_{GaN}=50\text{nm}$



Voltage difference v for $n_{ch\ ave}=1.0e10\text{cm}^{-3}$, $F_0=1e4-5e4\text{V/cm}$, and $th_{GaN}=50\text{nm}$

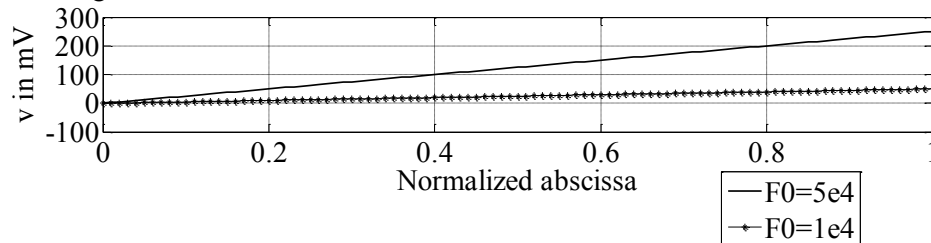
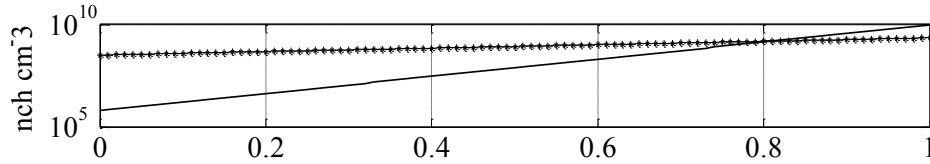
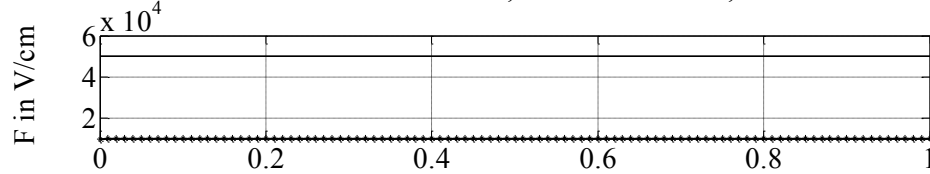


Figure 5-40: (n_{ch}, F, v) for input $(n_{ch\ ave}, th_{GaN})=(10^{+10}\text{cm}^{-3}, 10^4\sqrt{5}\cdot 10^{+4}\text{V/cm}, 50\text{nm})$

Free electron concentration for $n_{ch\ ave}=1.0e9cm^{-3}$, $F_0=1e4-5e4V/cm$, and $th_{GaN}=50nm$



Electric field F for $n_{ch\ ave}=1.0e9cm^{-3}$, $F_0=1e4-5e4V/cm$, and $th_{GaN}=50nm$



Voltage difference v for $n_{ch\ ave}=1.0e9cm^{-3}$, $F_0=1e4-5e4V/cm$, and $th_{GaN}=50nm$

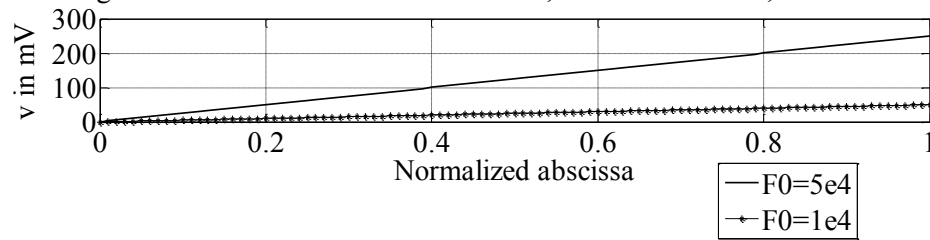
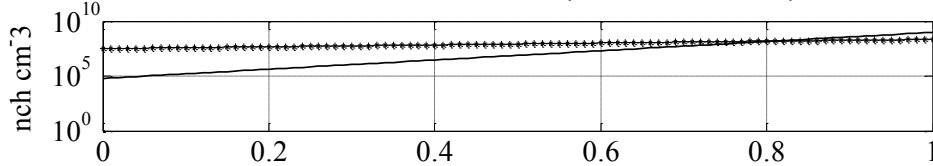
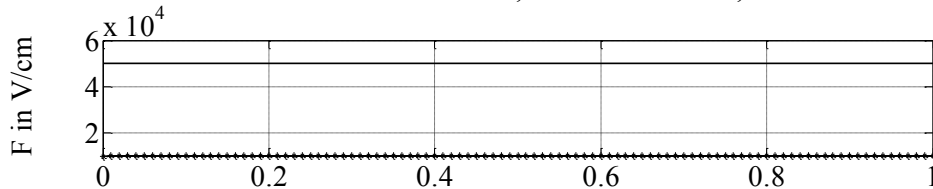


Figure 5-41: (n_{ch}, F, v) for input $(n_{ch\ ave}, th_{GaN})=(10^{+9}cm^{-3}, 10^{+4}\sqrt{5*10^{+4}}V/cm, 50nm)$

Free electron concentration for $n_{ch\ ave}=1.0e8cm^{-3}$, $F_0=1e4-5e4V/cm$, and $th_{GaN}=50nm$



Electric field F for $n_{ch\ ave}=1.0e8cm^{-3}$, $F_0=1e4-5e4V/cm$, and $th_{GaN}=50nm$



Voltage difference v for $n_{ch\ ave}=1.0e8cm^{-3}$, $F_0=1e4-5e4V/cm$, and $th_{GaN}=50nm$

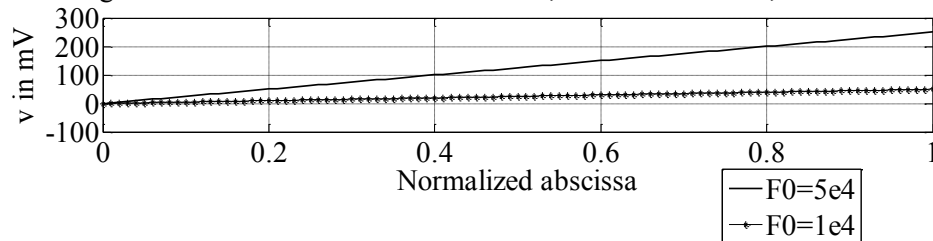


Figure 5-42: (n_{ch}, F, v) for input $(n_{ch\ ave}, th_{GaN})=(10^{+8}cm^{-3}, 10^{+4}\sqrt{5*10^{+4}}V/cm, 50nm)$

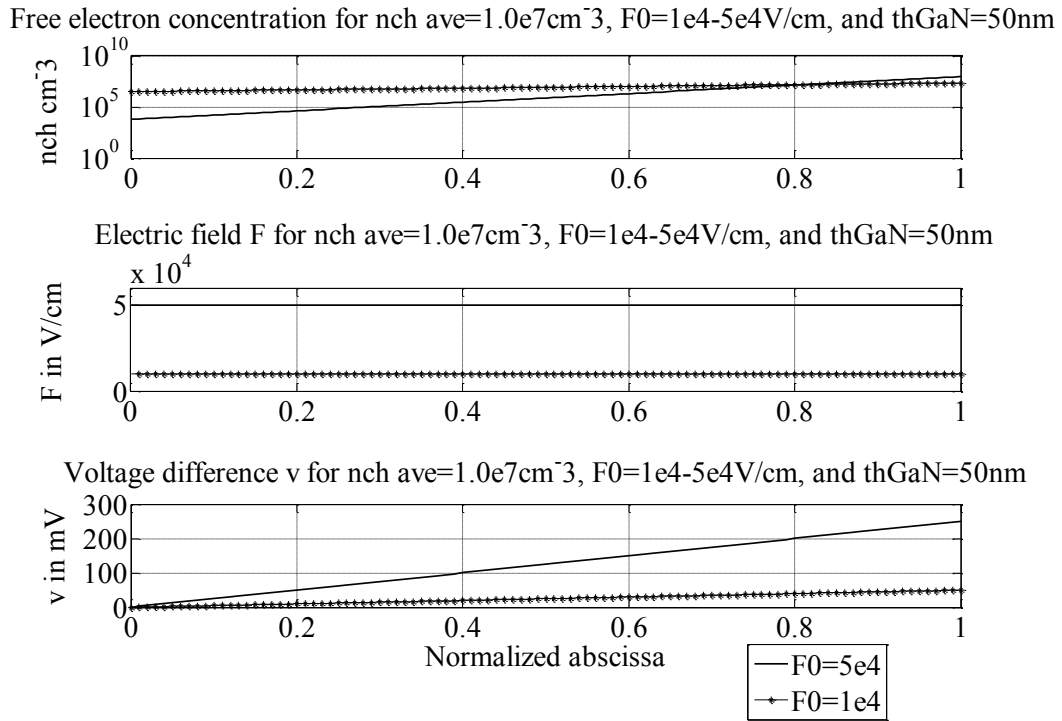


Figure 5-43: (n_{ch}, F, v) for input $(n_{ch\ ave}, th_{GaN})=(10^{+7} cm^{-3}, 10^{+4} \setminus 5 * 10^{+4} V/cm, 50nm)$

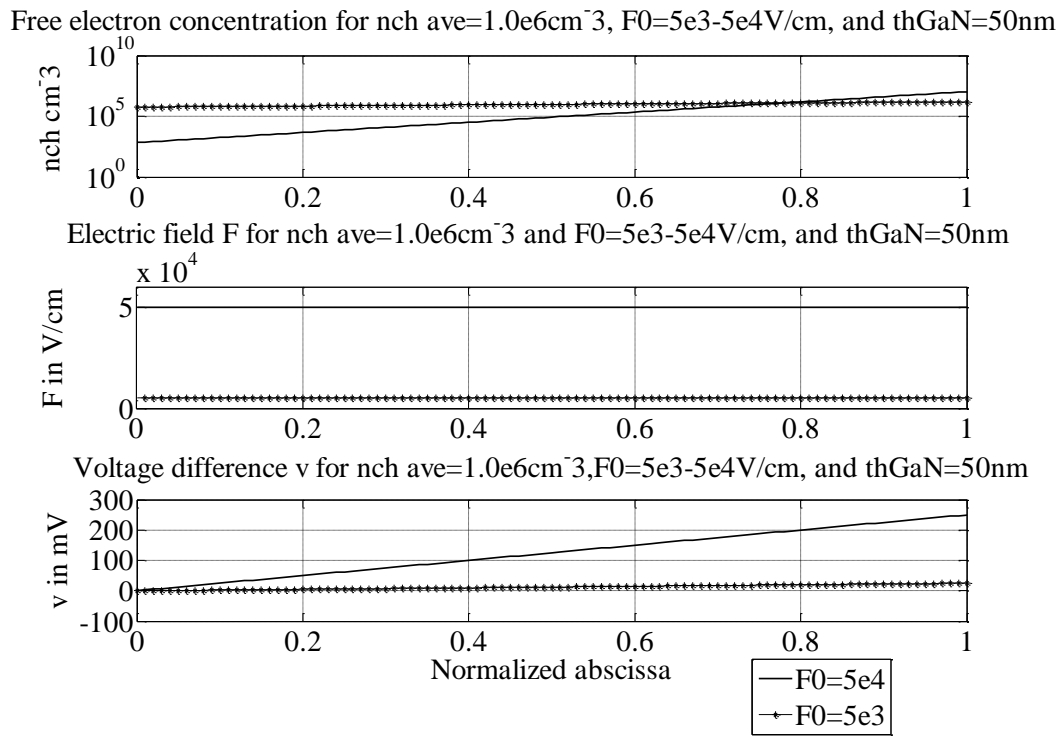
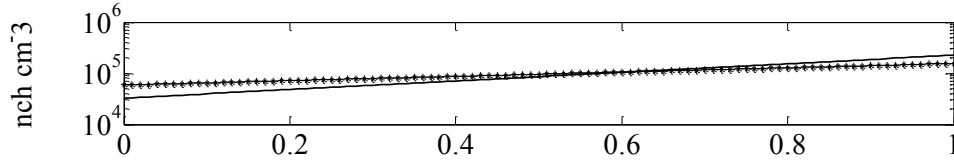
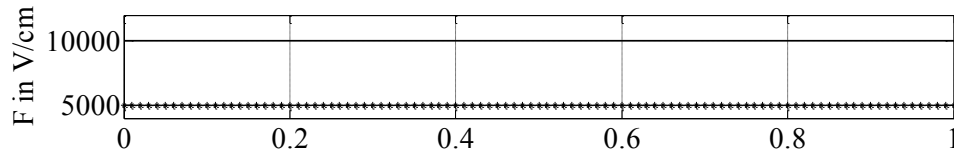


Figure 5-44: (n_{ch}, F, v) for input $(n_{ch\ ave}, th_{GaN})=(10^{+6} cm^{-3}, 5 * 10^{+3} \setminus 5 * 10^{+4} V/cm, 50nm)$

Free electron concentration for $n_{ch\ ave}=1.0e5\text{cm}^{-3}$, $F_0=5e3-1e4\text{V/cm}$, and $th_{GaN}=50\text{nm}$



Electric field F for $n_{ch\ ave}=1.0e5\text{cm}^{-3}$ and $F_0=5e3-1e4\text{V/cm}$, and $th_{GaN}=50\text{nm}$



Voltage difference v for $n_{ch\ ave}=1.0e5\text{cm}^{-3}$, $F_0=5e3-1e4\text{V/cm}$, and $th_{GaN}=50\text{nm}$

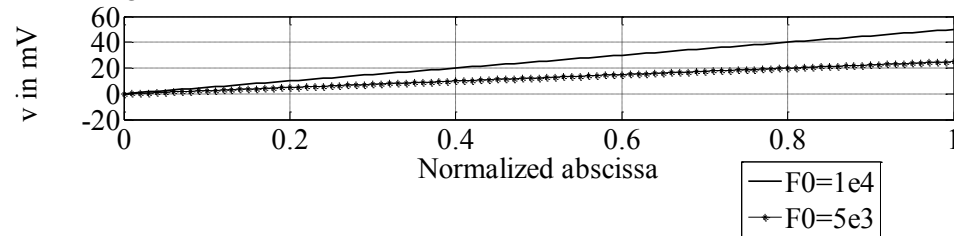
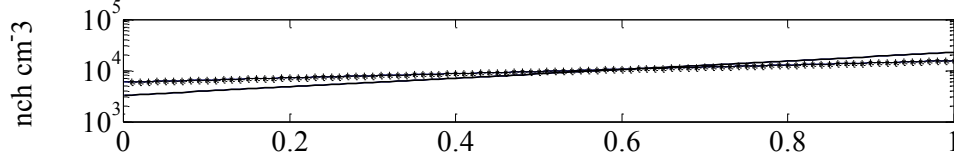
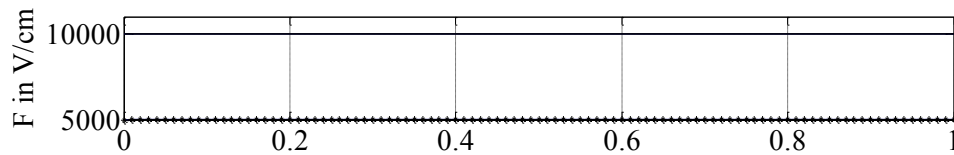


Figure 5-45: (n_{ch}, F, v) for input $(n_{ch\ ave}, th_{GaN})=(10^{+5}\text{cm}^{-3}, 5*10^{+3}\backslash 10^{+4}\text{V/cm}, 50\text{nm})$

Free electron concentration for $n_{ch\ ave}=1.0e4\text{cm}^{-3}$, $F_0=5e3-1e4\text{V/cm}$, and $th_{GaN}=50\text{nm}$



Electric field F for $n_{ch\ ave}=1.0e4\text{cm}^{-3}$ and $F_0=5e3-1e4\text{V/cm}$, and $th_{GaN}=50\text{nm}$



Voltage difference v for $n_{ch\ ave}=1.0e4\text{cm}^{-3}$, $F_0=5e3-1e4\text{V/cm}$, and $th_{GaN}=50\text{nm}$

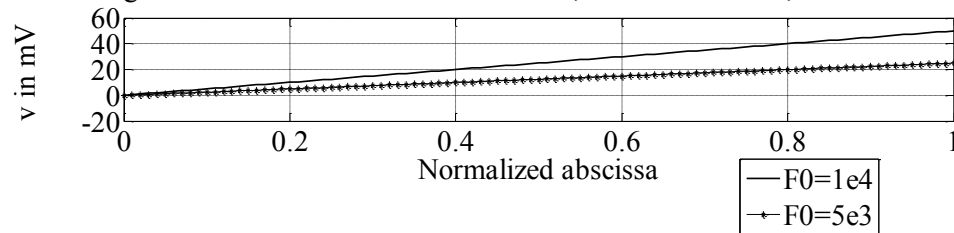


Figure 5-46: (n_{ch}, F, v) for input $(n_{ch\ ave}, th_{GaN})=(10^{+4}\text{cm}^{-3}, 5*10^{+3}\backslash 10^{+4}\text{V/cm}, 50\text{nm})$

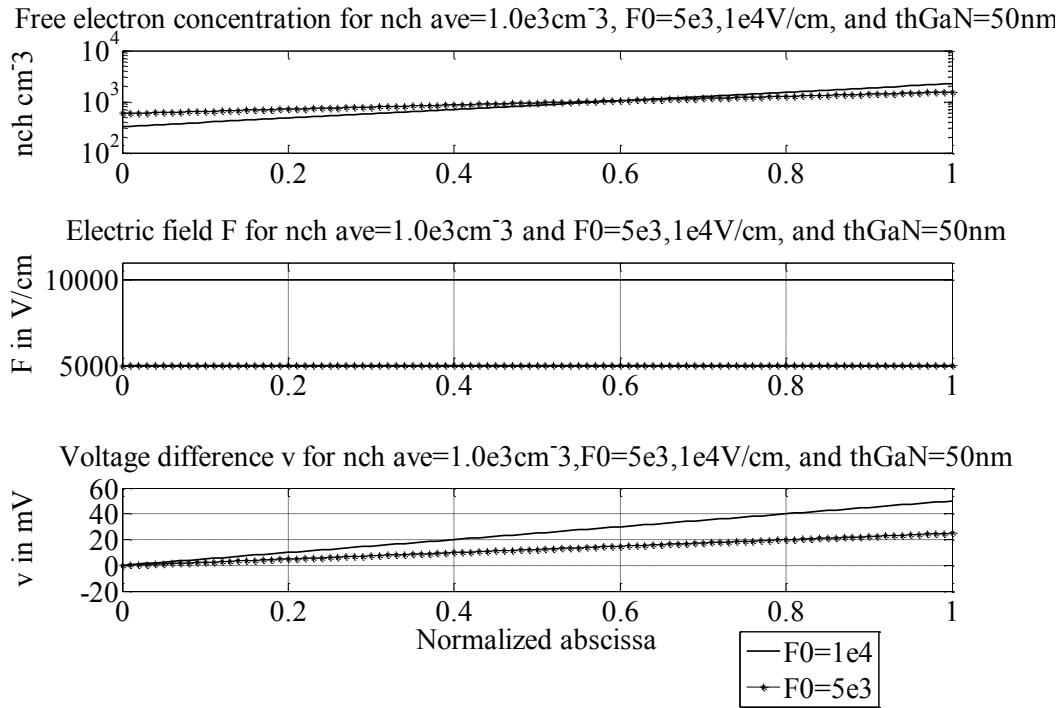


Figure 5-47: (n_{ch}, F, v) for input $(n_{ch\ ave}, th_{GaN})=(10^{+3}\text{cm}^{-3}, 5*10^{+3}\backslash 10^{+4}\text{V/cm}, 50\text{nm})$

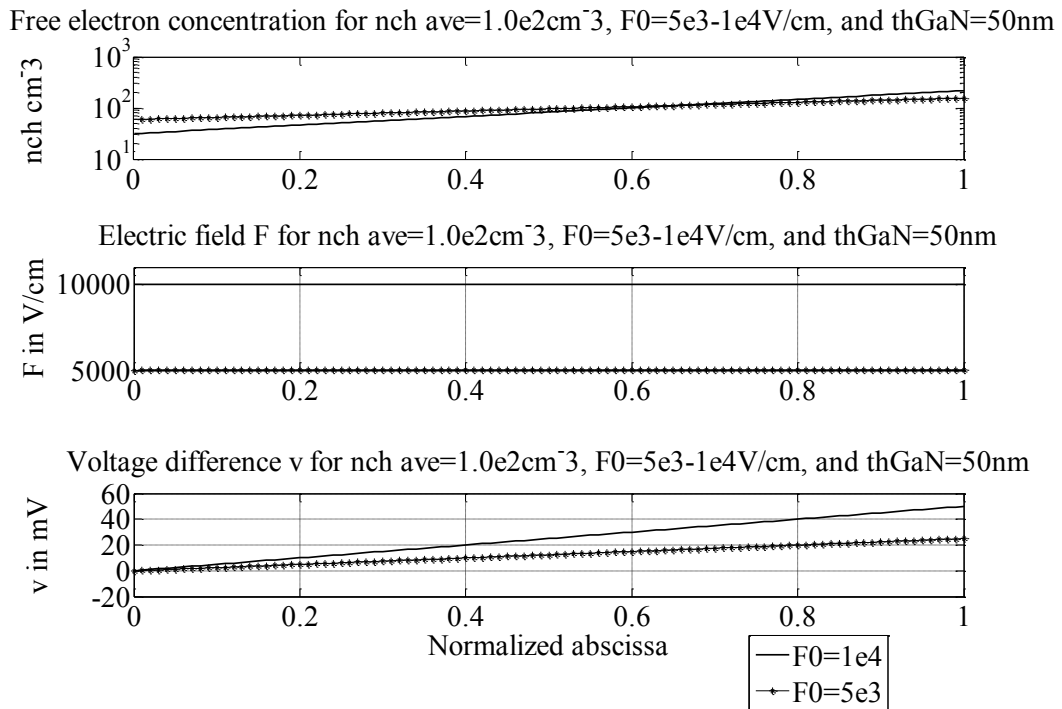


Figure 5-48: (n_{ch}, F, v) for input $(n_{ch\ ave}, th_{GaN})=(10^{+2}\text{cm}^{-3}, 5*10^{+3}\backslash 10^{+4}\text{V/cm}, 50\text{nm})$

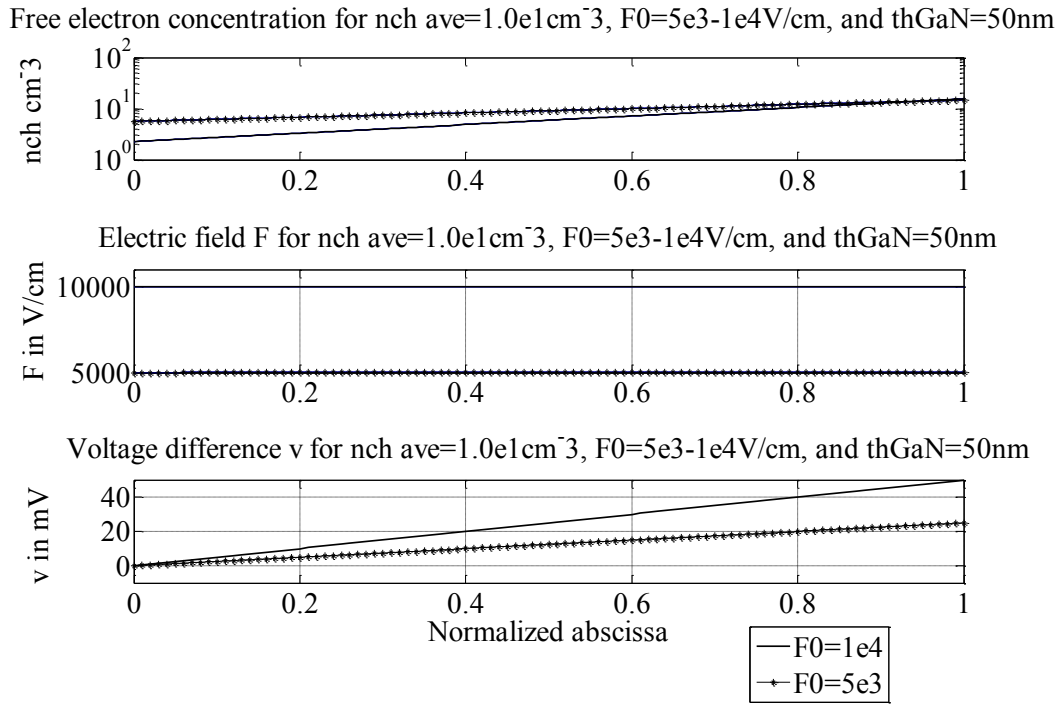


Figure 5-49: (n_{ch}, F, v) for input $(n_{ch\ ave}, th_{GaN})=(10^{+1}\text{cm}^{-3}, 5*10^{+3}\backslash 10^{+4}\text{V/cm}, 50\text{nm})$

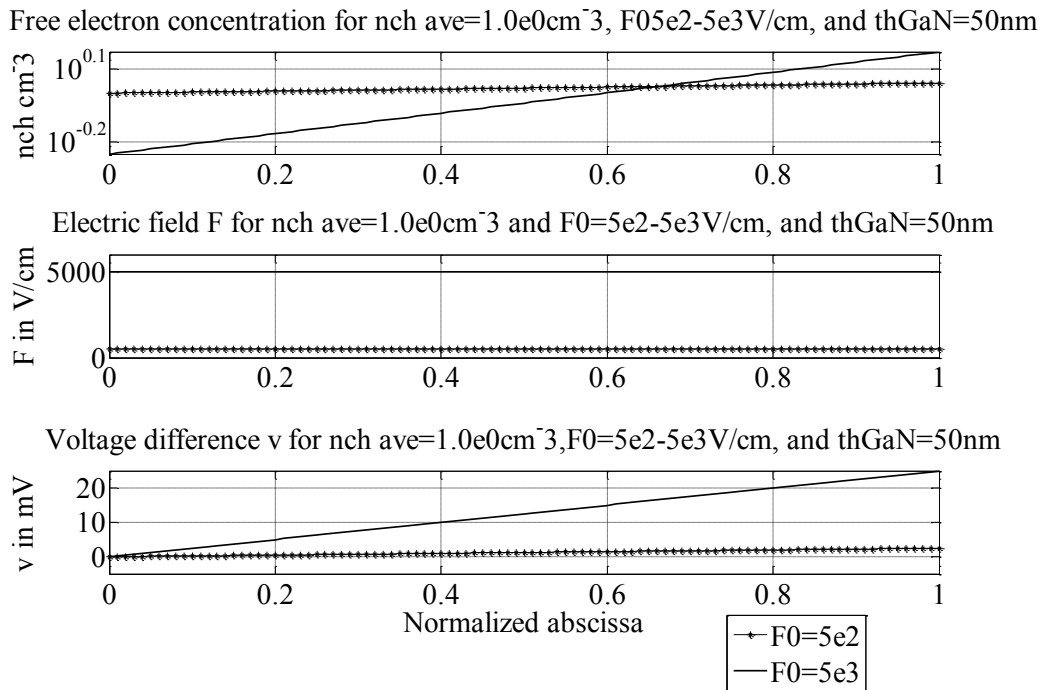


Figure 5-50: (n_{ch}, F, v) for input $(n_{ch\ ave}, th_{GaN})=(100\text{cm}^{-3}, 5*10^{+2}\backslash 5*10^{+3}\text{V/cm}, 50\text{nm})$

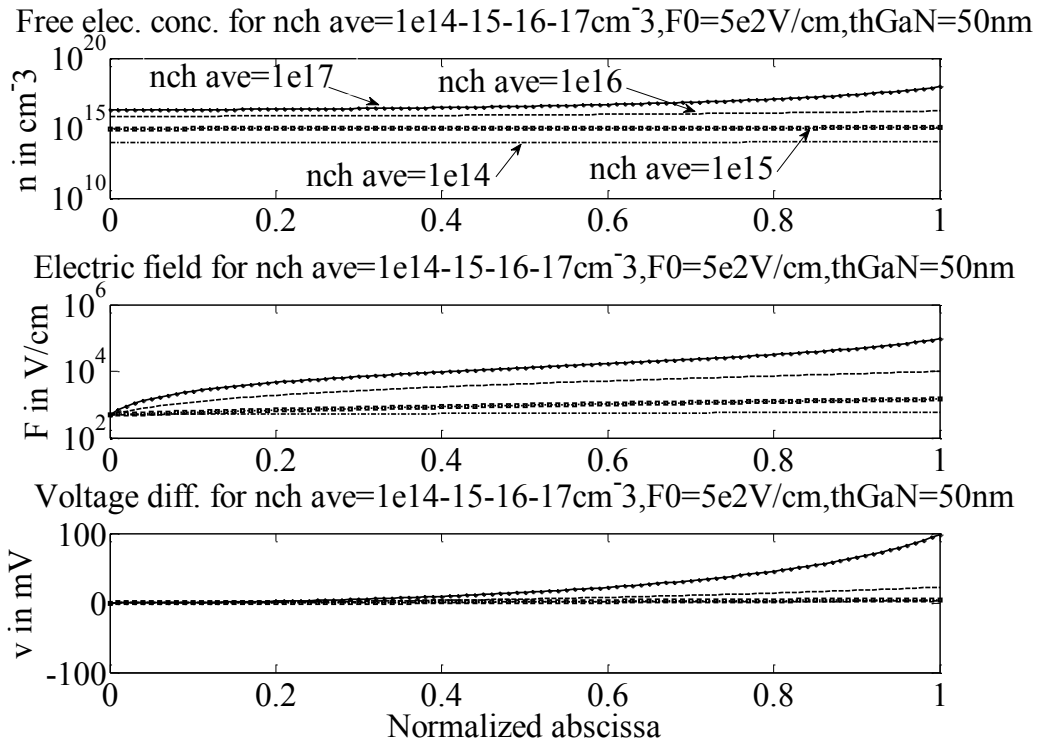
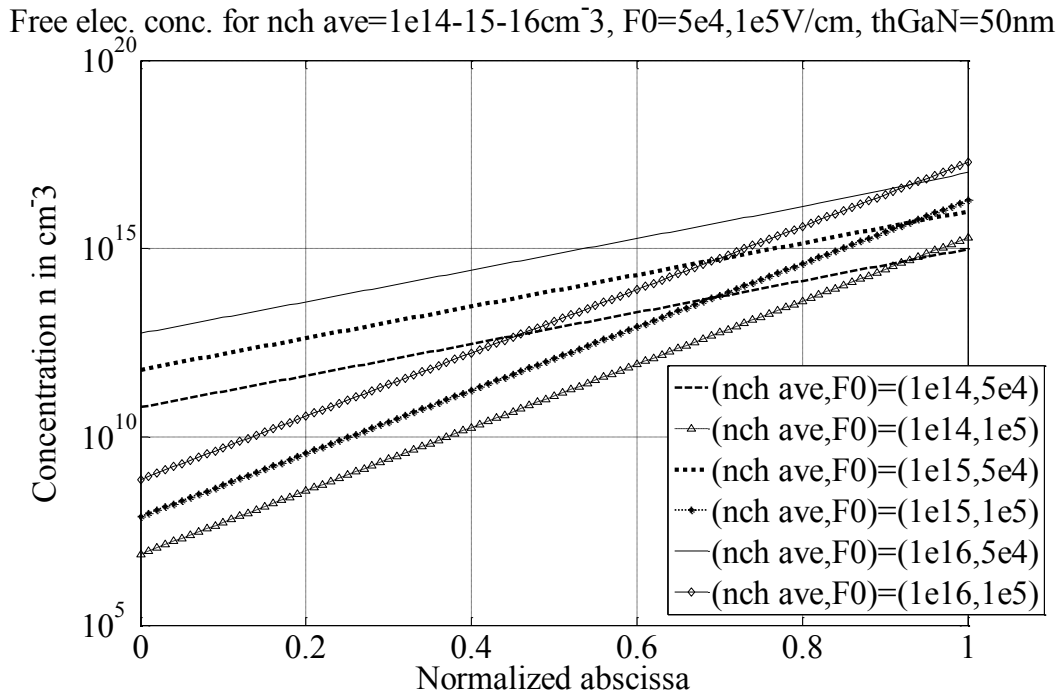
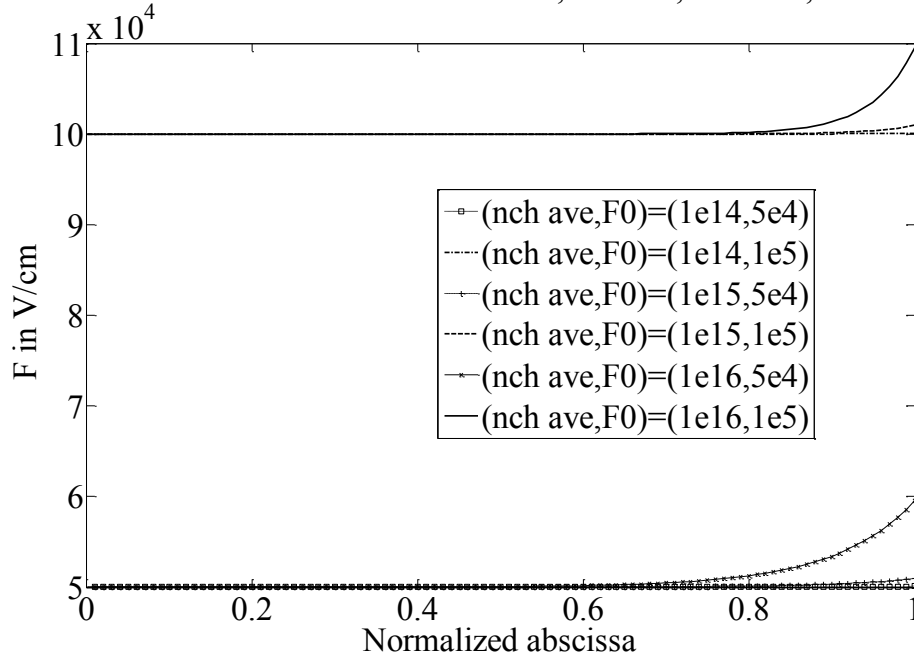


Figure 5-51: (n_{ch}, F, v) for input $(n_{ch\ ave}, th_{GaN}) = (10^{+14|15|16|17} cm^{-3}, 5 \cdot 10^{+2} V/cm, 50nm)$



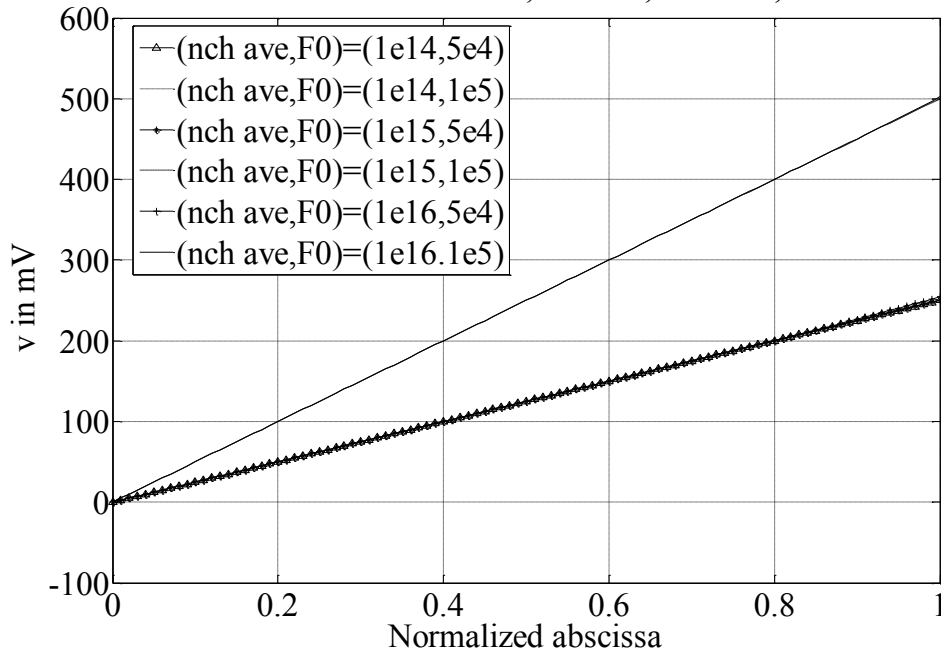
(a)

Electric field for $n_{ch\ ave}=1e14-15-16\ cm^{-3}$, $F_0=5e4, 1e5\ V/cm$, $th_{GaN}=50nm$



(b)

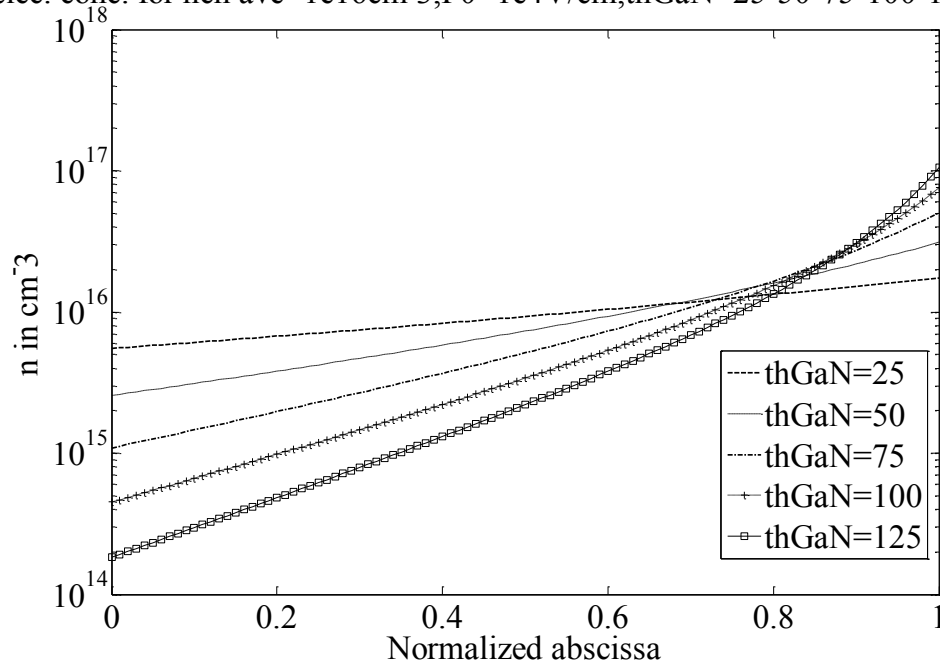
Volt diff. for $n_{ch\ ave}=1.0e14-15-16\ cm^{-3}$, $F_0=5e4, 1e5\ V/cm$, and $th_{GaN}=50nm$



(c)

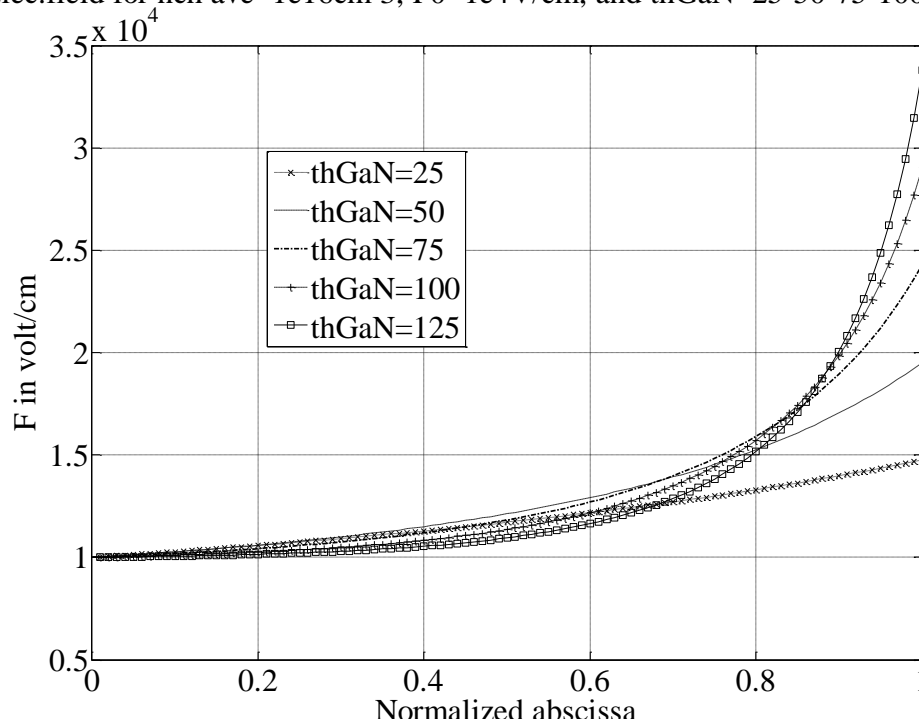
Figure 5-52 (a) Free electron concentration, (b) Electric field, and (c) Potential drop are plotted as functions of the normalized abscissa for inputs $(n_{ch\ ave}, F_0, th_{GaN}) = (10^{+14}, 10^{+5}, 16\ cm^{-3}, 5 \cdot 10^{+4}, 10^{+5}\ V/cm, 50nm)$

elec. conc. for nch ave= $1e16\text{cm}^{-3}$, $F_0=1e4\text{V/cm}$, thGaN=25-50-75-100-125nm



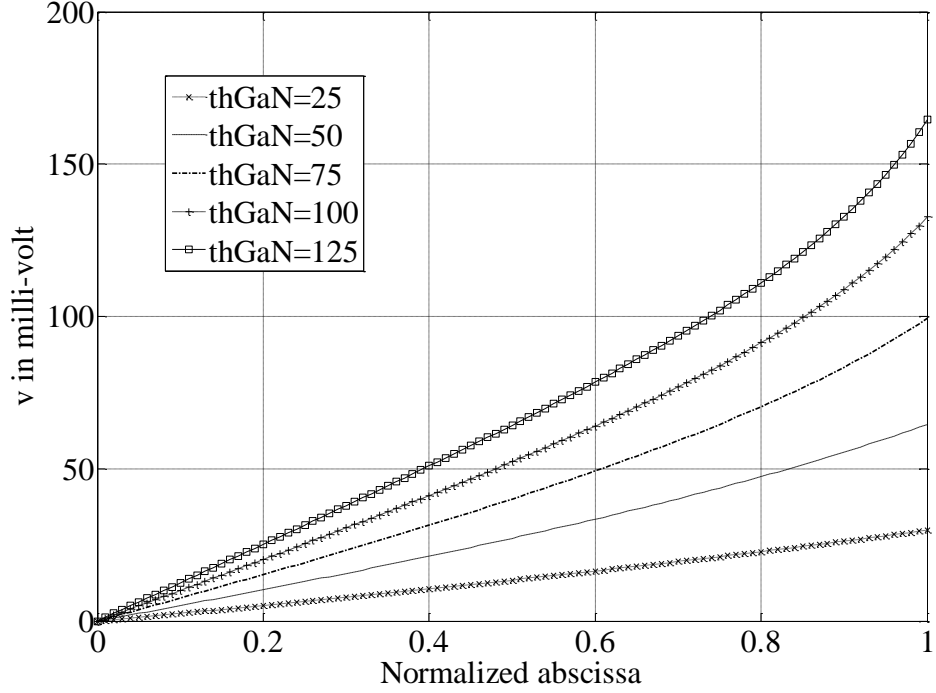
(a)

Elec. field for nch ave= $1e16\text{cm}^{-3}$, $F_0=1e4\text{V/cm}$, and thGaN=25-50-75-100-125nm



(b)

Volt. diff. for $n_{ch\ ave}=1.0e16cm^{-3}$ and $F_0=1e4V/cm$, $th_{GaN}=25-50-75-100-125nm$



(c)

Figure 5-53: (a) Free electron concentration, (b) Electric field, and (c) Potential drop are plotted as functions of the normalized abscissa for inputs $(n_{ch\ ave}, F_0, th_{GaN}) = (10^{+16} cm^{-3}, 10^{+4} V/cm, 50\ 75\ 100\ 125nm)$

Table 5-2: Initial and final values for the free electron concentration and the electric field, and the voltage drop across GaN layer of 50nm thickness

\bar{n}_{ch} (cm ⁻³)	F_0 (V/cm)	n_0 (cm ⁻³)	n_1 (cm ⁻³)	F_0 (computed) (V/cm)	F_1 (V/cm)	$F_deviation$ (%)	v (mV)
1.00E+00	5.00E+03	9.52111272391948E-01	1.04873284806836E+00	5.00000000000000E+02	5.00000000000000E+02	0.00E+00	2.49999999999999E+00
1.00E+01	5.00E+03	5.63379451119496E+00	1.48105996736925E+01	5.00000000000000E+03	5.00000000000001E+03	1.82E-13	2.50000000000001E+01
1.00E+01	1.00E+04	2.25351780447798E+00	1.55741472116882E+01	1.00000000000000E+04	1.00000000000000E+04	7.28E-14	4.99999999999999E+01
1.00E+02	5.00E+03	5.97182218186666E+01	1.56992356541141E+02	5.00000000000000E+03	5.00000000000010E+03	1.93E-12	2.50000000000001E+01
1.00E+02	1.00E+04	3.15492492626918E+01	2.18038060963636E+02	1.00000000000000E+04	1.00000000000001E+04	9.28E-13	5.00000000000002E+01
1.00E+03	5.00E+03	5.93238562028829E+02	1.55955614563993E+03	5.00000000000000E+03	5.00000000000095E+03	1.90E-11	2.50000000000020E+01
1.00E+03	1.00E+04	3.26760081649308E+02	2.25825134569493E+03	1.00000000000000E+04	1.00000000000010E+04	9.51E-12	5.00000000000017E+01
1.00E+04	5.00E+03	5.93351237919053E+03	1.55985235763449E+04	5.00000000000000E+03	5.00000000000095E+03	1.90E-10	2.500000000000200E+01
1.00E+04	1.00E+04	3.27210785210203E+03	2.26136617513857E+04	1.00000000000000E+04	1.00000000000095E+04	9.53E-11	5.000000000000166E+01
1.00E+05	5.00E+03	5.93385040686120E+04	1.55994122124341E+05	5.00000000000000E+03	5.0000000000009524E+03	1.90E-09	2.5000000000002003E+01
1.00E+05	1.00E+04	3.27030503785845E+04	2.26012024337468E+05	1.00000000000000E+04	1.000000000000952E+04	9.52E-10	5.0000000000001658E+01
1.00E+06	5.00E+03	5.93387294203925E+05	1.55994714559201E+06	5.00000000000000E+03	5.00000000000095237E+03	1.90E-08	2.50000000000020032E+01
1.00E+06	5.00E+04	6.76055341343395E+02	1.06585630202909E+07	5.00000000000000E+04	5.0000000000010502E+04	2.10E-09	2.500000000000543E+02
1.00E+07	1.00E+04	3.27035686876795E+06	2.26015606534734E+07	1.00000000000000E+04	1.00000000000095238E+04	9.52E-08	5.000000000000165772E+01
1.00E+07	5.00E+04	6.14083601720251E+03	9.68152807840694E+07	5.00000000000000E+04	5.00000000000095389E+04	1.91E-08	2.5000000000004932E+02

Table 5-2 (cont'd): Initial and final values for the free electron concentration and the electric field, and the voltage drop across GaN layer of 50nm thickness

\bar{n}_{ch} (cm ⁻³)	F_0 (V/cm)	n_0 (cm ⁻³)	n_1 (cm ⁻³)	F_0 (computed) (V/cm)	F_1 (V/cm)	$F_{deviation}$ (%)	v (mV)
1.00E+08	1.00E+04	3.27034988286276E+07	2.26015125039876E+08	1.00000000000000E+04	1.00000000952373E+04	9.52E-07	5.00000001657718E+01
1.00E+08	5.00E+04	6.16337119524729E+04	9.71705663855575E+08	5.00000000000000E+04	5.00000000957385E+04	1.91E-07	2.50000000049495E+02
1.00E+09	1.00E+04	3.27035603496637E+08	2.26015563251199E+09	1.00000000000000E+04	1.00000009523751E+04	9.52E-06	5.00000016577207E+01
1.00E+09	5.00E+04	6.13182194598459E+05	9.66731684324732E+09	5.00000000000000E+04	5.00000009524839E+04	1.90E-06	2.50000000492416E+02
1.00E+10	1.00E+04	3.27035513806628E+09	2.26015631637062E+10	1.00000000000000E+04	1.00000095237508E+04	9.52E-05	5.00000165772039E+01
1.00E+10	5.00E+04	6.13114589064325E+06	9.66625264295689E+10	5.00000000000000E+04	5.00000095237894E+04	1.90E-05	2.50000004923621E+02
1.00E+11	1.00E+04	3.27034703937399E+10	2.26016375641809E+11	1.00000000000000E+04	1.00000952375064E+04	9.52E-04	5.00001657718267E+01
1.00E+11	5.00E+04	6.13110082028716E+07	9.66619814614500E+11	5.00000000000000E+04	5.00000952372758E+04	1.90E-04	2.50000049235871E+02
1.00E+12	1.00E+04	3.27026664057421E+11	2.26023856214427E+12	1.00000000000000E+04	1.00009523750633E+04	9.52E-03	5.00016576973044E+01
1.00E+12	5.00E+04	6.13106363724339E+08	9.66630512717632E+12	5.00000000000000E+04	5.00009523751363E+04	1.90E-03	2.50000492357831E+02
1.00E+13	1.00E+04	3.26946288821099E+12	2.26098666200439E+13	1.00000000000000E+04	1.00095237506342E+04	9.52E-02	5.00165748772831E+01
1.00E+13	5.00E+04	6.13053859576392E+09	9.66713330886600E+13	5.00000000000000E+04	5.00095237511262E+04	1.90E-02	2.50004923367350E+02

Table 5-2 (cont'd): Initial and final values for the free electron concentration and the electric field, and the voltage drop across GaN layer of 50nm thickness

\bar{n}_{ch} (cm ⁻³)	F_0 (V/cm)	n_0 (cm ⁻³)	n_1 (cm ⁻³)	F_0 (computed) (V/cm)	F_1 (V/cm)	$F_deviation$ (%)	v (mV)
1.00E+14	5.00E+04	6.12529433588971E+10	9.67541704231428E+14	5.00000000000000E+04	5.00952375064319E+04	1.90E-01	2.50049212600281E+02
1.00E+14	1.00E+05	7.77328431476636E+06	1.93397506088434E+15	1.00000000000000E+05	1.00095234291331E+05	9.52E-02	5.00024626413467E+02
1.00E+15	5.00E+04	6.07334403557682E+11	9.75825931435339E+15	5.00000000000000E+04	5.09523750629475E+04	1.90E+00	2.50490032068009E+02
1.00E+15	1.00E+05	7.74040548999902E+07	1.94232917739370E+16	1.00000000000000E+05	1.00952377039080E+05	9.52E-01	5.00245746942549E+02
1.00E+16	5.00E+04	5.59851608089486E+12	1.05866866477085E+17	5.00000000000000E+04	5.95237506344161E+04	1.90E+01	2.54703195264787E+02
1.00E+16	1.00E+05	7.42374342163158E+08	2.02517389372321E+17	1.00000000000000E+05	1.09523756409511E+05	9.52E+00	5.02406460143396E+02
1.00E+17	5.00E+04	3.14197811146889E+13	1.88711891034415E+18	5.00000000000000E+04	1.45237506341180E+05	1.90E+02	2.84594982475882E+02
1.00E+17	1.00E+05	5.26846907795050E+09	2.85364722092265E+18	1.00000000000000E+05	1.95237501352260E+05	9.52E+01	5.20146848703239E+02
1.00E+18	5.00E+04	5.83148719836326E+13	1.01718414316966E+20	5.00000000000000E+04	1.00237506339983E+06	1.90E+03	3.71727127721840E+02
1.00E+18	1.00E+05	1.34977743542239E+10	1.11383968624473E+20	1.00000000000000E+05	1.05237512604219E+06	9.52E+02	5.90592572127487E+02

5.4 Conclusion

A channel second model was presented; its concept and analysis were discussed. Simulation results suggested a way for the free electrons, once injected in a thin GaN layer, to distribute under the influence of an electric field whose initial value is set independent from the free electron concentration average value. The potential and the electric field at any point in the GaN layer were computed.

Chapter 6 : Comparison

6.1 Introduction

So far, two channel models have been presented; their main difference besides the number of inputs resides in the fact that, for the first model, the initial field is inherent to the average free charge concentration while in the second model they are independent. A comparison of channel models 1 and 2 is performed. A set of four equations in terms of the potential drops ($\varphi_1, \varphi_2, \varphi_3, \varphi_4$) is obtained. Future work is defined.

6.2 Comparison

The quantum tunneling theory of electrons of exciton origin defined the range of electric field values at which excitons present in p-type $\text{In}_{0.5}\text{Ga}_{0.5}\text{N}$ will interact with the i-GaN/p- $\text{In}_{0.5}\text{Ga}_{0.5}\text{N}$ semiconductor heterojunction resulting in their destruction and in electron tunneling to the i-GaN layer (channel) [27]. The dependence of the transmission coefficient of electrons on the electric field strength at the semiconductor heterojunction showed that quantum tunneling occurs for values higher than 10^{+4}V/cm . If the initial value of the electric field in the i-GaN layer is taken at the i-GaN/p-type $\text{In}_{0.5}\text{Ga}_{0.5}\text{N}$ heterojunction, then table 4-2 gives the values of the initial electric field for different typical average concentrations of free charge carriers (electrons) that tunneled to the i-GaN material. In terms of the concordance with the exciton theory in Wurtzite $\text{In}_x\text{Ga}_{1-x}\text{N}$ [27], channel model 1 is not a candidate for the 2-terminal MOS capacitor analysis. However Channel model 2 can be used in our device analysis because it offers the possibility to set the initial electric field values to those which enable electron tunneling.

6.3 Set of equations

In section 3.4, the quasi analysis performed led to two equations of four unknowns ($\varphi_1, \varphi_2, \varphi_3, \varphi_4$). The third equation is obtained by finding the potential drop across the i-GaN channel. Its expression is that of the second equation in set 5-1 for $\lambda = 1$ if case 1 applies, or that of the second equation in set 5-2 for $\lambda = 1$ if case 2 applies. The fourth equation is obtained first, by finding the expression of the electric field final value and second, by using the flux continuity property at the oxide/GaN interface. The final value of the electric field in the GaN layer is obtained from the third equation in set 5-1 for $\lambda = 1$ if case 1 applies, or from the third equality in set 5-2 for $\lambda = 1$ if case 2 applies. The two additional equations are;

$$\left\{ \begin{array}{l} \varphi_3 = u_T \ln \left\{ d^2 \operatorname{csch}^2 \left[d \left(\frac{th_{GaN}}{L_d \sqrt{2}} - \frac{\sinh^{-1}(d)}{d} \right) \right] \right\} \\ \varepsilon_{ox} \frac{\varphi_4}{th_{ox}} = -\varepsilon_{GaN} \frac{u_T d \sqrt{2}}{L_d} \operatorname{cotanh} \left[d \left(\frac{th_{GaN}}{L_d \sqrt{2}} - \frac{\sinh^{-1}(d)}{d} \right) \right] \end{array} \right. \quad \text{Case 1} \quad (6-1)$$

$$\left\{ \begin{array}{l} \varphi_3 = u_T \ln \left\{ d^2 \operatorname{sec}^2 \left[d \left(\frac{th_{GaN}}{L_d \sqrt{2}} + \frac{1}{d} \arctan \left(\frac{\sqrt{1-d^2}}{d} \right) \right) \right] \right\} \\ \varepsilon_{ox} \frac{\varphi_4}{th_{ox}} = \varepsilon_{GaN} \frac{u_T d \sqrt{2}}{L_d} \tan \left[d \left(\frac{th_{GaN}}{L_d \sqrt{2}} + \frac{1}{d} \arctan \left(\frac{\sqrt{1-d^2}}{d} \right) \right) \right] \end{array} \right. \quad \text{Case 2} \quad (6-2)$$

In fact, instead of having one system of four equations, two systems are obtained. It will be demonstrated in a future paper that in the case where there is a presence of free charge carriers in the i-GaN channel, only case 1 is taken and thus the two equations 6-1 together with equations 3-1 and 3-6 form the needed four equations system.

The case corresponding to an initial zero-valued electric field was not discussed in this work because no charge tunneling occurs for this value [26][27], however this case will be considered in the discussion of the flat band condition of the MOS capacitor.

6.4 Conclusion

A set of four equations with respect to potential drops $(\varphi_1, \varphi_2, \varphi_3, \varphi_4)$ is obtained. For this, Channel model 2 was selected as a valid model after being compared against the theory of excitons in Wurtzite Indium Gallium Nitride [27].

Chapter 7 : Conclusion

7.1 Conclusion

This work aimed to set the first step towards providing the HF MOSFET on $\text{In}_x\text{Ga}_{1-x}\text{N}$ with a device model for circuit analysis and design.

In chapter 2, a qualitative description of the both the structure and the functioning of this 4-terminal device was presented.

In chapter 3, an ideal model for the MOS capacitor on $\text{In}_x\text{Ga}_{1-x}\text{N}$ was introduced. The idea that motivated the use of such a model was explained. A Quasi-static analysis was performed, although the CV characteristics are not obtained in this work, this analysis demonstrated the need for investigating the charge distribution, the electric field, and the voltage drop at any point in the channel.

In Chapter 4 and 5, two channel models were presented. Each one of these (1-D) models suggested a way for the free charge carriers (electrons) to distribute in the i-GaN once they tunneled.

In Chapter 6, a comparison between these models was performed; it used the concordance with the theory of the excitons of the structure in Wurtzite $\text{In}_x\text{Ga}_{1-x}\text{N}$ as a criteria. Channel model 2 has been retained.

Appendix A, B and C contain mathematical proofs needed to achieve a rigorous analysis. Including them directly in the text can create an off-topic tangent that would break the flow of the document.

7.2 Future work

Following the work described in this thesis, a number of directions could be taken up;

- 1- Solution of the non linear system of four equations taking the applied gate voltage as a parameter and computation of the gate capacitance per unit area.
- 2- Consideration of Fermi-Dirac distribution instead of Boltzmann distribution in the quasi-static analysis of the 2-terminal MOS capacitor. This way, the theoretical model is still valid even for degenerate semiconductors.

- 3- Comparison of the theoretical CV characteristics with measurements made on a test MOS capacitor.
- 4- Definition of a metric that expresses the dependence of the applied gate voltage on the Oxide and GaN layers thicknesses for the same level of doping. This can help define the drivability (per unit area) of the device as a function of its layers thicknesses.
- 5- The electrical quantities (current, voltage, and power) can be calculated based on the geometry of the device and its scaling down effects can be predicted.
- 6- Built a dc model for the MOSFET on Indium Gallium Nitride.

REFERENCES

- [1] J. E. Lilienfeld, "Method and Apparatus for controlling Electric Currents," U.S. Patents 1,745,175. Filed 1926. Granted 1930.
- [2] J. E. Lilienfeld, "Amplifier for Electric Currents," U.S. Patent 1,877,140. Filed 1928. Granted 1932.
- [3] J. E. Lilienfeld, "Device for Controlling Electric Current," U.S. Patent 1,900,018. Filed 1928. Granted 1933.
- [4] O. Heil, "Improvement in or Relating to Electrical Amplifiers and Other Control Arrangements and Devices," British Patent 439,457. Filed and granted 1933.
- [5] W. Shockley and G. L. Pearson, "Modulation of Conductance of Thin Films of Semiconductors by Surface Charges," *Phys. Rev.*, 74, 232, 1948.
- [6] J. R. Ligenza and W. G. Spitzer, "The Mechanism for Silicon Oxidation in Steam and Oxygen," *J. Phys. Chem. Solids*, 14, 131, 1960.
- [7] D. Kahng and M. M. Atalla, "Silicon-Silicon Dioxide Field Induced Surface Devices," in *IRE-AIEE Solid-State Device Res. Conf*, Carnegie Inst. of Tech., Pittsburgh, PA, 1960.
- [8] H. K. J. Ihantola and J. L. Moll, "Design Theory of a Surface Field-Effect Transistor," *Solid-State Electron*, 7, 423, 1964.
- [9] C. T. Sah, "Characteristics of The Metal-Oxide-Semiconductor Transistors," *IEEE Trans. Electron Dev*, ED11, 423, 1964.
- [10] S. R. Hofstein and F.P. Heiman, "The Silicon Insulated-Gate Field Effect Transistor," *Proc. IEEE*, 51, 1190, 1963.
- [11] J. R. Brews, "Physics of The MOS Transistor," in D. Kahng Ed., *Applied Solid State Science*. New York: Suppl. 2A, Academic, 1981.
- [12] Y. Tsididis, *Operation and Modeling of the MOS Transistor*, 2nd Ed. Oxford: Oxford University Press, 1999.
- [13] Y. Taur and T. H. Ning, *Fundamentals of Modern VLSI Devices*. Cambridge: Cambridge University Press, 1998.
- [14] R. M. Warner, Jr. and B. L. Grung, *MOSFET Theory and Design*. Oxford: Oxford University Press, 1999.
- [15] S. M. Sze and Kwok K. Ng, *Physics of Semiconductor Devices*, 3rd Ed. Hoboken, New Jersey: Wiley Interscience, 2007.
- [16] L. Esaki and R. Tsu, "Superlattice and Negative Conductivity in Semiconductors," *IBM Research*, RC2418, March 1969.
- [17] R. Dingle, H.L. Stormer, A.C. Gossard and W. Wiegmann, "Electron Mobilities in Modulation-Doped Semiconductor Heterojunction Superlattices," *Appl. Phys. Lett.*, 33, 665, 1978.
- [18] R. Dingle, A. C. Gossard, W. Wiegmann, and M. D. Sturge H. L. Stormer, "Two-Dimensional Electron Gas at a Semiconductor-Semiconductor Interface," *Solid State Commun.*, 29, 705, 1979.

References

- [19] S. Hiyamizu, T. Fujii, and K. Nambu T. Mimura, "A New Field Effect Transistor with Selectively Doped GaAs/n-Al_xGa_{1-x}As Heterojunctions," *Jpn. J. Appl. Phys.*, 19, L225, 1980.
- [20] T. Mimura, "The Early History of the High Electron Mobility Transistor (HEMT)," *IEEE Trans. Microwave Theory Tech.*, 50, 780, 2002.
- [21] D. DelageBeaudeuf, P. Delescluse, P. Etienne, M. laviron, J. Chaplart, and N. T. Linh "Two-Dimensional Electron Gas M.E.S.F.E.T. Structure," *Electron. Lett.*, 16, 667, 1980.
- [22] H. Daembkes, Ed., *Modulation-Doped Field-Effect Transistors: Principle, Design, and Technology*. Piscataway, New Jersey: IEEE Press, 1991.
- [23] H. Morkoc, H. Unlu, and G. Ji, *Principle and Technology of MODFET's : Principle, Design, and Technology. Vols. 1 and 2*. New York: Wiley, 1991.
- [24] C. Y. Chang and F. Kai, *GaAs High-Speed Devices*. New York: Wiley, 1994.
- [25] M. Golio and D. M. Kingsriter, Eds., *RF and Microwave Semiconductor Devices Handbook*. Boca Raton, Florida: CRC Press, 2002.
- [26] Dimiter Alexandrov, "Design of High Frequency Field Transistor on In_xGa_{1-x}N," in *21st Biennial symposium on Communications*, Kingston, Ontario, Canada, 2002.
- [27] Dimiter Alexandrov, "Excitons of the structure in wurtzite In_xGa_{1-x}N and their properties," *Journal of Crystal Growth*, vol. 246, pp. 325-340, 2002.
- [28] Tarik Menkad, Dimiter Alexandrov, Kenneth Scott A. Butcher, "Modeling of Metal-Oxide-Semiconductor Capacitor on Indium Gallium Nitride 1-Channel Model," accepted for publication in *CCECE/CCGÉI 2012*, Montreal, QC, Canada, May 2012.
- [29] G. C Dousmanis and R. C Duncun Jr, "Calculation on the Shape and Extent of Space Charge Regions in Semiconductor Surfaces," *Journal of Applied Physics*, vol. 29, no. 12, pp. 1267-1269, December 1958.
- [30] J. R Hause and M. A Littlejohn, "Approximations and Inversion Space Charge Layers in Semiconductors," *Solid-State Electronics*, vol. 11, no. 07, pp. 667-674, July 1968.
- [31] Levinshtein M.E., Rumyantsev S.L., Zubrilov A. Bougrov V., *Semiconductor Materials GaN, InN, SiC, SiGe*, Rumyantsev S.L., Shur M.S. Levinshtein M.E., Ed. New York: John Wiley & Sons, Inc, 2001.
- [32] New Semiconductor Materials Characteristics and Properties. [Online]. <http://www.ioffe.ru/SVA/NSM/Semicond/index.html>

Appendix A

A.1 Introduction

In Chapter 4 the localization and thus the existence of a thin i-GaN layer whose thickness is defined, and over which the free electron concentration has a known average value, is possible if and only if the i-GaN layer thickness th_{GaN} and the free electron average concentration $\overline{n_{ch}}$ satisfy condition 4-2 which is repeated below for convenience.

$$\overline{n_{ch}} > \frac{n_{i,GaN}L_D\sqrt{2}}{th_{GaN}} \frac{2 \left(-1 + \sqrt{1 + \tan^2 \left(\frac{th_{GaN}}{L_D\sqrt{2}} \right)} \right)}{\tan \left(\frac{th_{GaN}}{L_D\sqrt{2}} \right)} \quad (\text{A-1})$$

A proof of this condition is given.

A.2 Proof

The following statement to prove summarizes the condition given in Equality A-1

$$\forall (\overline{n_{ch}}, th_{GaN}) \in (\mathbb{R}_*^+)^2, \text{ such that } \overline{n_{ch}} > \frac{n_{i,GaN}L_D\sqrt{2}}{th_{GaN}} \frac{2 \left(-1 + \sqrt{1 + \tan^2 \left(\frac{th_{GaN}}{L_D\sqrt{2}} \right)} \right)}{\tan \left(\frac{th_{GaN}}{L_D\sqrt{2}} \right)},$$

$\exists! x_0 \in \mathbb{R}_*^+$ for which $N(x_0, th_{GaN}) = \overline{n_{ch}}$

Let us solve for the unknown x the equation

$$N(x, th_{GaN}) = \overline{n_{ch}} \quad (\text{A-2}),$$

where

$$N(x, th_{GaN}) = \frac{n_{i,GaN}L_D\sqrt{2}}{th_{GaN}} \left[\tan \left(\frac{x + th_{GaN}}{L_D\sqrt{2}} \right) - \tan \left(\frac{x}{L_D\sqrt{2}} \right) \right]$$

Expression A-2 leads to an equation of the 2nd degree with respect to the unknown $\tan\left(\frac{x}{L_D\sqrt{2}}\right)$;

$$\left[\tan\left(\frac{th_{GaN}}{L_D\sqrt{2}}\right)\right]\left[\tan\left(\frac{x}{L_D\sqrt{2}}\right)\right]^2 + \left[a * \tan\left(\frac{th_{GaN}}{L_D\sqrt{2}}\right)\right]\tan\left(\frac{x}{L_D\sqrt{2}}\right) + \left[\tan\left(\frac{th_{GaN}}{L_D\sqrt{2}}\right) - a\right] = 0 \quad (A-3),$$

where $a = \frac{\bar{n}_{ch} th_{GaN}}{n_{i,GaN} L_D \sqrt{2}}$

The Discriminant Δ of the Equation A-3 is given by the following expression

$$\Delta = \left[a * \tan\left(\frac{th_{GaN}}{L_D\sqrt{2}}\right)\right]^2 - 4 \left[\tan\left(\frac{th_{GaN}}{L_D\sqrt{2}}\right)\right]\left[\tan\left(\frac{th_{GaN}}{L_D\sqrt{2}}\right) - a\right]$$

The discriminant Δ itself can be considered as a polynomial of the 2nd degree with respect to the unknown a . Its reduced discriminant δ' is given by the following expression

$$\delta' = 4 \left[\tan\left(\frac{th_{GaN}}{L_D\sqrt{2}}\right)\right]^2 \left\{1 + \left[\tan\left(\frac{th_{GaN}}{L_D\sqrt{2}}\right)\right]^2\right\}$$

The reduced discriminant δ' is always positive; the discriminant Δ has two distinct real roots a_1 and a_2 of opposite sign. We suppose that,

$$a_2 < 0 < a_1 ,$$

the discriminant Δ can be put under the form

$$\Delta = \left[\tan\left(\frac{th_{GaN}}{L_D\sqrt{2}}\right)\right]^2 (a - a_1)(a - a_2)$$

Since the quantity a takes positive values only, the discriminant Δ is strictly positive for all

$a > a_1$. Root a_1 is given as;

$$a_1 = 2 \frac{-1 + \left\{1 + \left[\tan\left(\frac{th_{GaN}}{L_D\sqrt{2}}\right)\right]^2\right\}^{1/2}}{\tan\left(\frac{th_{GaN}}{L_D\sqrt{2}}\right)}$$

For all values $a > a_1$, Equation A-3 accepts one positive solution;

$$\tan\left(\frac{x_0}{L_D\sqrt{2}}\right) = -\frac{a}{2} + \frac{1}{2}\cotan\left(\frac{th_{GaN}}{L_D\sqrt{2}}\right)\Delta^{1/2}$$

The condition given by Inequality A-1 is proven.

The abscissa (location of the thin GaN layer) x_0 is,

$$x_0 = L_D\sqrt{2} * \arctan\left(-\frac{a}{2} + \frac{1}{2}\cotan\left(\frac{th_{GaN}}{L_D\sqrt{2}}\right)\Delta^{1/2}\right)$$

For the intrinsic GaN material, the room temperature Debye length L_D has the value $2.46 * 10^7 cm$. All considered GaN layers have thicknesses th_{GaN} in the range of hundreds of nanometers. The following two approximations to the first degree are thus justified;

$$\tan\left(\frac{th_{GaN}}{L_D\sqrt{2}}\right) \sim \frac{th_{GaN}}{L_D\sqrt{2}},$$

and

$$a_1 \sim \frac{th_{GaN}}{L_D\sqrt{2}}$$

The condition A-1 becomes,

$$\overline{n_{ch}} > n_{i,GaN}$$

This concludes the proof.

A.3 Conclusion

For any given value of $(\overline{n_{ch}}, th_{GaN})$, the fact that $(\overline{n_{ch}}, th_{GaN})$ satisfies condition A-1 is a *cine qua non* condition for the existence of a GaN layer where this value applies. A proof of this statement has been presented.

Appendix B

B.1 Introduction

In Chapter 5, any input $(\overline{n_{ch}}, F_0, th_{GaN})$ that satisfies condition 1 ensures the existence and the uniqueness of a solution to equation 5-6. This solution allows the computation of the initial free electron concentration that falls under case 1. In this appendix, a proof of the sufficiency and the necessity of condition 1 is presented. Equation 5-6 and Condition 1 are repeated for convenience in B-1 and B-2 respectively.

$$Z = \ln \left[1 + \frac{Z}{-\frac{b}{2a}(Z-a)(Z+\frac{a(b+1)}{b})} \right], \quad Z \in]0, a[\quad (\text{B-1})$$

Where $a = \frac{F_0 th_{GaN}}{u_T}, \quad b = \frac{\varepsilon_o \varepsilon_{GaN} F_0}{q \overline{n_{ch}} th_{GaN}}$

$$a(b+1) > 2 \quad (\text{B-2})$$

B.2 Proof

A proof of the following statement is presented

$\forall (a, b) \in (\mathbb{R}_*^+)^2$, such that $a(b+1) > 2, \exists ! Z_r \in]0, Z_r[$ for which

$$Z_r = \ln \left[1 + \frac{Z_r}{-\frac{b}{2a}(Z_r-a)(Z_r+\frac{a(b+1)}{b})} \right]$$

f, g are two functions defined on $[0, a[$ by

$$\begin{cases} f(Z) = \ln \left[1 + \frac{Z}{-\frac{b}{2a}(Z-a)(Z+\frac{a(b+1)}{b})} \right], & (a, b) \in (\mathbb{R}_*^+)^2 \\ g(Z) = Z \end{cases}$$

We notice that $f(0) = g(0) = 0$, the derivatives f' , g' are given as;

$$\begin{cases} f'(Z) = \frac{2a}{b} \frac{Z^2 + \frac{a^2(b+1)}{b}}{(z-a)(z+a) \left(z - \frac{a(b+1)}{b}\right) \left(z + \frac{a(b+1)}{b}\right)} \\ g'(Z) = 1 \end{cases} \quad (\text{B-3})$$

f' and g' are strictly positive functions on $[0, a[$. Second derivatives f'' , g'' are given as follow

$$\begin{cases} f''(Z) = \frac{4b}{a} Z \frac{-Z^4 + 2 \frac{a^2(b+1)}{b} Z^2 + \frac{a^2(b+1)}{b} a^2 \left[1 + \frac{(b+1)}{b} + \left(\frac{(b+1)}{b}\right)^2\right]}{(Z^2 - a^2)^2 \left[Z^2 - \left(\frac{a(b+1)}{b}\right)^2\right]^2} \\ g''(Z) = 0 \end{cases}$$

Function f'' can be written as

$$f''(Z) = -\frac{4b}{a} Z \frac{\left[Z^2 - \frac{a^2(b+1)}{b} + \Delta^{1/2}\right] \left[Z^2 - \frac{a^2(b+1)}{b} - \Delta^{1/2}\right]}{(Z^2 - a^2)^2 \left[Z^2 - \left(\frac{a(b+1)}{b}\right)^2\right]^2},$$

where

$$\begin{cases} \Delta = \left[\frac{a^2(b+1)}{b}\right]^2 + \frac{a^2(b+1)}{b} a^2 \left[1 + \frac{(b+1)}{b} + \left(\frac{(b+1)}{b}\right)^2\right] \\ \Delta^{1/2} > \frac{a^2(b+1)}{b} \end{cases}$$

Besides $Z = 0$, function f'' has two real (and opposite) zeros whose square value is equal to $\frac{a^2(b+1)}{b} + \Delta^{1/2}$. Function f'' is positive on $[0, a[$ since $a^2 < \frac{a^2(b+1)}{b} < \frac{a^2(b+1)}{b} + \Delta^{1/2}$. So, f and $f - g$ are convex functions on $[0, a[$.

Suppose that $f'(0) \geq g'(0) = 1$, by integrating both sides (left and right) of the double inequality $f'(Z) \geq f'(0) \geq 1$ on $[0, Z[$ where $Z \in [0, a[$, we get $f(Z) \geq g(Z)$. Since $f - g$ is positive, convex on $[0, a[$ and $(f - g)(0) = 0$, then $(f - g) > 0$ on $]0, a[$. Equation $f - g = 0$ has only one solution (trivial) $Z = 0$. Equation B-1 has no solution on $]0, a[$.

Suppose that $f'(0) < g'(0) = 1$. Since function f' is continuous on $[0, a[$, there exists a point $Z' \in]0, a[$ such that $f'(0) < f'(Z) < g'(0) = 1$ for all $Z \in [0, Z']$. Integrating both sides (middle and right) of previous double inequality, we obtain $f(Z) < g(Z)$ for all $Z \in [0, Z']$, and thus function $(f - g)$ satisfies : $(f - g) < 0$ on $[0, Z']$. Function f diverges at point $x = a : \lim_{x \rightarrow a^-} f = +\infty$. Using the definition of limits in \mathbb{R} , we get;

$$\forall A > 0 \exists \varepsilon > 0 \text{ such that, } Z \in]a - \varepsilon, a[\Rightarrow f(Z) > A$$

It is sufficient to take $A = g(a^-) = a$, we get as a result $(f - g) > 0$ for all $Z \in]a - \varepsilon, a[$.

Application of Intermediate value theorem on function $f - g$ shows that there exists at least one point $Z_r \in]0, a[$ such that $(f - g)(Z_r) = 0$. Equation B-1 has at least one solution on $]0, a[$.

So far it has been proven that the condition $f'(0) < g'(0) = 1$ is sufficient for the equation $(f - g)(Z) = 0$ to accept at least one solution $Z_r \in]0, a[$. The uniqueness of this solution is guaranteed by the convexity of the function $(f - g)$ on $[0, a[$ and the fact that $(f - g)(0) = 0$.

Now, a proof that the condition $f'(0) < g'(0) = 1$ is also necessary for the solution existence is given. Suppose there exists a point $Z_r \in]0, a[$ such that $(f - g)(Z_r) = 0$. Application of Rolle's Theorem shows that there is at least one point $Z_0 \in]0, Z_r[$ such that $(f - g)'(Z_0) = 0$. Point Z_0 is unique because of convexity of function $(f - g)$. Using the following statement: $(f - g)'(Z_0) = 0 \Leftrightarrow f'(Z_0) = 1$, together with the fact that function f' is monotonically increasing on $[0, a[$, we obtain $f'(Z) < 1$ for all $Z \in [0, Z_0[$ and $f'(Z) \geq 1$ for all $Z \in [Z_0, a[$. So $f'(0) < g'(0) = 1$ is also a necessary condition for the equation 8-1 to have a solution on $]0, a[$.

The equation $(f - g) = 0$ admits a unique solution on $]0, a[$ if and only if the following condition 9-4 is satisfied

$$f'(0) < g'(0) = 1 \tag{B-4}$$

Substituting $f'(0)$ by its expression obtained from expression B-3 for $Z = 0$ in inequality B-4, constants (a, b) satisfy the following condition

$$a(b + 1) > 2$$

This concludes the proof.

B.3 Computation of the solution

Equation B-1 has always a trivial solution $Z = 0$. When condition B-2 is satisfied, Equation B-1 has also a second solution $Z_r \in]Z_0, a[$.

An approximate value of solution Z_r can be obtained using an iterative method. Fixed point method cannot be applied since $f'(Z_r) > 1$ because $Z_r \in]Z_0, a[$. Newton-Raphson or Bisection methods can be used. The success of these methods relies in part on the choice of an adequate starting point $Z = Z_{init}$.

The point $Z_{init} \in]Z_0, a[$ will be taken as the barycenter of points $Z = Z_0$ and $Z = a$, fitted with coefficients $1 - \alpha$ and α respectively. The coefficient α is chosen so that iterative variable initial value Z_{init} will be as close as necessary to point $Z = a$. The value Z_{init} is given as

$$Z_{init} = (1 - \alpha)Z_0 + \alpha a \quad (\text{B-5})$$

The determination of point $Z = Z_0$ is essential to ensure that initial point $Z = Z_{init}$ is on the right side ($f'(Z_{initial}) > 1$), otherwise the iterative method will converge to the second, unwanted and trivial, solution $Z = 0$. The value Z_0 is a solution for equation $f'(Z) = 1$.

Using the expression of the derivative f' in B-3, Z_0 is a root of polynomial Γ defined on $]0, a[$ as

$$\Gamma(Z) = Z^4 - \left[\left(\frac{a}{b} \right)^2 + 2 \frac{a^2}{b} + \frac{2a}{b} + 2a^2 \right] Z^2 + \frac{a^2(b+1)}{b} \left(a^2 + \frac{a^2}{b} - \frac{2a}{b} \right)$$

Γ can be considered as a second degree polynomial with respect to unknown Z^2 . Its discriminant Δ has the following expression

$$\Delta = \left[\left(\frac{a}{b} \right)^2 + 2 \frac{a^2}{b} + \frac{2a}{b} + 2a^2 \right]^2 - 4 \frac{a^3(b+1)}{b^2} [a(b+1) - 2], \Delta \text{ is always positive.}$$

Its square root satisfies the following inequality

$$\Delta^{1/2} < \left[\left(\frac{a}{b} \right)^2 + 2 \frac{a^2}{b} + \frac{2a}{b} + 2a^2 \right] \quad \text{since } a(b+1) > 2$$

If Z_1^2 and Z_2^2 , we take $Z_1^2 < Z_2^2$, denote roots of polynomial Γ with respect to unknown Z^2 , theirs sum and product are given as

$$\begin{cases} Z_1^2 + Z_2^2 = \left[\left(\frac{a}{b}\right)^2 + 2\frac{a^2}{b} + \frac{2a}{b} + 2a^2 \right] (> 0) \\ Z_1^2 \cdot Z_2^2 = \frac{a^2(b+1)}{b} \left(a^2 + \frac{a^2}{b} - \frac{2a}{b} \right) (> 0) \end{cases}$$

To see which root is accepted or discarded, we compute $\Gamma(a)$

$$\Gamma(a) = -2a \left(\frac{a}{b}\right)^2 - 4a^2 \left(\frac{a}{b}\right)$$

Since $\Gamma(a) < 0$, we obtain $Z_1^2 < a^2 < Z_2^2$ (comparison of a real number with real roots of a second degree polynomial), root Z_1^2 is accepted and root Z_2^2 is discarded. Our point $Z = Z_0$ is given as;

$$Z_0(= |Z_1|) = \left\{ \frac{\left(\frac{a}{b}\right)^2 + \frac{2a^2}{b} + \frac{2a}{b} + 2a^2 - \Delta^{1/2}}{2} \right\}^{1/2} \quad (\text{B-6})$$

B.4 Conclusion

A proof of the necessity and sufficiency of condition B-2 for equation B-1 to have a unique non-zero valued solution was given. Choice of the iterative method used was made. The iterative method initial point was defined by B-5 and B-6.

Appendix C

C.1 Introduction

In Chapter 5, any input $(\overline{n_{ch}}, F_0, th_{GaN})$ that satisfies condition 2 ensures the existence and the uniqueness of a solution for equation 5-7. This solution allows the computation of the initial free electron concentration that falls under case 2. In this appendix, a proof of the sufficiency and necessity of condition 2 is presented. Equation 5-7 and Condition 2 are repeated for convenience in C-1 and C-2 respectively.

$$Z = \arctan \left[\frac{2Z}{\frac{4b}{a}Z^2 + a(b+1)} \right], Z \in \left[0, \arctan \left(\frac{d}{\sqrt{1-d^2}} \right) \right] \left[\subset \left[0, \frac{\pi}{2} \right] \right] \quad (\text{C-1})$$

Where

$$a = \frac{F_0 th_{GaN}}{u_T}, \quad b = \frac{\varepsilon_o \varepsilon_{GaN} F_0}{q \overline{n_{ch}} th_{GaN}}$$

$$a(b+1) < 2 \quad (\text{C-2})$$

C.2 Proof

A proof of the following statement is presented

$$\forall (a, b) \in (\mathbb{R}_*^+)^2, \text{ such that } a(b+1) < 2, \exists ! Z_r \in \left] 0, \frac{\pi}{2} \right[\text{ for which}$$

$$Z_r = \arctan \left[\frac{2Z_r}{\frac{4b}{a}Z_r^2 + a(b+1)} \right]$$

We can follow an approach similar to that used in appendix B and apply it on functions f, g defined on interval $\left[0, \frac{\pi}{2} \right]$ as follow;

$$\begin{cases} f(Z) = \arctan\left(\frac{2z}{\frac{4b}{a}z^2 + a(b+1)}\right) \\ g(z) = z \end{cases}$$

Or we can work on function h defined on $\left[0, \frac{\pi}{2}\right]$ as

$$h(Z) = \arctan\left(\frac{2z}{\frac{4b}{a}z^2 + a(b+1)}\right) - z$$

The second option is considered. We notice that $h(0) = 0$ and $h\left(\frac{\pi}{2}\right) < 0$ since $\arctan(m(x)) < \frac{\pi}{2}$ for any real function m of variable x . h is a class C^2 -function on $\left[0, \frac{\pi}{2}\right]$, its first derivative h' is given as follow;

$$h'(z) = 2 \frac{-\frac{4b}{a}z^2 + a(b+1)}{4z^2 + \left[\frac{4b}{a}z^2 + a(b+1)\right]^2} - 1 \quad (\text{C-3})$$

Its value at $z = 0$ is $h'(0) = \frac{2}{a(b+1)} - 1$

Suppose that $h'(0) > 0$, that is $a(b+1) < 2$, then function h is positive (increasing from $h(0) = 0$) in the neighbourhood of $z = 0$. On the other side, $h\left(\frac{\pi}{2}\right) < 0$ means that function h is negative in the neighborhood of $z = \frac{\pi}{2}$. The existence of these two neighborhoods is guaranteed by the fact that h is continuous on $\left[0, \frac{\pi}{2}\right]$.

Application of the Intermediate Value theorem on function h shows that there exists at least one point $z_r \in \left]0, \frac{\pi}{2}\right[$ where $h(z_r) = 0$. Thus, $h'(0) > 0$ is a sufficient condition for the existence of at least one solution to equation $h(Z) = 0$ in $\left]0, \frac{\pi}{2}\right[$. Since $h(0) = h(z_r) = 0$, function h has at least one maximum at $(z_0, h(z_0))$, where $z_0 \in \left]0, z_r\right[$, and $h(z_0) > 0$ according to Rolle's Theorem.

The first derivative h' at $Z = Z_0$ satisfies $h'(Z_0) = 0$. Using the expression of h' in C-3, $Z = Z_0$ is a root of the polynomial Γ defined as follow,

$$\Gamma(z) = -\left(\frac{4b}{a}\right)^2 z^4 - \left[8b(b+1) + \frac{8b}{a} + 4\right] z^2 - a(b+1)[a(b+1) - 2] \quad \text{C-4}$$

Γ is a polynomial of the 4th degree composed of even power monomials only . It has four roots in \mathbb{C} according to d'Alembert-Gauss theorem. Γ has its coefficients in \mathbb{R} , this implies that if Z is a root of Γ , then $-Z$ and \bar{Z} are also roots of Γ , and thus either $\bar{Z} = Z$ or $\bar{Z} = -Z$; roots are real or pure imaginary complex. So, the real numbers Z_0 and $-Z_0$ are two roots of Γ .

We can consider Γ as a polynomial of second degree with respect to unknown Z^2 , then Z_0^2 is one of its two roots. The reduced discriminant is given as follow

$$\Delta' = \left(4b(b+1) + \frac{4b}{a} + 2\right)^2 - \left(\frac{4b}{a}\right)^2 a(b+1)(a(b+1) - 2) \quad \text{(C-5),}$$

and it satisfies the following inequality

$$\Delta' > \left(4b(b+1) + \frac{4b}{a} + 2\right)^2 \text{ since } a(b+1) < 2 \quad \text{(C-6)}$$

The second root Z_1^2 is negative since

$$Z_0^2 Z_1^2 = \frac{a(b+1)(a(b+1) - 2)}{\left(\frac{4b}{a}\right)^2} < 0$$

Γ , as a second degree polynomial, has two real roots of opposite sign Z_0^2 and Z_1^2 . Γ , as a fourth degree polynomial, has four roots Z_0 , $-Z_0$, $j\sqrt{-Z_1^2}$, and $-j\sqrt{-Z_1^2}$. Γ has a unique positive root $Z_0 \in]0, \frac{\pi}{2}[$. Polynomial Γ can be put in the following form,

$$\Gamma = -\left(\frac{4b}{a}\right)^2 (Z - Z_0)(Z + Z_0)(Z^2 - Z_1^2)$$

We can see that $\Gamma > 0$ on $]0, Z_0[$ and $\Gamma < 0$ on $]Z_0, \frac{\pi}{2}[$.

The function h is monotonically increasing on $]0, Z_0[$ and monotonically decreasing on $]Z_0, \frac{\pi}{2}[$. $Z = Z_0$ is the unique point where $h'(Z_0) = 0$. The value of this root is given as follow;

$$Z_0 = \frac{-\left[4b(b+1) + \frac{4b}{a} + 2\right] + \sqrt{\Delta'}}{\left(\frac{4b}{a}\right)^2} \quad (C-7)$$

So far, it has been proven that $a(b+1) < 2$ is a sufficient condition for the equation $h(Z) = 0$ to have a unique solution $Z = Z_r \in]Z_0, \frac{\pi}{2}[$ ($\subset]0, \frac{\pi}{2}[$). Notice that if $h'(0) = 0$, that is $a(b+1) = 2$, the function h is strictly decreasing, and thus negative on $]0, \frac{\pi}{2}[$. In fact, we know that

$$h(Z) \leq \frac{2z}{\frac{4b}{a}z^2 + a(b+1)} - z \text{ for all } Z \in \left]0, \frac{\pi}{2}\right[$$

Developing the right side of the previous inequality results in the following;

$$h(Z) \leq Z \frac{-\frac{4b}{a}Z^2 - a(b+1) + 2}{\frac{4b}{a}Z^2 + a(b+1)},$$

setting $a(b+1) = 2$ makes $h < 0$ on $]0, \frac{\pi}{2}[$.

Let's prove the necessity of condition C-2 for equation C-1 to have a unique solution on $]0, \frac{\pi}{2}[$. Suppose that equation C-1 has a unique solution $Z = Z_r$. Applying Rolle's Theorem on function h results in the existence of a point $Z = Z_0 \in]0, Z_r[$ where $h'(Z_0) = 0$. Considering polynomial Γ as of second degree with respect to unknown Z^2 , it is found that it has two roots Z_0^2 and Z_1^2 , then their sum is given as,

$$Z_0^2 + Z_1^2 = -\frac{\left[8b(b+1) + \frac{8b}{a} + 4\right]}{\left(\frac{4b}{a}\right)^2} < 0$$

Second root Z_1^2 is negative, thus Γ has a one positive root $Z = Z_0$. For this to happen, the reduced discriminant Δ' must satisfy inequality C-6. This is achieved for all values (a, b) for which $a(b+1) < 2$. The necessity of condition C-2 is proven

C.3 Computation of the solution

Equation C-1 has always a trivial solution $Z = 0$. When condition C-2 is satisfied, equation C-1 has also a second solution $Z_r \in]0, \frac{\pi}{2}[$.

An approximate value of solution Z_r can be obtained using an iterative method, Newton-Raphson or Bisection methods can be used. For The Bisection method, initial points are $(Z_0, h(Z_0))$ and $(\frac{\pi}{2}, h(\frac{\pi}{2}))$. For Newton-Raphson method, the initial point $Z_{init} \in]Z_0, \frac{\pi}{2}[$ is taken as the barycenter of points $Z = Z_0$ and $Z = \frac{\pi}{2}$, fitted with the same coefficient $\frac{1}{2}$.

The value Z_{init} is given as

$$Z_{init} = \frac{1}{2} \left(Z_0 + \frac{\pi}{2} \right) \quad (C-8)$$

Where the value of Z_0 is given in expression C-7.

C.4 Conclusion

A proof of the necessity and sufficiency of condition C-2 for the equation C-1 to have a unique non-zero valued solution was given. Choice of the iterative methods used to get an approximate value of the solution was made. Initial points for the candidate methods were defined in C-7 and C-8.